Aus der

Medizinischen Klinik und Poliklinik III

Klinikum der Ludwig-Maximilians-Universität München



The Impact of Obesity-Associated Environment on Differentiation, Metabolism and Function of Natural Killer Cells

Dissertation

zum Erwerb des Doctor of Philosophy (Ph.D.)

an der Medizinischen Fakultät der

Ludwig-Maximilians-Universität München

vorgelegt von:

Jingke Tu

aus

ChongQing (China)

Jahr:

2025

Mit Genehmigung der Medizinischen Fakultät der Ludwig-Maximilians-Universität München

Erstes Gutachten: Prof. Dr. Sebastian Theurich

Zweites Gutachten: Prof. Dr. Elfriede Nößner

Drittes Gutachten: Prof. Dr. Barbara Schraml-Schotta

Viertes Gutachten: Priv.Doz.Dr.Philipp Freiherr von Hundelshausen

Dekan: Prof. Dr. med. Thomas Gudermann

Tag der mündlichen Prüfung: 02.10.2025

1.	Abs	tract	1
2.	Intr	oduction	. 4
	2.1.	Natural killer cell differentiation from hematopoietic stem cell	4
	2.2.	Anti-tumour Function of NK cell	6
	2.3.	The impact of obesity microenvironment on NK cell	8
	2.4.	The molecular pathways involved in obesity associated NK regulation	10
	2.5.	Research Hypothesis and objective	13
3.	Mat	rerials and Methods	15
	3.1.	Compounds	15
	3.2.	Antibodies	17
	3.3.	Technical devices	19
	3.4.	Cell lines	20
	3.5.	Differentiation of 3T3-L1 cell line into adipocyte	20
	3.6.	BD Rhapsody single cell whole transcriptome analysis	21
	3.7.	Isolation of murine bone marrow cells	21
	3.8.	Isolation of murine splenocytes	22
	3.9.	Differentiation of BMCs into NK cells	22
	3.10.	Flow Cytometry	22
	3.11.	Seahorse real-time cell metabolic analysis	23
	3.12.	Cytation-based NK cell killing assay	24
	3.13.	Single-cell transcriptomics: data analysis	24
	3.14.	Statistical Analysis	25
	3.15.	Software	25
4.	Res	ults	26

4.	.1. Estab	lishment of a NK cell differentiation model from murine	
h	ematopoiet	ic stem/progenitor cell <i>in vitro</i>	26
	4.1.1.	Flow cytometry analysis of frequency of hematopoietic stem cell, NK cell	
	progenitor a	nd NK cell in murine bone marrow	26
	4.1.2.	Establishing an in vitro NK cell differentiation model under the induction of	
	different cyto	okines	27
	4.1.3.	Analysis of the dynamic changes of lymphoid and myeloid lineages in the	
	model over t	ime	28
4.	.2. The si	mulation of obesity condition in the NK cell differentiation model	
in	iduced by fa	itty acids	29
	4.2.1.	Dose-dependent cytotoxicity induced by palmitate in different linages within	1
	the different	iation model	29
	4.2.2.	Effects of varying palmitate concentrations on the frequency of lineage	
	specific cells	s in the NK cell differentiation model.	31
	4.2.3.	Dynamic changes in CD36, IL-6R, and CSF1R expression levels across	
	lineage-spec	sific cell populations during differentiation.	32
	4.2.4.	Increasing frequency of obesity-associated specific NK cell subsets in the	
	differentiatio	on model	33
4.	.3. Simul	ating obesity conditions through co-culture with adipocytes to	
		ne effects on NK cell differentiation and phenotype	36
	4.3.1.	Establishment of an <i>in vitro</i> adipocyte induction and NK cell co-culture	
		on model	36
	4.3.2.	Dynamic changes in the frequency of different lineage cells in the co-culture	
	differentiatio	on model	
	4.3.3.	Increasing frequency of obesity-associated NK cell subsets in the adipocyte	
		ifferentiation model	38
	4.3.4.	Flow cytometry analysis of surface markers of NK cell subsets indicating a	
		ession pattern in obese-associated NK cell.	41

4.4.	Analysis of mitochondrial metabolism and cytotoxic function in NK cells
induc	ed under obesity conditions
4.4.	1. NK cells induced in adipocytes co-culture model exhibiting reduced mitochondrial
met	abolic activity
4.4.	2. Analysis of mitochondrial mass, membrane potential, and reactive oxygen species
leve	els elucidated impaired NK cell function in obese environment
4.4.	3. NK cells induced under obesity conditions exhibit reduced tumor cell
cyto	otoxicity
4.5.	Using single-cell RNA sequencing to analyze the impact of obesity
condi	tions on the NK cell from the <i>in vitro</i> differentiation model 49
4.5.	1. The Adipocytes induce generally upregulation of pro-inflammatory genes and fatty
acio	d metabolism related genes 50
4.5.	2. Identification of obesity-associated NK cell subsets in adipocytes coculture
mod	del53
4.5.	3. Comparative gene set enrichment analysis of the differential expression genes in
NKp	o46+ NK cell subsets 55
4.5.	4. Pseudotime analysis showing distinct differentiation regulation pathways of
obe	sity-associated NK cells
5. Dis	cussion 63
5.1	Summary of the results 63
5.2	The NK cell generation facilitated by cytokines <i>in vitro</i>
5.3	Phenotypic differences in obesity-associated NK cells 65
5.4	Impaired NK cell function in obese environment 65
5.5	Transcriptomic profile of NK cells induced in different environment 66
5.6	Clinical perspective in obesity associated cancer 67
6. Co.	nclusion and Outlook 69
7 Su	nnlamentary 71
	0010000019FV /1

8.	List of Figures	<i>7</i> 3
9.	List of Abbreviations	<i>7</i> 5
10.	References	77
11.	Acknowledgments	86
12.	Affidavit	88
13.	Confirmation of congruency	89

Abstract

Natural killer cells represent a distinct lymphocyte subset which are traditionally classified within the innate immune compartment. They play a central role in host defense, particularly in antitumor and anti-viral immunity. Obesity is a global epidemic, currently affecting over 600 million adults and 124 million children. It is well established that obese individuals exhibit chronic lowgrade inflammation, which also affects the composition and function of NK cells. In earlier studies, we identified the expansion of a specific NK cell subpopulation that expresses the interleukin-6 receptor alpha (IL6Ra), in both obese humans and mouse models. This subpopulation is characterized by the expression of several myeloid-associated genes, such as the colonystimulating factor 1 receptor (CSF1R). This obesity-associated NK cell population contributes to the development of insulin resistance and correlates with the extent of systemic low-grade inflammation. In the present study, we describe an in vitro model for generating murine, obesityassociated NK cells from hematopoietic progenitor cells, using additional fatty acid supplementation as well as adipocyte co-culture, both serving as obesity-mimicking microenvironments. Immunophenotypic analyses using flow cytometry show that NK cells generated from bone marrow under such obesity-mimicking conditions exhibit increased expression of IL6Ra and CSF1R, while displaying a specific expression pattern of key receptors and maturation markers of other myeloid genes. Functional analyses reveal reduced mitochondrial respiration and glycolytic capacity in adipocyte-induced NK cells, as well as a diminished cytotoxic capacity against the colorectal cancer cell line MC38. Single-cell RNA sequencing ultimately reveals transcriptomic changes in these NK cells, notably an upregulation of genes associated with myeloid cell differentiation, fatty acid uptake, and inflammatory signaling pathways. Additionally, potential regulatory differentiation pathways of these obesityassociated NK cells are depicted from the RNA sequencing data. In summary, this study highlights the phenotypic and functional impacts of the obese microenvironment on NK cells. It contributes to a better understanding of how NK cell immunity is reshaped by obesity and offers potential strategies to improve immune responses in obesity-associated cancers.

Deutsche Zusammenfassung

Natürliche Killerzellen stellen eine bestimmte Untergruppe von Lymphozyten dar, die traditionell dem angeborenen Immunsystem zugeordnet werden. Sie spielen eine zentrale Rolle im Schutz des Wirts, insbesondere in der Anti-Tumor- und Anti-Virus-Immunität. Fettleibigkeit ist eine globale Epidemie, von der mittlerweile über 600 Millionen Erwachsene und 124 Millionen Kinder betroffen sind. Es ist gut etabliert, dass adipöse Individuen eine chronische niedriggradige Entzündung aufweisen, die auch die Zusammensetzung und Funktion der NK-Zellen beeinflusst. In früheren Studien identifizierten wir die Expansion einer spezifischen NK-Zell-Subpopulation, die den Interleukin-6-Rezeptor alpha (IL6Ra) exprimiert, sowohl in adipösen Menschen als auch in Mausmodellen. Diese Subpopulation ist durch die Expression mehrerer myeloid-assoziierter Gene, darunter der Koloniestimulierende Faktor 1 Rezeptor (CSF1R) charakterisiert. Die adipositasassoziierte NK-Zell-Population trägt zur Entwicklung einer Insulinresistenz bei und korreliert mit dem Ausmaß der systemischen niedriggradigen Entzündung. In der vorliegenden Studie beschreiben wir ein in-vitro-Modell zur Generierung muriner, adipositasassoziierter NK-Zellen aus hämatopoetischen Vorläuferzellen durch zusätzliche Fettsäuresupplementierung sowie durch Adipozyten-Kokultur – beides als adipositas-imitierendes Mikromilieu. Immunphänotypische Analysen mittels Durchflusszytometrie zeigen, dass aus Knochenmark gerenierte NK-Zellen unter solchen Adipositas-imitierenden Bedingungen eine verstärkte Expression von IL6Ra und CSF1R aufweisen, während sie ein spezifisches Expressionsmuster wichtiger Rezeptoren und Reifungsmarker weiterer myeloischer Gene zeigen. Funktionelle Analysen offenbaren eine reduzierte mitochondriale Atmung und Glykolysekapazität in Adipozyten-induzierten NK-Zellen sowie eine verminderte zytotoxische Kapazität gegenüber der Kolonkarzinom-Zelllinie MC38. Einzelzell-RNA-Sequenzierung Die zeigt transkriptomische Veränderungen in diesen NK-Zellen, insbesondere eine Hochregulation von Genen, die mit einer Differenzierung myeloischer Zellen, der Fettsäureaufnahme und entzündlichen Signalwegen assoziiert sind. Darüber hinaus werden potenzielle regulatorische Differenzierungswege dieser adipositasassoziierten NK-Zellen aus den RNA-Sequenzierungsdaten abgeleitet. Zusammenfassend hebt diese Studie die phänotypischen und funktionellen Auswirkungen des adipösen Mikromilieus auf NK-Zellen hervor. Dies trägt zu einem

Abstract

besseren Verständnis der Umgestaltung der NK-Zell-Immunität durch Adipositas bei und liefert potenzielle Strategien zur Verbesserung der Immunantwort in adipositasassoziierten Krebserkrankungen.

Introduction

2.1 Natural killer cell differentiation from hematopoietic stem cells

Natural Killer (NK) cells, first discovered in the 1970s (Horowitz et al. 2013), are large granular lymphocytes that can spontaneously kill tumor cells without prior sensitization, representing about 5-15% of circulating lymphocytes in humans (Rosenstock et al. 2020). They represent a critical component of the innate immune system, serving as a first line of defense against viral infections and cancer.

In mice, NK cell development begins in the bone marrow with CD34⁺ hematopoietic stem cells progressing through well-defined stages. The developmental sequence starts with Common Lymphoid Progenitors (CLPs) expressing IL-7Rα, which then differentiate into Pre-NK Cell Progenitors (Pre-NKPs) marked by IL-7Rα and CD244 expression (Luo et al. 2023). These cells then progress to NK Cell Progenitors (NKPs) characterized by CD122 (IL-2/15Rβ) expression, marking their commitment to the NK lineage and dependence on IL-15 signaling (Stokic-Trtica et al. 2020). The immature NK cell (iNK) stage follows, during which cells sequentially acquire NK1.1 and NKp46 expression, followed by CD11b and CD43 (Baranek et al. 2017). Final maturation is marked by the expression of CD49b and the acquisition of Ly49 receptors, with terminal maturation characterized by distinct CD27/CD11b expression patterns. This process is regulated by key transcription factors including E2A, EBF, Id2, and E4BP4/NFIL3, with IL-15 serving as the critical cytokine throughout development (Di Vito et al. 2019).

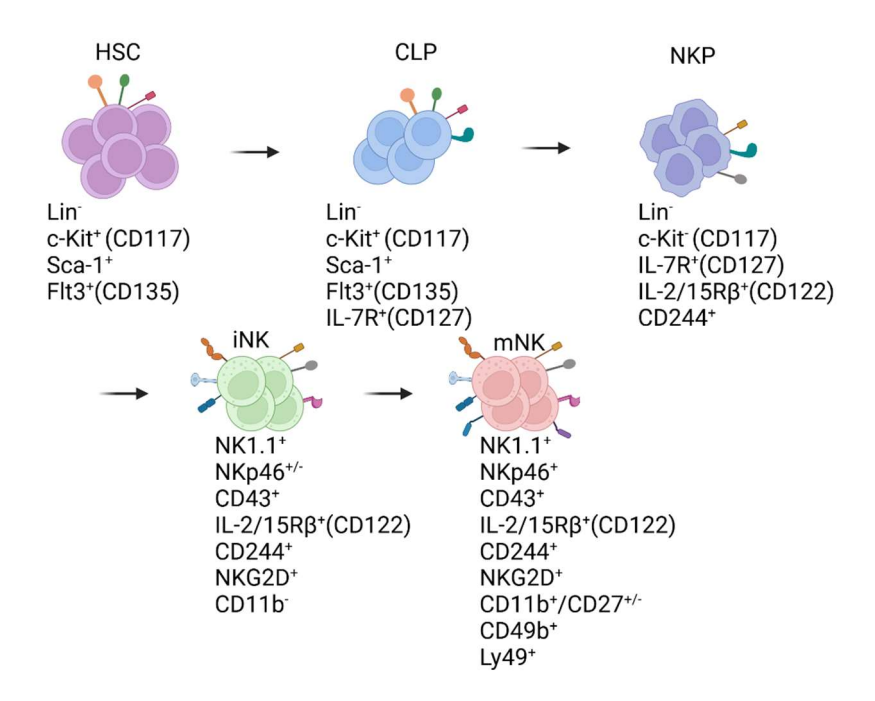


Figure 1 Key makers of murine NK cell at distinct developmental stages from HSC. HSC = Hematopoietic Stem Cell; Lin⁻ = Lineage maker negative; CLP = Common Lymphoid Progenitor; NKP = Natural Killer Progenitor; iNK = immature NK; mNK = mature NK. Created with BioRender.com.

Human NK cell development shares fundamental similarities with mice but follows a distinct pathway. Starting from CD34* HSCs, human NK cells develop through stages beginning with Multi-Lymphoid Progenitors (MLPs) expressing CD34*CD38*CD45RA*CD10* (Karamitros et al. 2018). These cells progress to Common Lymphoid Progenitors marked by CD34*CD38*CD123*CD45RA* and CD7/CD10 expression. The NK-committed progenitors emerge with CD122 expression and IL-15 responsiveness, followed by pre-NK cells (CD34*CD117*CD94*) that begin expressing NK cell-associated markers (Persyn et al. 2022). A unique feature of human NK cell development is the prominent CD56bright immature stage, characterized by CD94/NKG2A expression and limited cytotoxicity (Nguyen et al. 2005). Final maturation involves transition to a CD56dim phenotype, acquisition of KIR receptors (unlike mouse Ly49 receptors), and development of potent cytotoxic capabilities. This process is governed by similar transcription factors as in mice (E4BP4/NFIL3, T-bet, Eomes, Id2) but results in distinct tissue distribution patterns, with significant populations in lymph nodes and tonsils compared to the predominantly splenic and bone marrow distribution in mice (Damele et al. 2018).

2.2 Anti-tumor Function of NK cell

NK cells play a pivotal role in the body's defense against infections, cancer, and other pathological conditions. These innate immune cells operate through the "missing self" principle, utilize a sophisticated array of receptors including inhibitory receptors (KIRs in humans, Ly49 in mice), activating receptors, and natural cytotoxicity receptors (NCRs) to identify their targets (Beaulieu 2021). Upon activation, NK cells execute their functions through direct cytotoxicity (releasing perforin and granzymes), cytokine production (particularly IFN- γ and TNF- α), and antibody-dependent cellular cytotoxicity (ADCC) (Jiao et al. 2023). Over the past few decades, extensive research has elucidated the multifaceted functions of NK cells, highlighting their importance in immune system.

1.Rapid response to tumors and infections: NK cells are essential for the early detection and elimination of virus-infected cells and tumor cells. Unlike adaptive immune cells, which require days to mount a response, NK cells can act within hours of encountering a threat. This rapid response is mediated by their ability to recognize stress-induced ligands which are upregulated on the cellular surface of infected or malignant cells (Batlle et al. 2019). For example, NK cells detect the downregulation of MHC-I molecules, a common evasion strategy employed by viruses and tumors. Many research has shown that NK cells are particularly effective against cytomegalovirus (CMV) infections, where they play a critical role in controlling viral replication and preventing disease progression (Leone et al. 2020).

2.Cytotoxicity and target cell killing: one of the most well-defined functions of NK cells is their ability to induce apoptosis in target cells through cytotoxic mechanisms. NK cells release cytotoxic granules containing perforin and granzymes, which penetrate the target cell membrane and trigger programmed cell death (Littwitz-Salomon et al. 2021). This process is tightly regulated by a balance of activating and inhibitory receptors on the NK cell surface. Activating receptors, such as NKG2D and natural cytotoxicity receptors, recognize stress ligands on target cells, while inhibitory receptors, such as killer cell immunoglobulin-like receptors (KIRs), bind to MHC-I molecules on healthy cells to prevent inappropriate killing (Shaver et al. 2021). This dual-receptor system ensures that NK cells selectively eliminate abnormal cells while sparing normal ones.

- 3. Cytokine production and immune regulation: In addition to their cytotoxic functions, NK cells are potent producers of cytokines and chemokines, which play a crucial role in shaping the immune response. For instance, NK cells secrete interferon-gamma (IFN-γ), a cytokine that enhances the antiviral and antitumor activities of macrophages and T cells. IFN-γ also promotes the differentiation of T helper 1 (Th1) cells, which are essential for combating intracellular pathogens (Oh et al. 2013). Furthermore, NK cells produce tumor necrosis factor-alpha (TNF-α) and granulocyte-macrophage colony-stimulating factor (GM-CSF), which contribute to inflammation and immune cell recruitment (Barnes et al. 2020). These cytokine-mediated functions underscore the role of NK cells as immune regulators, bridging the innate and adaptive immune systems.
- 4. ADCC: NK cells also mediate antibody-dependent cellular cytotoxicity, a process in which they recognize and kill cells coated with antibodies. This function is facilitated by the FcyRIIIa receptor (CD16) on NK cells, which binds to the Fc region of IgG antibodies. ADCC is particularly essential in the context of viral infection and cancer immunotherapy (O'Sullivan et al. 2015). For example, monoclonal antibodies used in cancer treatment, such as rituximab and trastuzumab, rely on NK cell-mediated ADCC to eliminate tumor cells. Recent studies have highlighted the potential of enhancing ADCC through genetic engineering of NK cells or the use of cytokines to boost their activity (Omer et al. 2021; Sordo-Bahamonde et al. 2020).

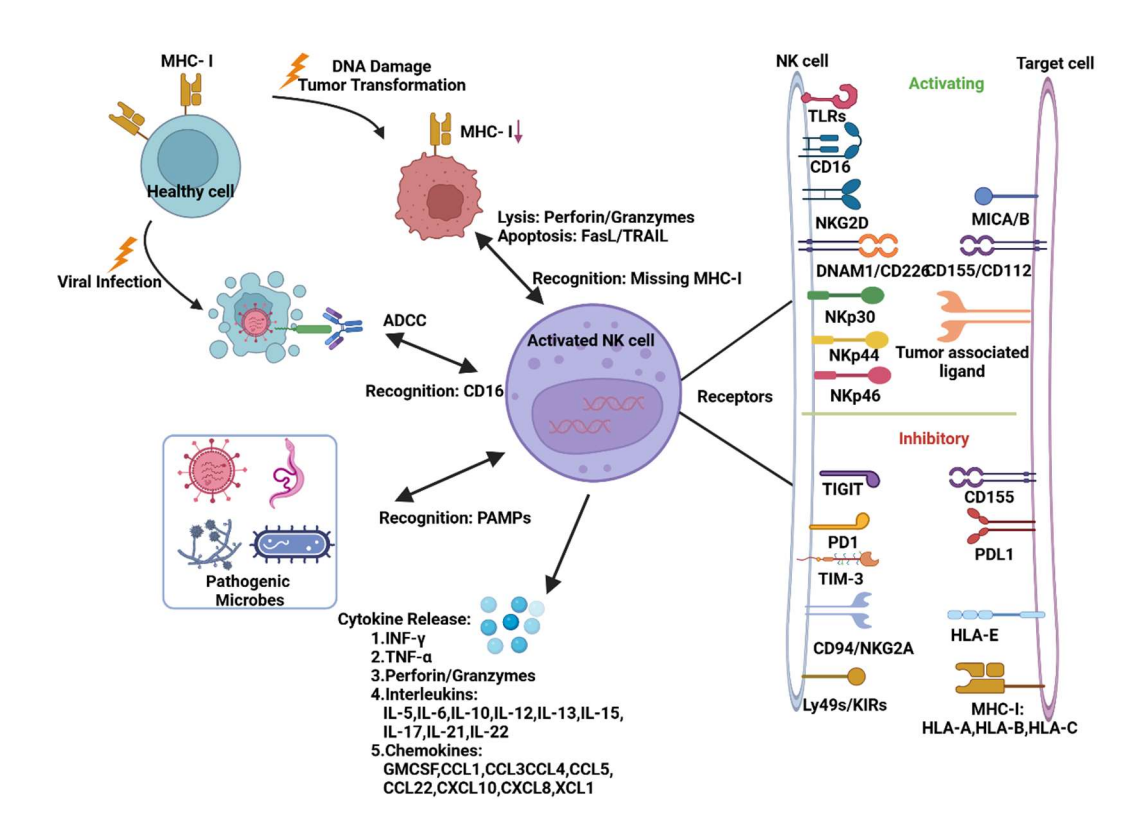


Figure 2 Mechanism of NK cell recognition and killing against target cell. MHC-I = Major histocompatibility complexes I; FasL = Fas ligand; TRAIL = Tumor necrosis factor-related apoptosis-inducing ligand; PAMPs = Pathogen-associated molecular patterns; GM-CSF = Granulocyte-macrophage colony-stimulating factor; CCL = C-C motif chemokine ligand; CXCL = C-X-C motif chemokine ligand; XCL = X-C motif chemokine ligand; TLRs = Toll-like receptors; MICA/B = MHC class I chain-related protein A/B; Created with BioRender.com. Adapted from (Chan et al. 2014; Leischner et al. 2016; Rados et al. 2024).

2.3 The impact of obesity microenvironment on NK cell

Obesity has emerged as a global health crisis, significantly influencing immune system function through its association with chronic low-level inflammation and metabolic dysfunction (Li et al. 2023). One of the most affected components of the immune cells in this condition are NK cells, which are crucial for innate and adaptive immune surveillance. Obesity-induced alterations can lead to compromised NK cell function, thereby increasing susceptibility to various diseases including obesity associated cancer (Johnson et al. 2012). The relationship between adipose tissue expansion, metabolic dysregulation, and NK cell dysfunction is a critical area of study for understanding the immune responses associated with obesity. The environment created by excessive adipose tissue, characterized by persistent inflammation and metabolic disturbances, can profoundly affect NK cell functionality through several aspects.

The expanding adipose tissue generates a distinct microenvironment marked by elevated levels of circulating free fatty acids, increased glucose concentrations, and altered lipid metabolism, all of which contribute to systemic metabolic dysfunction (Quail et al. 2019). This metabolic disruption is accompanied by enhanced secretion of pro-inflammatory adipokines and cytokines, including TNF-α, IL-6, IL-1β and IFN-gamma, secretion of inflammatory adipokines and cytokines that act both locally and systemically to induce peripheral insulin resistance (Zatterale et al. 2019). The inflammatory reaction could be sustained by adipocyte-derived chemoattractants such as CCR2, monocyte chemoattractant protein (MCP), and semaphorin 3A. The creating state of chronic inflammation could dramatically diminish NK cell function (Kawai et al. 2021). The adipose tissue expansion also leads to increased leptin production but decreased adiponectin levels, disrupting the delicate balance of metabolic regulation and immune function (Ouchi et al. 2011).

The general impact of obesity on NK cell function manifests through several mechanisms. First, obesity significantly impairs NK cell cytotoxicity by reducing the expression of critical activating receptors such as NKG2D and NKp46, compromising cytolytic granule formation, and impairing immunological synapse formation. The production and release of cytotoxic molecules, including perforin and granzymes, are also diminished, further impairing NK cell ability to eliminate transformed or infected cells (Bahr et al. 2020). Second, obesity induces profound metabolic reprogramming in NK cells, leading to impaired glycolytic capacity, compromised mitochondrial function, and dysregulated mTOR signaling. This metabolic dysfunction is particularly significant because NK cells rely heavily on metabolic flexibility to mount effective immune responses (Michelet et al. 2018). Third, obesity leads to the development of leptin resistance in NK cells, resulting in reduced JAK-STAT signaling and impaired metabolic adaptation, which further compounds the functional deficits (Richard et al. 2014).

The tissue-specific effects of obesity on NK cells are also noteworthy and contribute to various pathological conditions. In adipose tissue, resident NK cells undergo significant modifications to their tissue residency programs and develop an enhanced pro-inflammatory phenotype, with the increasing levels of granzyme B and perforin, upregulation of chemokines receptor CCR5 and adhesion molecule CD54, contributing to local inflammation and insulin resistance (Haugstoyl et

al. 2023). Hepatic NK cells show reduced frequency and impaired anti-fibrotic function, potentially contributing to the onset and progression of non-alcoholic fatty liver disease (NAFLD). These tissue-specific alterations not only affect local immune surveillance but also contribute to systemic inflammation (Stiglund et al. 2019).

The implications of obesity-induced NK cell dysfunction are also extensive and multifaceted in clinic. In the context of cancer, impaired NK cell function leads to reduced tumor immunosurveillance, compromised anti-metastatic responses, and potentially decreased efficacy of immunotherapy approaches. The relationship between obesity and cancer becomes particularly concerning when considering that NK cells play a crucial role in early detection and elimination of transformed cells (Spielmann et al. 2017). In viral immunity, NK cell dysfunction results in decreased antiviral protection and impaired viral clearance, potentially explaining the increased susceptibility to viral infections observed in obese individuals. This has become particularly relevant in the context of respiratory viral infections, where obesity is often associated with more severe disease outcomes (Bjorkstrom et al. 2022; Yu et al. 2022).

The relationship between obesity and NK cell dysfunction thus represents a complex interplay of metabolic, inflammatory, and immune processes that significantly impact human health. The widespread effects of this dysfunction on various physiological systems underscore the importance of maintaining metabolic health for optimal immune function. As research continues to uncover new mechanisms and therapeutic targets, the development of more effective interventions to restore NK cell function in obesity remains a critical area of investigation in both basic research and clinical studies (De Barra et al. 2023).

2.4 The molecular pathways involved in obesity associated NK regulation

The oxidative stress and epigenetic modifications induced by obesity represent another layer of complexity in NK cell dysfunction (Long et al. 2024). Increased oxidative stress leads to mitochondrial dysfunction, DNA damage, and altered cell signaling pathways in NK cells (Bald et al. 2020). These changes are often accompanied by epigenetic modifications, including altered histone modifications, DNA methylation patterns, and changes in microRNA expression, which

can have long-lasting effects on NK cell function even after weight loss (Leong et al. 2014). The cumulative impact of these molecular alterations contributes to a persistent state of immune dysfunction that may require targeted therapeutic interventions to reverse (S. Y. Wu et al. 2020).

The molecular pathways underlying obesity-induced NK cell dysfunction shape an intricate network of interconnected signaling cascades that collectively impair NK cell function. The mTOR pathway, particularly through mTORC1 activation, plays a central role by disrupting cellular metabolism, glycolytic reprogramming, and lipid metabolism, while mTORC2 dysregulation affects cytoskeleton reorganization and immunological synapse formation (Paul et al. 2017). This metabolic disruption is compounded by reduced AMPK activation, leading to decreased fatty acid oxidation and compromised metabolic flexibility, which is further aggravated by disrupted AMPK-mTOR cross-talk (Terren et al. 2020).

The inflammatory environment in obesity also intensely impacts the JAK-STAT pathway, where leptin resistance develops through SOCS3 upregulation and reduced STAT3 phosphorylation, ultimately impairing cytokine signaling and IFN-γ production (likuni et al. 2008). Concurrently, enhanced NF-κB pathway activation leads to increased pro-inflammatory cytokine production and modified receptor expression. Impaired signaling in NK cells is particularly manifested through modifications in the NKp46 receptor, which affect the recruitment of adaptor proteins and disrupt signal transduction (Liu et al. 2017). Additionally, the NKG2D pathway exhibits deficiencies, characterized by impaired DAP10-mediated signaling, reduced activation of PI3K, and compromised calcium mobilization (Segovis et al. 2009).

Metabolic regulation is significantly impacted as well by disruptions in glucose utilization pathways in obese environment. In particular, obesity-associated insulin resistance can lead to GLUT1 transporter dysfunction, resulting in reduced glucose uptake and impaired glycolytic flux (Berbudi et al. 2025). Meanwhile, altered lipid metabolism through CPT1a-mediated pathway changes negatively affecting mitochondrial function and fatty acid oxidation (Sheppard et al. 2024). The stress response pathways are significantly activated, with enhanced ROS-mediated signaling through NADPH oxidase pathway activation and elevated endoplasmic reticulum stress affecting protein folding capacity through the UPR and PERK-eIF2a pathways (X. Chen et al. 2023).

Epigenetic regulation is also markedly altered, with changes in histone modifications (particularly H3K27me3 and H3K4me3) affecting gene accessibility and expression patterns, while DNA methylation changes through modified DNMT activity and TET enzyme functions lead to altered gene expression and cellular plasticity (Benayoun et al. 2014; Lau et al. 2022). These pathways interact and reinforce each other, creating a complex feedback loop that maintains NK cell dysfunction in obesity, with implications for both metabolic disease and immune surveillance, particularly affecting cytotoxicity, cytokine production, and cellular activation thresholds.

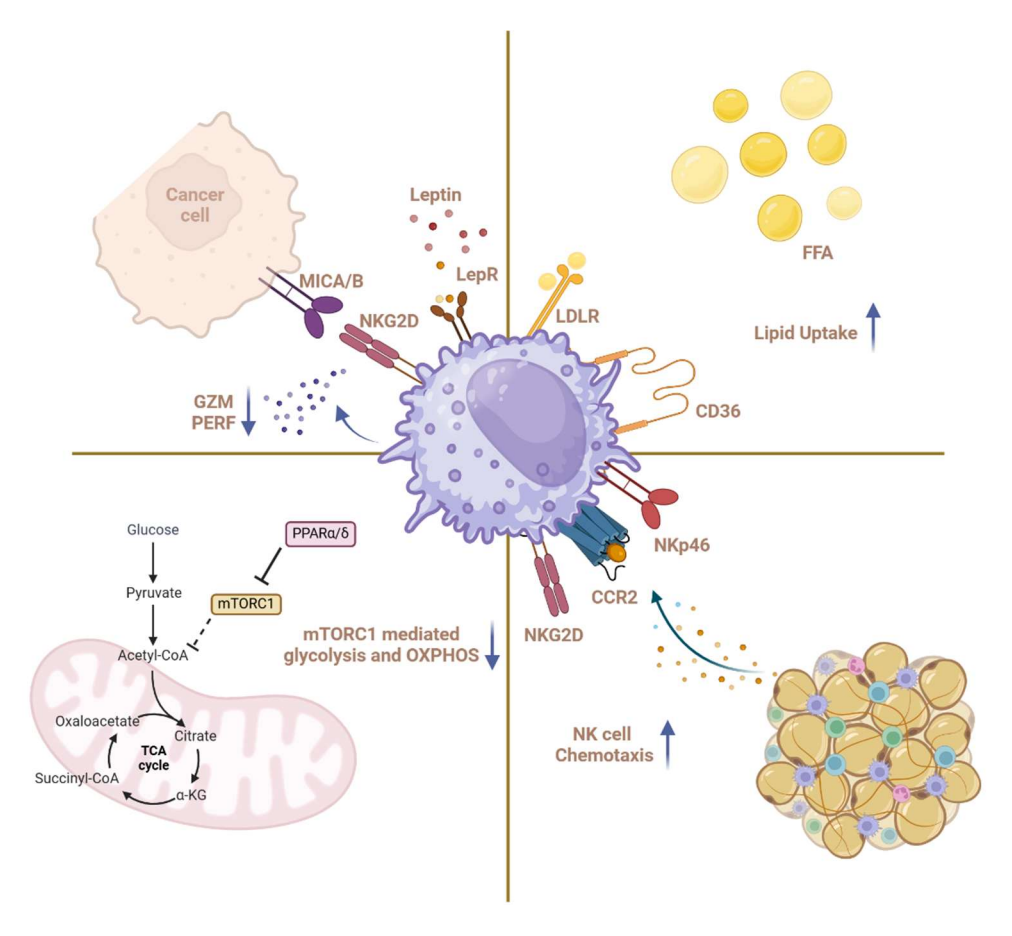


Figure 3 Phenotypically and functionally adaptation of NK cell in obesity. a, impaired NK cell cytotoxicity mediated by Leptin signaling pathway; b, Increased lipid uptake in NK cells; c) Metabolic reprogramming of NK cells through PPARα/δ-mTORC1 pathway; d, upregulation of NK cell chemotaxis and activating receptor in obese environments. Created with BioRender.com. Adapted from (de Andrade et al. 2025).

Understanding these complex interactions has led to the development of various therapeutic strategies aimed at restoring NK cell function in obesity. These approaches include metabolic interventions targeting specific pathways, structured exercise programs designed to enhance NK cell activity, and dietary interventions focused on reducing inflammation and improving metabolic health (Syed et al. 2024). Novel immunotherapeutic approaches are also needed to specifically

target NK cell dysfunction in obesity in combination with lifestyle intervention (Riggan et al. 2021). In this project, we establish an obesity mimic microenvironment in vitro to investigate the modification and regulatory of obesity associated NK cell, providing a better understanding of interactions between obese micro-environment and NK cell.

2.5 Research hypothesis and objective

From our previous research, we identify an expanding subset of NK cell population which is induced under high fat diet. Those NK cell play a vital role in developing insulin resistance as well as systemic meta-inflammation (Theurich et al. 2017). So, we hypothesize that high-lipid culture conditions in vitro will enlarge this NK cell subset and significantly alter the differentiation, metabolic profile, and functional properties of NK cells compared to normal condition. Specifically, high-lipid environments may induce phenotypic changes, impair mitochondrial metabolism, reduce cytotoxic activity, and modulate transcriptional programs in NK cells, ultimately affecting their immune surveillance and effector functions. Understanding these changes will provide insights into how lipid metabolism influences NK cell biology and its implications for immune responses in metabolic disorders such as obesity. The objectives of this project are as followed: 1, phenotypic characterization: to compare the surface marker expression and differentiation status of NK cells cultured under high-lipid and normal lipid conditions; 2, metabolic profiling: to assess the impact of high-lipid conditions on mitochondrial metabolism, including mitochondrial membrane potential, reactive oxygen species (ROS) production, and oxidative phosphorylation (OXPHOS) activity in NK cells; 3, functional analysis: to evaluate the cytotoxic capacity of NK cells under both conditions using in vitro killing assays against target cells; 4, transcriptional profiling: to perform single-cell RNA sequencing (scRNA-seq) to uncover differentially expressed genes and pathways in NK cells under high-lipid versus normal conditions, identifying key molecular mechanisms driving phenotypic and functional changes; 5, integration of findings: to correlate phenotypic, metabolic, functional, and transcriptional data to provide a comprehensive understanding of how obese conditions modulate NK cell biology. By addressing these objectives, this study aims to elucidate the effects of lipid metabolism on NK cell differentiation and function, contributing to a deeper understanding of the interplay between metabolism and immunity in health and disease.

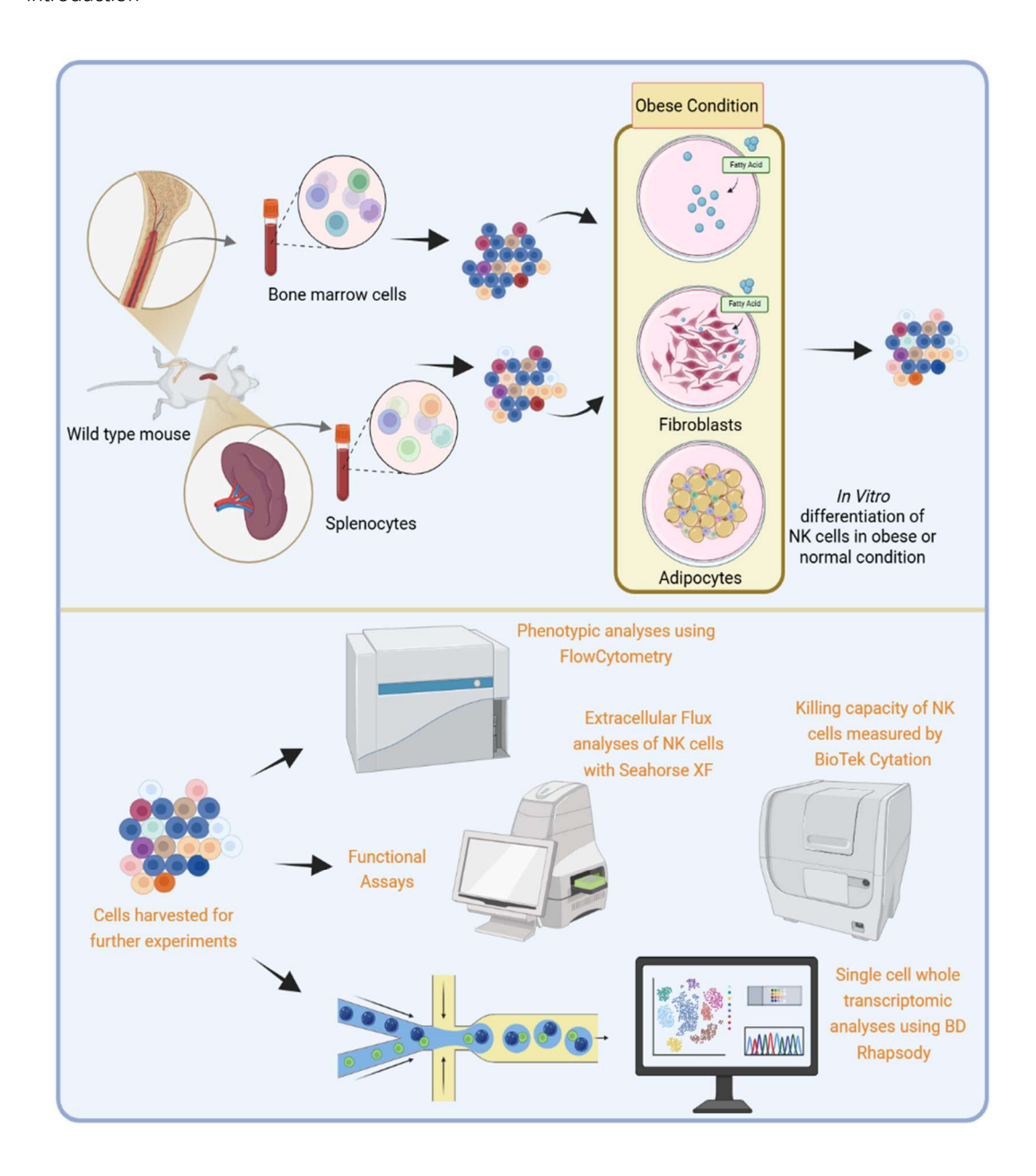


Figure 4 Schematic presentation of project objectives. Establish the In Vitro NK cell differentiation protocol under obese and normal condition. NK cells are collected for further experiments including phenotypic analysis, metabolic stress test and single cell RNA sequencing to characterize their profile and regulatory pathway. Created with BioRender.com.

Materials and Methods

3.1 Compounds

Compound	Manufacturer	Catalog ID
100X Non-Essential Amino Acids	Thermo Fisher	11140050
2-DG	Sigma Aldrich	D8375
Agencourt AMPure XP magnetic beads	Beckman	A63880
	Coulter	
Antimycin A	Sigma Aldrich	A8674
Beta-Mercaptoethanol	Sigma Aldrich	M6250
BSA	Car Roth	284.3
BD Stain Buffer	BD	554656
	Biosciences	
BD Mouse Immune Single-Cell Multiplexing	BD	633793
Kit	Biosciences	
BD Rhapsody Enhanced Cartridge Reagent Kit	BD	664887
	Biosciences	
BD Rhapsody cDNA Kit	Biosciences	633773
BD Rhapsody cDNA Kit		633773
BD Rhapsody cDNA Kit BD Rhapsody WTA Amplification Kit	BD	633773
	BD Biosciences	
	BD Biosciences BD	633801
BD Rhapsody WTA Amplification Kit	BD Biosciences BD Biosciences	633801
BD Rhapsody WTA Amplification Kit Calcein AM	BD Biosciences BD Biosciences Thermo Fisher	633801 C1430
BD Rhapsody WTA Amplification Kit Calcein AM CellROX Deep Red	BD Biosciences BD Biosciences Thermo Fisher Thermo Fisher	633801 C1430 C10491
BD Rhapsody WTA Amplification Kit Calcein AM CellROX Deep Red CellTrace Blue	BD Biosciences BD Biosciences Thermo Fisher Thermo Fisher Thermo Fisher	633801 C1430 C10491 C34568

Dexamethasone	Jenapharm	08704321
D-Glucose min 99,5% CELLPURE	Carl Roth	HN06.1
Dimethyl sulfoxide	Sigma Aldrich	D2650
DMEM	PAN-Biotech	P04-05550
DRAQ7	BD	564904
	Pharmingen	
Dead Cell Removal Kit	Miltenyi Biotic	130090101
eBioscience™ UltraComp eBeads	Thermo Fisher	1-2222-41
EDTA	AppliChem	A1103
Ethanol Absolute >99,8%	Carl Roth	9065.1
Fetal Bovine Serum	Gibco	A5256701
FCCP	Sigma Aldrich	C2920
Fixation Buffer	Biolegend	420801
Human Insulin (100 I.E.)	Lilly	HI0210
HEPES Buffer 1M	PAN Biotech	P05-01100
IBMX	Biomol	AG-CR1-
		3512-M500
Intracellular Staining Permeabilization Wash	Biolegend	421002
Buffer (10x)		
Ionomycin Calcium Salt	Peprotech	5608212
L-Glutamine	Car Roth	HN08.2
MitoSOX Green	Thermo Fisher	M36006
MitoTracker Red FM	Thermo Fisher	M22425
MitoTracker™ Green FM Dye	Thermo Fisher	M46750
MojoSort Mouse Hematopoietic Progenitor	Biolegend	480004
Cell Isolation Kit		
MojoSort Mouse NK Cell Isolation Kit	Biolegend	480050

MojoSort Mouse CD3 Selection Kit	Biolegend	480100
Nuclease-Free Water	Thermo Fisher	AM9937
Oligomycine	Sigma Aldrich	495455
Oil red O staining solution	Sigma Aldrich	1024190250
PBS	PAN Biotech	P04-36503
Penicillin/Streptomycin	PAN Biotech	P06-07100
Phorobol 12-myristate 13-acetate (PMA)	Peprotech	1652981
Poly-D-Lysine	Santa Cruz	11131D
Recombinant Mouse Interleukin 2	Immunotools	12340027
Recombinant Mouse Interleukin 7	Immunotools	12340075
Recombinant Mouse Interleukin 15	Immunotools	12340155
Recombinant Mouse FLT-3L	Immunotools	12343303
Recombinant Mouse SCF	Immunotools	12343325
Rotenone	Takara	T100B
RPMI 1640, w: L-Glutamine, w: 2.0g/L NaHCO3	PAN Biotech	P04-16500
Seahorse XFE96 FluxPak	Agilent	102416-100
Sodium Pyruvate (100 mM)	Gibco	11360070
True-Nuclear transcription factor buffer	Biolegend	424401
Trypan Blue Stain (0.4%)	Invitrogen	T20282
XF RPMI Medium PH 7.4, 1mM HEPES	Agilent	103576
Zombie UV Fixable Viability Kit	Biolegend	423108

3.2 Antibodies

Antibody	Clone	Manufacturer	Catalog ID
Alexa Fluor 488 anti-mouse	M1/70	Biolegend	101217
CD11B			

Alexa Fluor 488 anti-mouse CD3	17A2	Biolegend	100212
Alexa Fluor 488 anti-mouse NK1.1	PK136	Biolegend	108718
Alexa Fluor 700 anti-mouse CD19	6D5	Biolegend	115528
Alexa Fluor 700 anti-mouse CD45	A20	Biolegend	110724
Alexa Fluor 700 anti-mouse NK1.1	PK136	Biolegend	108730
APC anti-mouse CD115	AFS98	Biolegend	135510
APC anti-mouse CD126	D7715A7	Biolegend	115811
APC anti-mouse Sca1	D7	Biolegend	108112
APC/Cy7 anti-mouse CD11b	M1/70	Biolegend	101226
APC/Cy7 anti-mouse F4/80	BM8	Biolegend	123118
Biotin anti-mouse NK1.1	PK136	eBioscience	135941-82
Brilliant Violet 421 anti- mouse CD3	17A2	Biolegend	100228
Brilliant Violet 421 anti- mouse CD45	30-F11	Biolegend	103134
Brilliant Violet 510 anti- mouse CD27	LG.3A10	Biolegend	124229
Brilliant Violet 785 anti- mouse CD69	H1.2F3	Biolegend	104543
FITC anti-mouse CD127	LG.3A10	Biolegend	124207

FITC anti-mouse F4/80	BM8	Biolegend	123108
FITC anti-mouse KLRG1	2F1	Biolegend	138410
PE anti-mouse CD126	M24	Biolegend	363406
PE/Cy7 anti-mouse CD117	2B8	Biolegend	105814
PE/Dazzle 594 anti-mouse	H1.2F3	Biolegend	104536
CD69			
PerCP/Cy5.5 anti-mouse	RA36B2	Biolegend	103236
CD45			

3.3 Technical devices

Device	Manufacturer
Agilent 4200 Tapestation System	Agilent Technologies
BD Rhapsody Scanner	BD Biosciences
BD Rhapsody Express Instrument	BD Biosciences
BD Rhapsody P1200M pipette	BD Biosciences
BD Rhapsody P5000M pipette	BD Biosciences
BioTek Cytation 1 Cell Imaging Multimode	BioTek/Agilent
Reader	
CelldropFL Cellcounter	Biozym
Centrifuge 5424 R G	Eppendorf
Centrifuge 5910 R G	Eppendorf
Centrifuge Rotina 420R	Hettich GmbH
CO ₂ -Incubator (BD6220)	Heraeus, Thermo Fischer
	Scientific
Cytoflex LX MPL	Beckmann Coulter

DS11FC+ Spektrophotometer	Biozym
Multi-Detection Reader Cytation 1	Biotek/Agilent
Qubit 3.0 Fluorometer	Thermo Fischer Scientific
Seahorse XFe96 Analyzer, S7800A	Agilent Technologies
T100 thermal cycler	Biorad
Thermomixer C	Eppendorf
Thunder Imager 3D	Leica

3.4 Cell lines

Cell lines used in experiments were 3T3-L1 and MC38. 3T3-L1 is a fibroblast cell line that was isolated from the embryo of a mouse (Rizzatti et al. 2013). The MC38 cell line is an established and well-characterized cellular model for colorectal cancer deriving from a female C57BL/6 mouse (Schrors et al. 2023). 3T3-L1 cells were kindly provided by Professor Djabali, TUM School of Medicine and Health. The MC38 cell line was kindly provided by Professor Per Thor Straten, Herlev Hospital of Copenhagen University. Both cell lines were cultivated in 10% FBS (Thermo Fisher), +1% Penicillin/Streptomycin (Pan Biotech) + Dulbecco's Modified Eagle's Medium (Pan Biotech) and maintained at a concentration of 500,000 cells/mL. Cell lines were cultured in a humidified CO_2 (5%) incubator at 37°C.

3.5 Differentiation of 3T3-L1 cell line into adipocyte

To differentiate 3T3-L1 fibroblasts into adipocytes, cells are first cultured in DMEM supplemented with 10% calf serum and maintained at 37°C with 5% CO_2 until they reach 80% full confluence (approximately 2-3 days). Differentiation is then induced (Day 0) by replacing the medium with DMEM containing 10% FBS, 10 μ g/mL insulin, 0.5 μ M dexamethasone, and 0.5 mM IBMX, followed by incubation for 48 hours. On Day 2, the medium is replaced with DMEM containing 10% FBS and 10 μ g/mL insulin only, and refreshed every two days. Cells are maintained under these conditions until Day 8-10, when lipid droplets become visible,

indicating successful differentiation. Differentiation is validated by Oil Red O staining to detect lipid accumulation.

3.6 BD Rhapsody single cell whole transcriptome Analysis

Collect all the bone marrow derived cells after 16 days differentiation in vitro for Single-cell RNA transcriptome analysis using the BD Rhapsody system, filtered through a 40 µm strainer, and counted to ensure high viability (>85%), followed by dead cell removal (Dead Cell Removal Kit from Miltenyi Biotic). The cell suspension is then loaded into the BD Rhapsody cartridge, allowing single-cell capture in microwells containing barcoded beads via gravitybased settling, after which unbound cells are washed away (BD Single cell Labeling Protocol). Following cell lysis, mRNA is captured on barcoded beads and reverse-transcribed into cDNA, which is subsequently amplified using the BD Rhapsody system (BD Single cell capture and cDNA synthesis protocol). Whole transcriptome amplification is performed afterwards, followed by enzymatic fragmentation, end repair, and adapter ligation to generate sequencing libraries (BD WTA library preparation protocol). Quality control is performed using TapeStation to assess fragment size, while quantification is done via qPCR or fluorometric assays before sequencing on an Illumina platform, typically targeting 50,000 reads per cell. The sequencing data is processed using Seven Bridges pipeline for demultiplexing, barcode error correction, and quality filtering. Further downstream analysis, including normalization, clustering, differential gene expression, and cell-type annotation, is conducted with tools Seurat, enabling detailed transcriptomic insights at the single-cell level.

3.7 Isolation of murine bone marrow cells

The 8 to 12-week-old C57BL/6 WT mouse is euthanized and disinfected in the hind limbs with ethanol before dissecting the femur and tibia. To collect the bone marrow cells (BMCs), the bones are cleaned of muscle tissue and placed in cold PBS. Both ends of the bones are cut, BMCs are flushed out with cold PBS using a syringe and passed through a 70 μ m cell strainer to remove debris. The cell suspension is centrifuged at 300 × g for 5 minutes, and the pellet is resuspended in red blood cell lysis buffer (BioLegend) for 1-2 minutes to remove the

erythrocyte. After another centrifugation and washing step in 1xPBS, cells are counted and resuspended with the concentration of 1,000,000 cells/mL in the RPMI 1640 complete medium (NK basal medium) supplemented with 10% FBS (Gibco), 1mM sodium pyruvate (Gibco), 1mM HEPES (PAN Biotech), 1x nonessential amino acid (Thermo Fisher), 1% Penicillin-Streptomycin (Pan Biotech), 0.1mM Beta-Mercaptoethanol (Sigma Aldrich) for NK cell induction.

3.8 Isolation of murine splenocytes

8 to 12 weeks old wild type mouse (C57BL/6) were sacrificed and spleens were harvested, then dissociated through a 70µm cell strainer. Erythrocytes were lysed by incubating the cell suspension in erythrocyte lysis buffer (BioLegend) for 1-2 minutes. Following lysis, cells were washed with 1X PBS and resuspended in NK basal medium then used for further experiments.

3.9 Differentiation of BMCs into NK cells

Isolated BMCs were cultivated in NK basal medium in a density of 500,000-1,000,000 cells/mL. To differentiate them towards NK cells, from day 1 to day 8, IL-7 20ng/mL, SCF 50ng/mL, Flt3L 50ng/mL were added in the medium and cells were kept in a humidified CO2 (5%) incubator at 37°C, medium is refreshed every 2-4 days according to the PH value. Since day 9, change the medium to NK expansion medium (NK basal medium + IL-2 500U/mL + IL-15 50ng/mL). Throughout the 16-day in vitro differentiation cycle of NK cells, the feeder layer cells should be replaced in a timely manner based on their condition, typically every 3-5 days. During replacement, all cells are resuspended using a pipette, passed through a 70μ m strainer, and then collected and transferred to a new culture dish with fresh feeder cells. At last days, fully resuspended all the cells and passed through 70μ m strainer, collected cells for further experiments.

3.10 Flow cytometry

Flow cytometry was applied to characterized bone marrow and NK cell phenotypes in vitro with the combination of fluorescent antibodies. The Fc receptors were blocked using TruStain FcX (10 µg/ml, Biolegend) for 10 minutes at room temperature before extracellular and viability staining. Cells underwent 20-minute incubation at 4°C in FACS buffer containing 2.5 µg/ml fluorophore conjugated antibodies or isotype control and Zombie UV Live/Dead dyes according to specifications. CellROX Deep Red and MitoSOX Green (2 µM, Thermo), MitoTracker Red FM and MitoTracker Green (5 µM, Thermo) staining occurred alongside antibody labeling. After washing, cells were suspended in 100-200 µL FACS buffer (PBS, 0.1% BSA, 0.5 mM EDTA) for immediate assessment or FACS Fix (FACS buffer with 3% formaldehyde) for delayed analysis. Flow cytometry data were acquired on CytoFLEX LX (Beckman Coulter GmbH) and analyzed in FlowJo 10.8.1.

3.11 Seahorse real-time cell metabolic analysis

Magnetic sorted NK Cells were cultivated in NK basal medium with 20U/ml IL-2 for 6 hours. Following PBS washing, cells underwent resuspension in respective media: Mito Stress Test Medium (Seahorse XF RPMI containing 5mM Glucose, 2mM L-Glutamine, Agilent) Glycolysis or Stress Test Medium (Seahorse XF RPMI supplemented with 2mM L-Glutamine, Agilent). Poly-L-Lysine precoated (0.05mg/ml) Seahorse cell culture microplates received 200,000 cells per well for subsequent metabolic flux analysis via Seahorse XF analyzer, with Wave Desktop 2.6 facilitating data interpretation. Sequential reagent administration for Mito Stress Test comprised: A. 1.5µM Oligomycin (Sigma Aldrich), B. 1µM FCCP (Sigma Aldrich), C. 0.5µM Rotenone/ Antimycin A (Sigma Aldrich) plus 8µM Hoechst (ThermoFisher). Glycolysis Stress Test also consisted of three injections including A. 5mM Glucose (Roth), B. 1.5µM Oligomycin (Sigma Aldrich), C. 50mM 2-DG (Sigma Aldrich) with 8µM Hoechst (ThermoFisher). Flux assessment protocol comprised triple baseline measurements succeeded by injection A to C with three measurement cycles respectively. Individual measurement cycles incorporated 3 minutes mixing periods followed by 3 minutes measurement intervals. Normalization methodology employed Hoechst-based cell quantification via BioTek Cytation1 analyzer (Agilent) utilizing cell measurement software Gen5 Microplate Reader (Agilent).

3.12 Cytation-based NK cell killing assay

To measure the killing capacity of NK cells, NK cells were enriched by CD3 negative, NK1.1 positive magnetic cell sorting and subsequently cultivated in NK basal medium with IL-2 20U/mL. To perform the real-time NK cell killing assay, MC38 target cells were Hoechst3342 (ThermoFisher) and Cell Trace Far Red (ThermoFisher) stained (10µM) at 37°C, for 15 min, washed and seeded at 30,000 cells per well in NK medium for 4h. NK cells were then stained (10µM) with Cell Trace CFSE (ThermoFisher) in PBS at room temperature for 20 min, washed and resuspended in NK basal medium with IL-2 20U/mL. Then effector cells (NK cells) were co-cultivated with target cells (MC38) at 5:1 effector to target (E/T) ratios. The confluency of target cells was monitored with Cytation for 4 days and images were taken every 1.5h.

3.13 Single-cell transcriptomics: data analysis

Initial dataset preprocessing employed Seurat methodology for cellular origin identification, with subsequent exclusion of multiplets (exhibiting multiple hashtag positivity) and hashtagnegative cells. Computational workflow implementation adhered to developer-provided protocols (https://satijalab.org/seurat/v3.1/hashing_vignette.html). During pre-processing, quality control filtering was also performed with exclusion of cells with high mitochondrial transcripts content. To correct for potential batch effects and technical differences in sequencing, data obtained from different libraries pooled for analysis were batch-corrected using Harmony. Clustering was performed using the "FindClusters" function in Seurat. The number of clusters obtained using "FindClusters" in Seurat depends on the so-called "resolution" parameter, which needs to be adjusted to avoid under- or over-clustering. To fully uncover cell transcriptional state heterogeneity while avoiding generating "false heterogeneity" with poorly defined cell clusters, we performed iterative clustering analysis with increasing resolutions, and examined differential gene expression across clusters using heatmaps. Pseudo-time analysis was performed in Monocle v2.8 (Qiu et al. 2017). Differentially expressed genes were determined using the differential GeneTest function in Monocle. Statistical analysis was performed via one-way ANOVA followed by Tukey's test for multiple comparison. Adjusted p values <0.05 were considered statistically significant.

3.14 Statistical analysis

Statistical analyses were conducted using GraphPad Prism (versions 9.5 to 10.0). For comparisons between two groups, either the student's t-test was used, depending on the normality of the data. For multiple group comparisons, one-way or two-way analysis of variance (ANOVA) was performed with Brown-Forsythe and Welch corrections. Data are reported as mean \pm SEM or median with 95% confidence intervals (CIs). Statistical significance was defined as p < 0.05. Statistical significance was represented as *<0.05, **<0.01, ***<0.001 and ****<0.0001.

3.15 Software

Software

CytExpert 2.3	Beckmann Coulter
LAS X Office	Leica Microsystem
Wave Desktop	Agilent
lmageJ	National Institutes of Health (NIH)
FlowJo™ 10.7.1-10.8.1	BD
R-Studio	Open Source
GraphPad Prism 9.5 – 10.0	Graphpad Software, Inc

Results

4.1 Establishment of a NK cell differentiation model from murine hematopoietic stem/progenitor cell *in vitro*

As described previously, NK cells are derived from Lin⁻Sca-1⁺c-Kit⁺ (LSK) hematopoietic stem cells and undergo differentiation via precursor NK cells in bone marrow through sequential acquisition of functional surface receptors (Yang et al. 2005). In general, differentiation of NK cells from HSC is largely divided into two-stages, lineage committed differentiation of NK precursor and expansion of mature NK. To induce the in vitro differentiation of murine HSC into NK cells, we established a 16-day differentiation model. This model utilizes SCF, FLT3 to expand the HSC pool, IL-7 to promote differentiation into common lymphoid progenitors (Kumar et al. 2017), and IL-15, IL-2 in the later stages to drive NK cell differentiation and expansion (Ali et al. 2015).

4.1.1 Flow cytometry analysis of frequency of HSC, NK cell progenitor and NK cell in murine bone marrow

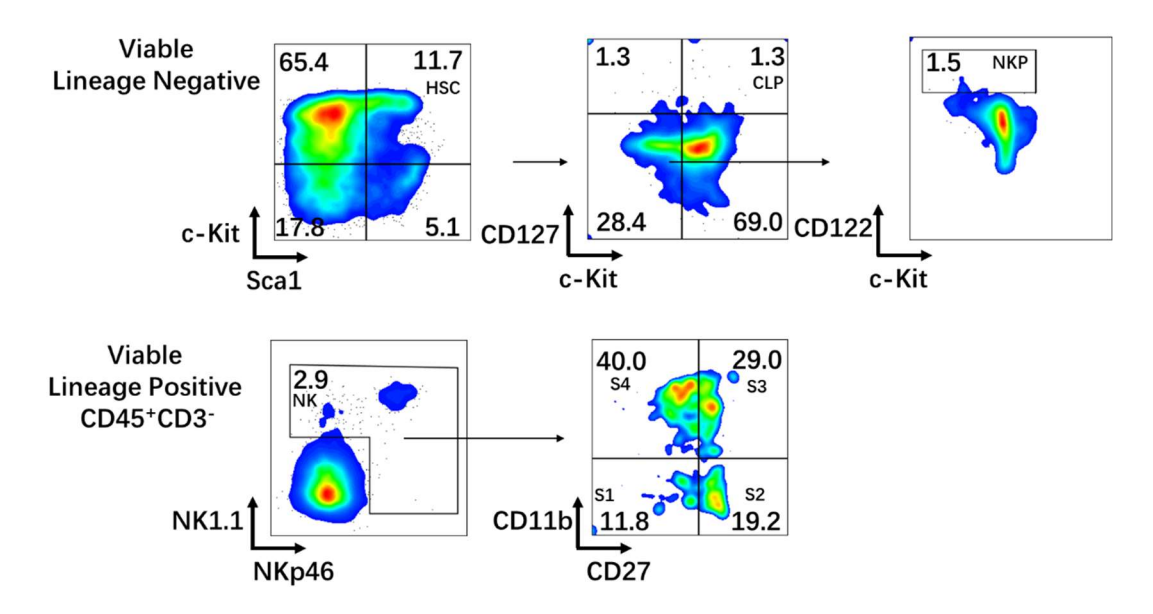


Figure 5 Identification of hematopoietic stem cells, NK cell progenitors, and NK cells in murine bone marrow. Flow cytometry analysis of bone marrow cell populations using multi-color immunofluorescence staining. Viable cells were Zombie UV Live/Dead staining negative, Lineage negative mean CD5, CD45R, CD11b, Ly-6G/C, 7-4, and Ter-119 were all negative. Cell populations were identified based on specific surface marker expression: 1. HSC: gated on Lineage Sca1+ c-Kit+ population; 2. CLP: gated on Sca1+ CD127+ c-Kit+ population, percentage of CLPs indicated in plot; 3. NKP: identified by CD122+

and c-Kit⁻ expression; 4. NK: gated on CD45⁺CD3⁻ population, identified by NK1.1 and NKp46 markers, further subdivided into 4 subsets (S1-S4) based on CD11b and CD27 expression.

Prior to differentiation initiation, we performed flow cytometric analysis to examine HSCs, CLPs, and NKPs in the bone marrow niche of C57/BL6 wild type mice, and identified four distinct maturation stages of NK cells (Figure 5), the gating strategy was shown in figure Sup 1. The results demonstrated that even after hematopoietic stem and progenitor cell enrichment, the bone marrow samples retained only approximately 12% primitive HSCs, with even lower quantities of CLPs and NKPs. Within the lineage positive cell compartment of mouse bone marrow, four distinct NK cell maturation stages S1-S4 were clearly delineated based on CD11b and CD27 expression levels.

4.1.2 Establishing an *in vitro* NK cell differentiation model under the induction of different cytokines

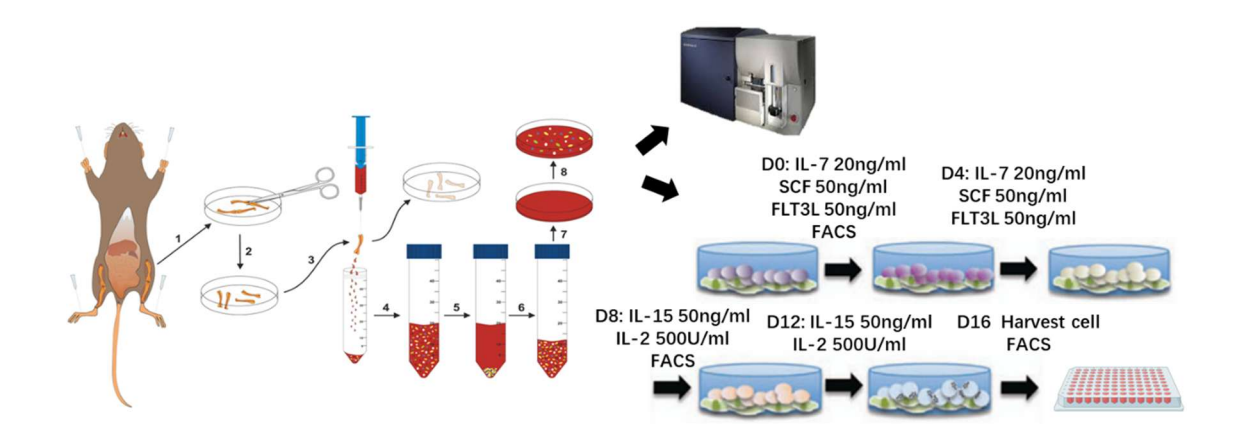
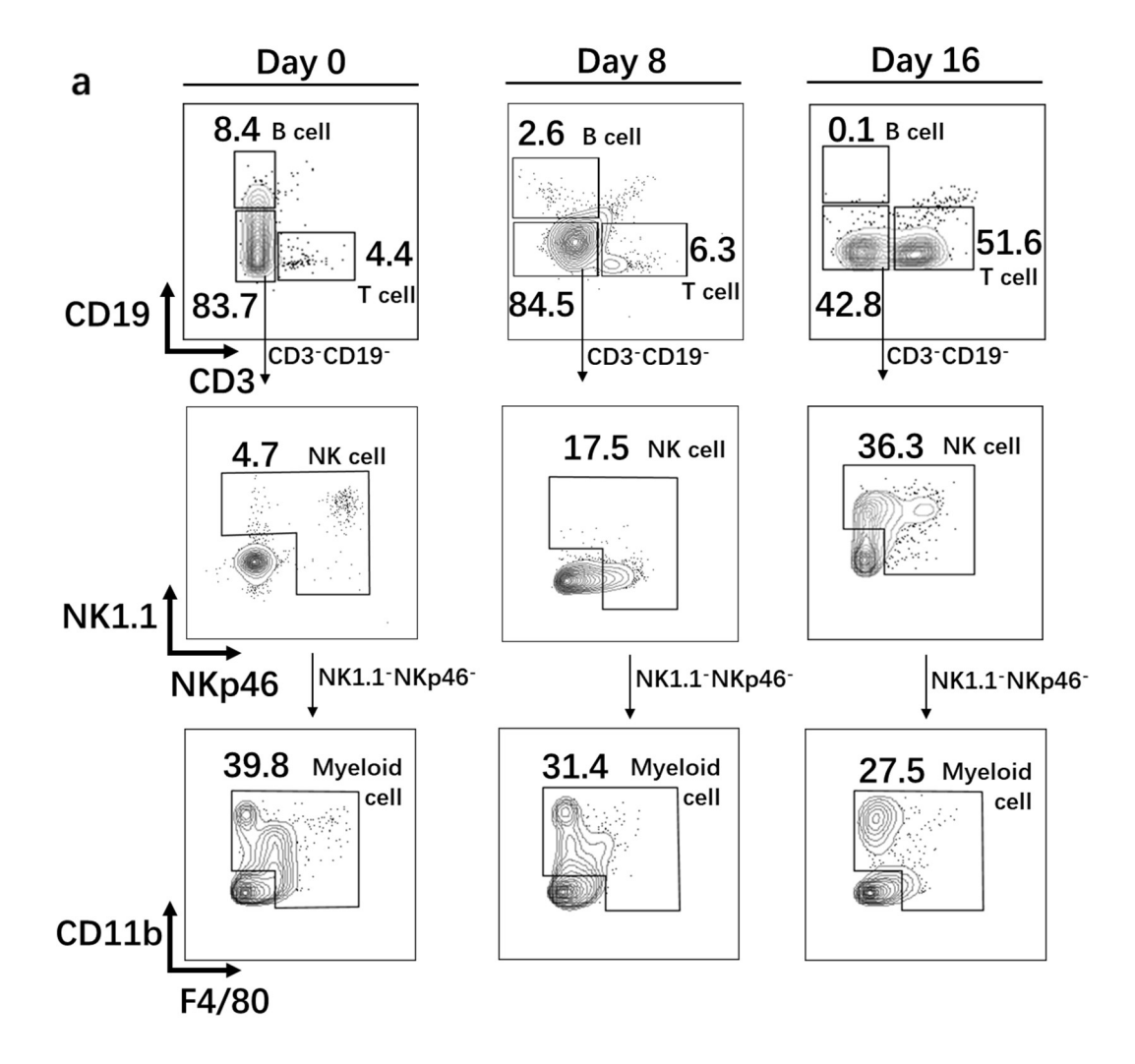


Figure 6 In Vitro NK cell differentiation protocol. Schematic representation of a stepwise in vitro NK cell differentiation protocol from murine bone marrow cells. The experimental workflow demonstrates the sequential cytokine stimulation for generating NK cells:1. Day 0-7: Initial culture setup with cytokine cocktail including IL-7 20ng/ml, SCF 50ng/ml, Flt3L 50ng/ml; 2. Day 8-16: Cytokines switch to IL-15 50ng/ml, IL-2 500U/ml. Multiple FACS analysis applied to track cellular differentiation.

As shown above, in our *in vitro* NK cell differentiation model, we first euthanized mice and isolated the tibia and femur to extract fresh bone marrow cells (Figure 6). These cells were then processed into a single-cell suspension and cultured in RPMI complete medium for 16 days. During the initial 8 days, the culture was supplemented with 20 ng/mL IL-7, 50 ng/mL SCF, and 50 ng/mL FLT3L to promote HSC differentiation and facilitate the expansion of CLPs. In the subsequent 8 days, cytokine supplementation was switched to 50 ng/mL IL-15 and 500 U/mL IL-2 to drive CLP differentiation toward the NK cell lineage and enhance their proliferation.

4.1.3 Analysis of the dynamic changes of lymphoid and myeloid lineages in the model over time

Throughout the differentiation process, we performed flow cytometry analysis at the beginning, on day 8, and at the end of the culture to assess the proportions of myeloid and lymphoid cell populations. The results showed that CD19⁺ B lymphocytes gradually decreased and eventually disappeared as the culture progressed, while the proportions of CD3⁺ T cells and NKP46⁺ or NK1.1⁺ NK cells steadily increased. By the end of differentiation, NK cells accounted for approximately 20% of the total cell population, while myeloid cells, initially the dominant population, decreased to a level comparable to that of NK cells (Figure 7). These findings indicate that under sequential cytokine stimulation, NK cells can be successfully induced from HSCs and expanded in vitro.



Result

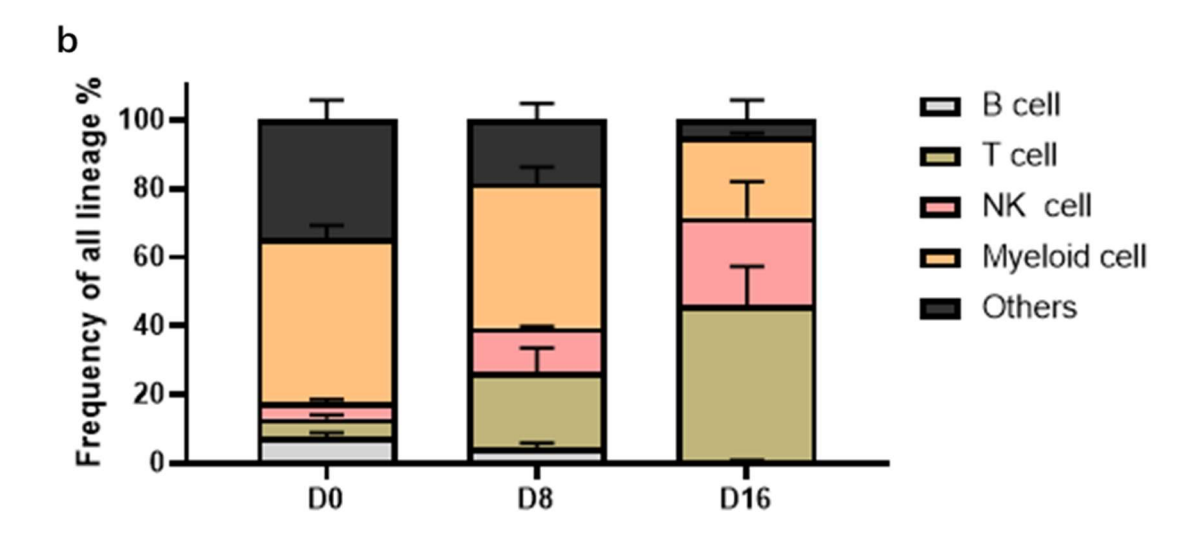
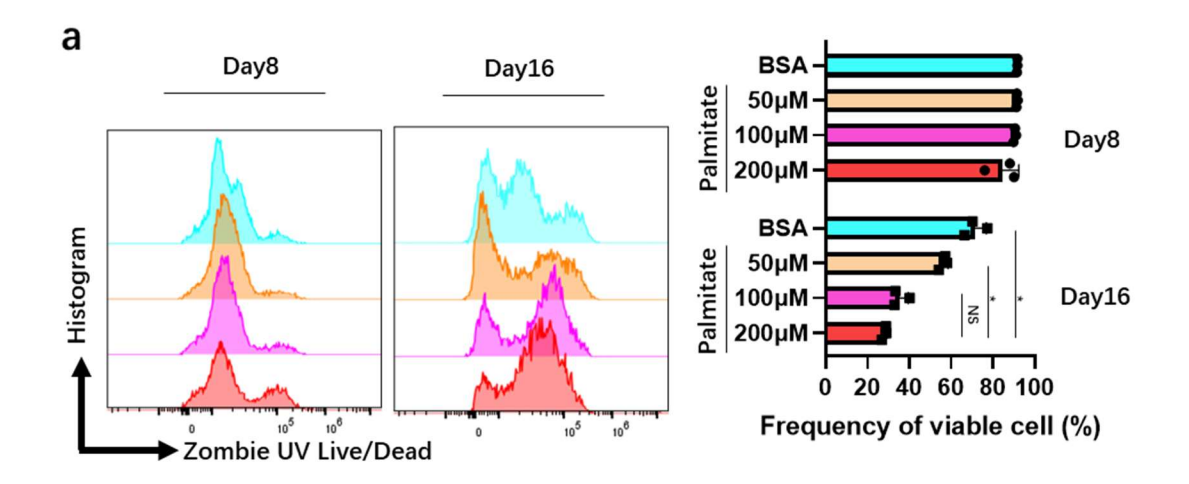


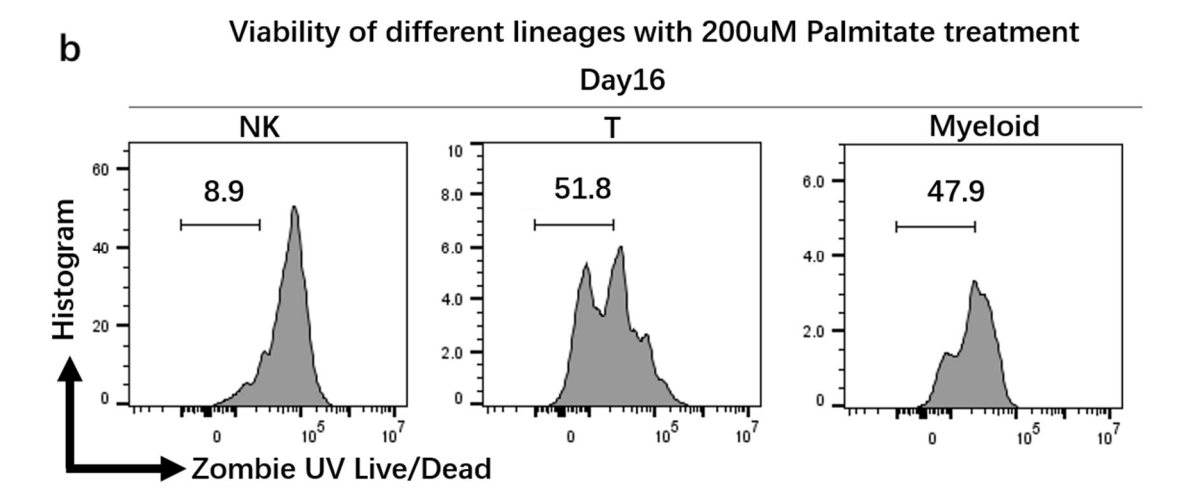
Figure 7 Dynamic changes in lymphoid and myeloid lineage populations during in vitro NK cell differentiation. Flow cytometry analysis tracking the temporal progression of cell lineage composition during NK cell differentiation from murine bone marrow cells, a) all cells are gated on viable (Zombie Live/Dead staining negative) CD45⁺ cells, T cells are identified as CD3⁺ CD19⁻, B cells are gated on CD3⁻ CD19⁺, NK cells are identified CD3⁻CD19⁻ NK1.1⁺ or NKp46⁺, while Myeloid are CD3⁻CD19⁻ NK1.1⁻ NKp46⁻ CD11b⁺ or F4/80⁺; b) quantitative analysis of cell lineage frequencies. Error bars indicate standard deviation from n=3 independent experiments. Plots demonstrate the dynamic shifts in cellular composition during the NK cell differentiation protocol.

4.2 The simulation of obesity condition in the NK cell differentiation model induced by fatty acids

In obese mice and humans, excessive accumulation of saturated fatty acids is commonly observed in peripheral blood and bone marrow, with palmitate being one of the most prevalent saturated fatty acids (Murru et al. 2022). To simulate an obesity-associated differentiation environment *in vitro*, we incorporated varying concentrations of palmitate into the differentiation model to investigate its effects on NK cell differentiation and phenotype.

4.2.1 Dose-dependent cytotoxicity induced by palmitate in different linages within the differentiation model







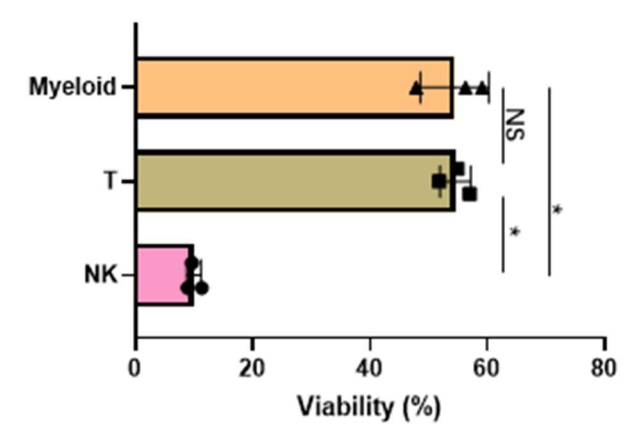


Figure 8 Dose-dependent cytotoxicity of palmitate on different cell lineages during NK cell differentiation. flow cytometry analysis demonstrating the differential cytotoxic effects of palmitate on cell viability at D8 and D16 of NK cell differentiation. BSA: Bovine serum albumin. a) overlaid histograms with viability profiles at increasing palmitate concentrations accompanied by quantifying the frequency of viable cells; b) toxicity of 200µM palmitate across different cell lineages. Error bars represent SD from n=3

independent experiments, statistical significance was calculated by one-way ANOVA and indicated with * (p<0.05) or NS (non-significant).

The accumulation of excessive fatty acid in non-adipose tissues is a hallmark of metabolic disease (Jin et al. 2023). Upon lipid accumulation surpassing cellular storage or oxidative capacity, lipotoxic reaction is triggered, manifesting through organelle membrane disruption, stress pathway induction, and programmed cell death cascades (Brookheart et al. 2009). To determine the optimal palmitate concentration for cell growth, we assessed cell viability on days 8 and 16. The results showed that on day 8, all concentration groups exhibited high cell viability, exceeding 90%. However, by the end of differentiation, palmitate at 100µM and 200µM demonstrated significant cytotoxicity, leading to a substantial decrease in cell viability with statistically significant differences. In the 50µM group, viability was slightly reduced compared to the control group but remained above 60%. Palmitate exhibited differential cytotoxic effects on various cell lineages, with statistically significant differences. Notably, NK cells were the most affected (Figure 8).

4.2.2 Effects of varying palmitate concentrations on the frequency of lineage specific cells in the NK cell differentiation model

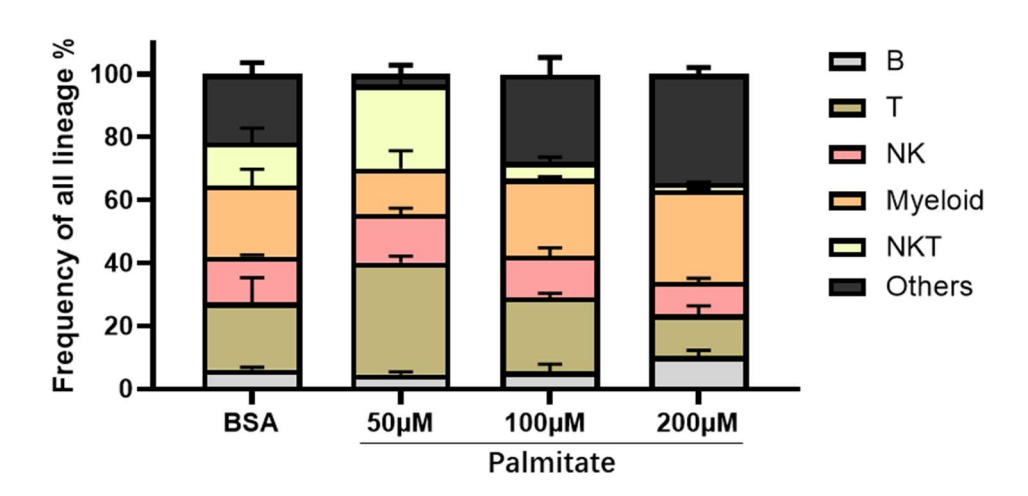


Figure 9 Dose-dependent effects of palmitate on cell lineage composition on D16. stacked bar graph depicting the percentage distribution of cell lineages on Day 16 of NK cell differentiation under varying palmitate concentrations. Error bars indicate SD from n=3 independent experiments.

On day 16 of differentiation, we further analyzed the proportions of various cell lineages in the culture system to determine whether palmitate affects NK cell differentiation and proliferation (Figure 9). The results indicated that, compared to the BSA control group, palmitate did not

directly alter the overall NK cell differentiation trend, with the final proportion of mature NK cells ranging between 10% and 20%. However, at an optimal concentration of 50µM, the proportions of NKT cells and T cells were notably increased.

4.2.3 Dynamic changes of CD36, IL-6R, and CSF1R expression levels across lineage-specific cell populations during differentiation

CD36 functions as a cell surface scavenger receptor abundantly expressed across various immune and non-immune cell types (Y. Chen et al. 2022). It serves as a receptor detecting both pathogen-associated molecular patterns (PAMPs) and damage-associated molecular patterns (DAMPs), while simultaneously facilitating long-chain fatty acid transport (Ma et al. 2024). To investigate whether palmitate induces a meta-inflammatory response and whether it upregulates cellular uptake channels, we examined the expression of CD36 in different cell lineages during differentiation (Figure 10). The results showed that on day 8, NK cells treated with 50µM palmitate exhibited a differential upregulation of CD36 expression on their surface compared to the control group, and this difference was maintained through day 16. In contrast, CD36 expression on the surface of NKT cells decreased following palmitate treatment. Meanwhile, no statistically significant differences in CD36 expression were observed among T cells treated with different concentrations of palmitate.

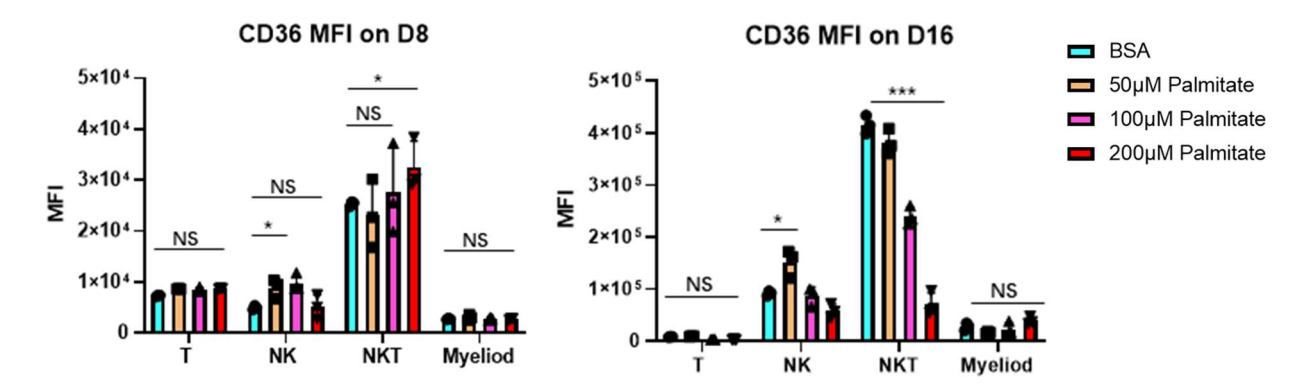


Figure 10 Palmitate-induced CD36 expression variations in different cell lineages, the mean fluorescence intensity of CD36 expression across T, NK, NKT and Myeloid cells under increasing palmitate concentrations at D8 and D16 of cell differentiation. Error bars indicating standard deviation from n=3 independent experiments. Statistical significance was calculated by one-way ANOVA and indicated with * (p<0.05), *** (p<0.001) or NS (non-significant).

In addition to CD36, we also examined two myeloid-associated pro-inflammatory surface receptors, IL6R and CSF1R which are upregulated in high fat diet induced mouse and obese

individuals from our previous results (Theurich et al. 2017). Flow cytometry analysis on D16 of differentiation revealed a significant upregulation in the mean fluorescence intensity of both markers on the surface of palmitate-treated NK cells (Figure 11). However, no such differences were observed among NKT cells and T cells.

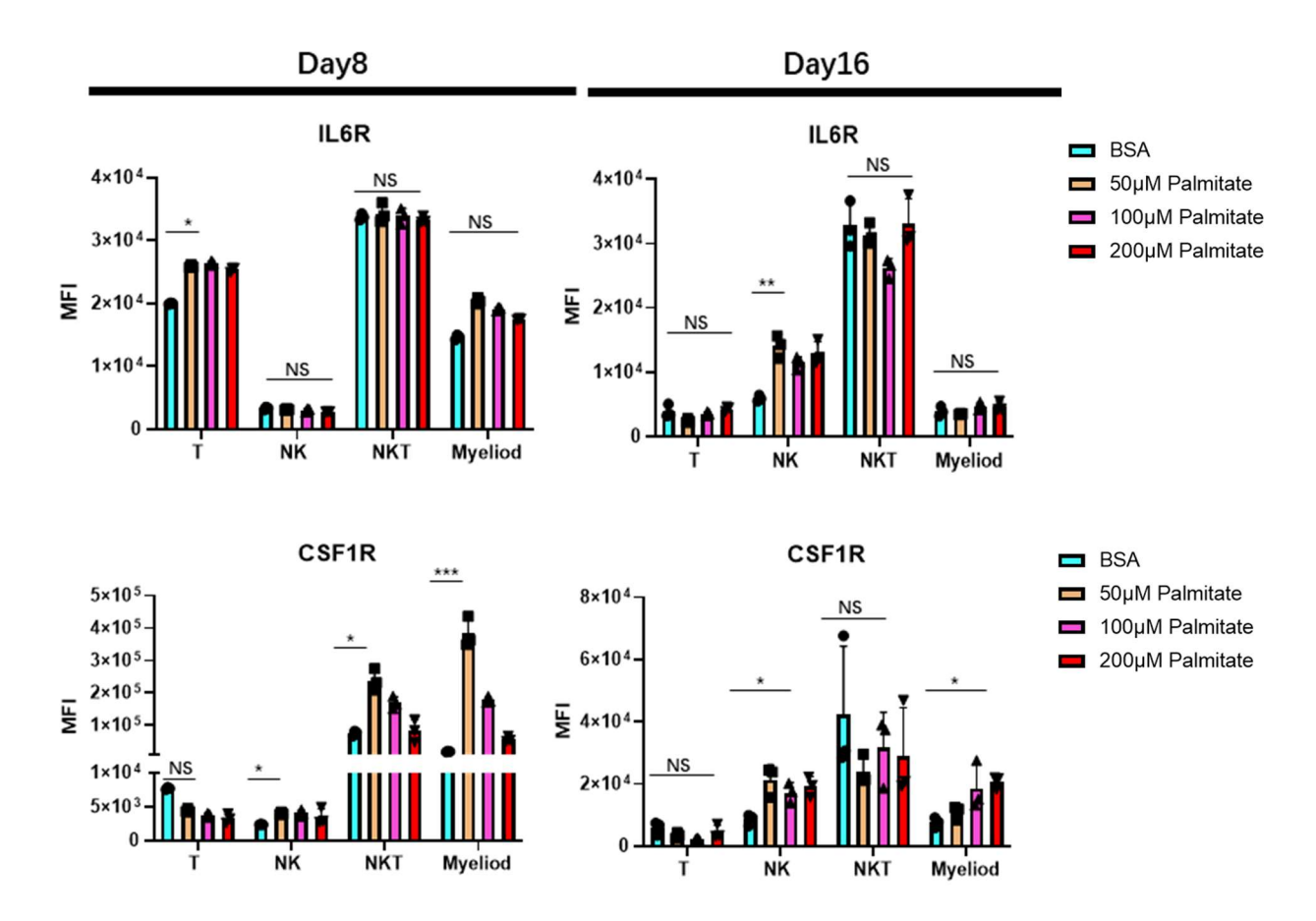
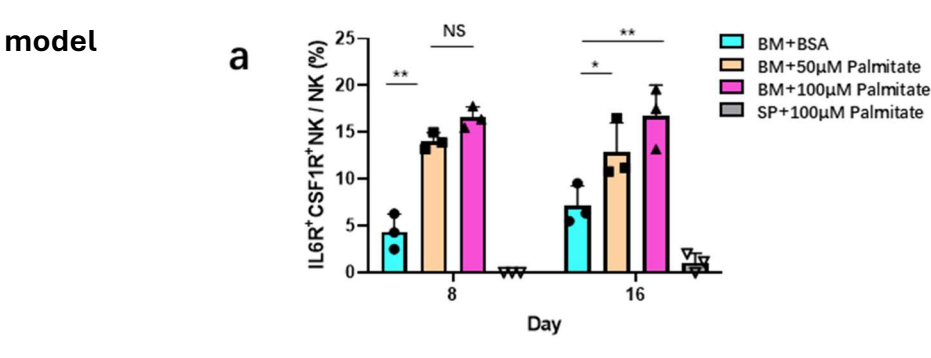


Figure 11 Palmitate-induced IL6R and CSF1R expression variations in different cell lineages. the mean fluorescence intensity of IL6R and CSF1R receptor expression across T, NK, NKT and Myeloid cells under increasing palmitate concentrations at D8 and D16 of cell differentiation. Error bars indicating standard deviation from n=3 independent experiments. Statistical significance was calculated by one-way ANOVA and indicated with * (p<0.05), ** (p<0.01), *** (p<0.001) or NS (non-significant).

4.2.4 Increasing frequency of IL6R⁺ CSF1R⁺ obesity-associated NK cell subsets in the from bone marrow derived palmitate treated differentiation



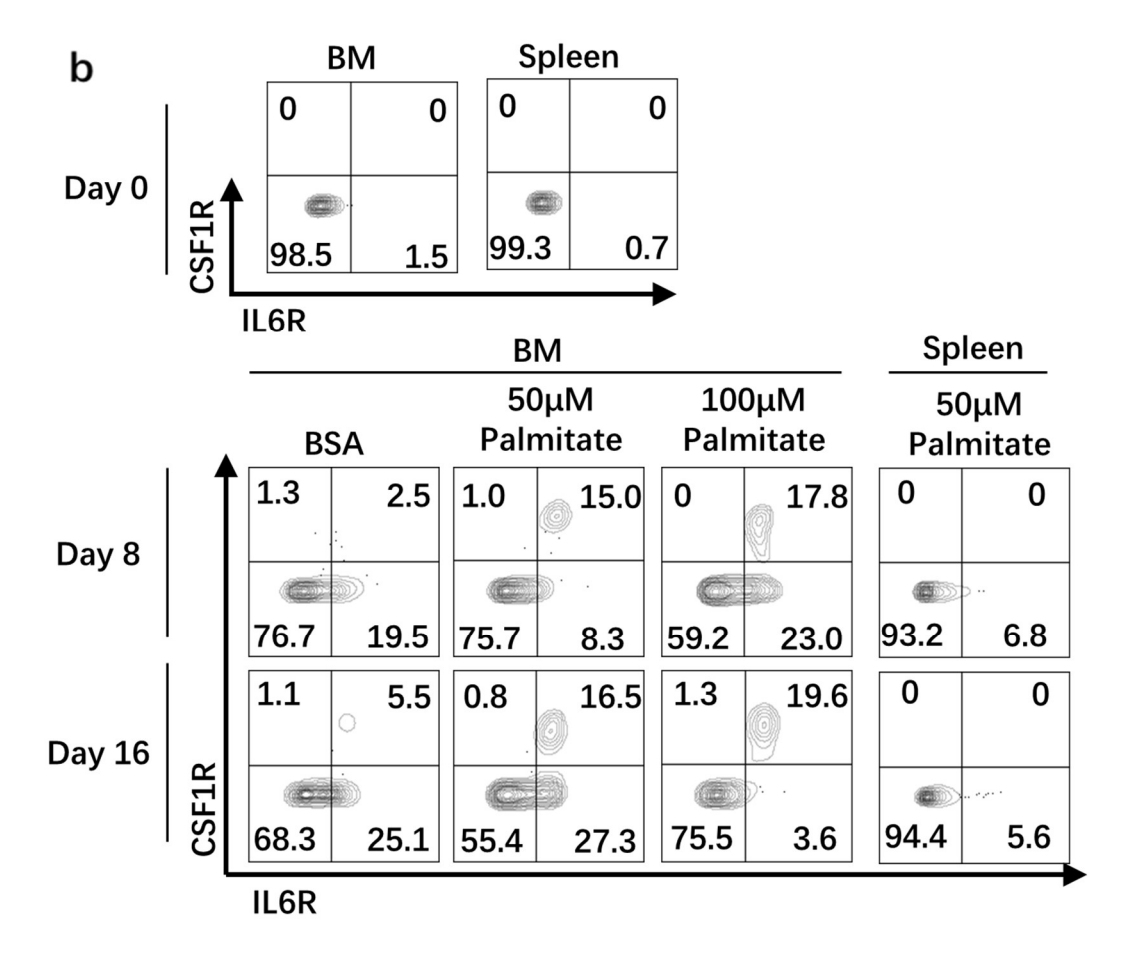


Figure 12 Frequency of bone marrow and spleen derived IL6R and CSF1R positive obesity-associated NK cells. Flow cytometry analysis of the frequency of IL6R and CSF1R double-positive obesity-associated NK cells across different palmitate concentrations on D8 and D16, gated on CD45⁺ CD3⁻ NK1.1⁺ or NKp46⁺ cells. BM: bone marrow; SP: splenocytes; BSA: Bovine serum albumin. a) quantifying the percentage of IL6R⁺CSF1⁺ obesity-associated NK cells, comparing bone marrow and spleen derived across different palmitate concentrations on D8 and D16; b) representative flow cytometry dot plots of IL6R and CSF1R expression in bone marrow and spleen from D0 to D16. Error bars represent standard deviation from n=3 independent experiments. Statistical significance was calculated by one-way ANOVA and indicated with * (p<0.05), ** (p<0.01) or NS (non-significant)

To further investigate whether IL6⁺ and CSF1R⁺ obesity-associated NK cells with a unique phenotype can only be induced through in vitro differentiation from hematopoietic progenitor cells, we used mature NK cells isolated from the mouse spleen as a control and cultured them under the same conditions. As shown in the figure 12, palmitate treatment induced the expression of myeloid-associated markers in bone marrow-derived NK cells, with IL6⁺ and CSF1R⁺ NK cells accounting for 10–20% of the total NK cell population. However, this subset could not be directly induced from mature splenic NK cells.

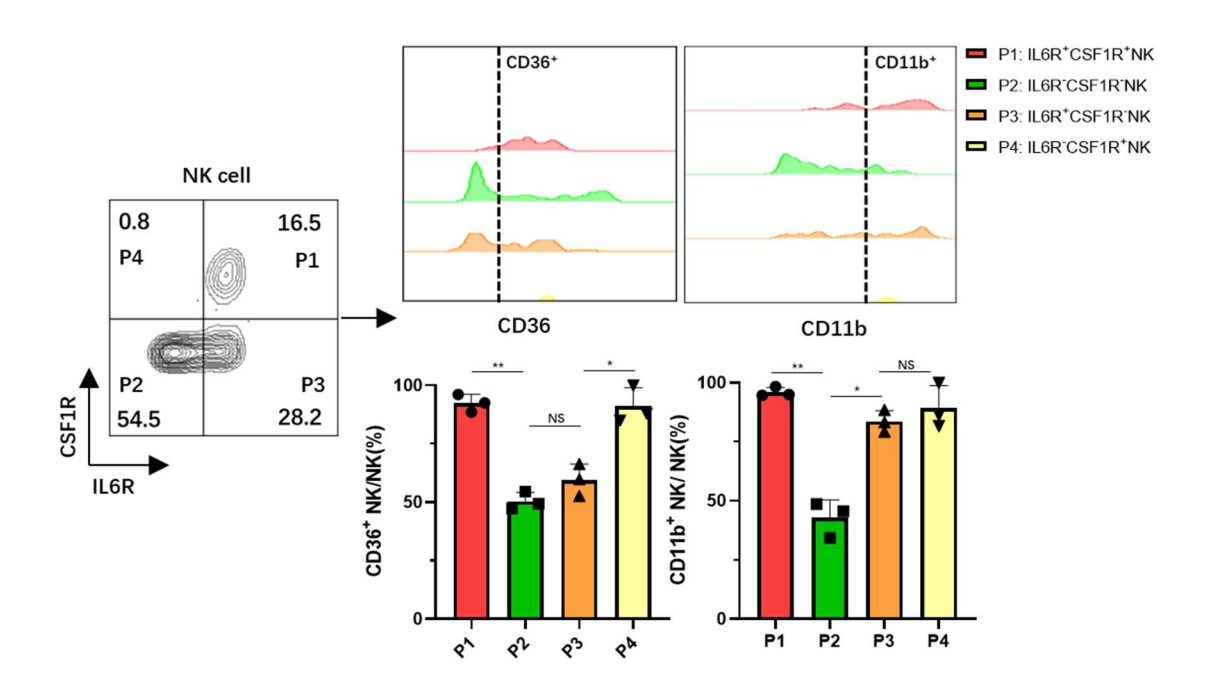


Figure 13 Differential expression of CD36 and CD11b on NK cell subpopulations. Comprehensive flow cytometry histogram revealing the expression patterns of CD36 and CD11b across different NK cell subpopulations based on IL6R and CSF1R expression, NK cells were gated on CD45⁺ CD3⁻ NK1.1⁺ or NKp46⁺ cells; Bar graph shows quantification of the percentage of CD36 and CD11b expression NK cells, with error bars representing standard deviation from n=3 independent experiments. Statistical significance was calculated by one-way ANOVA and indicated with * (p<0.05), ** (p<0.01) or NS (non-significant).

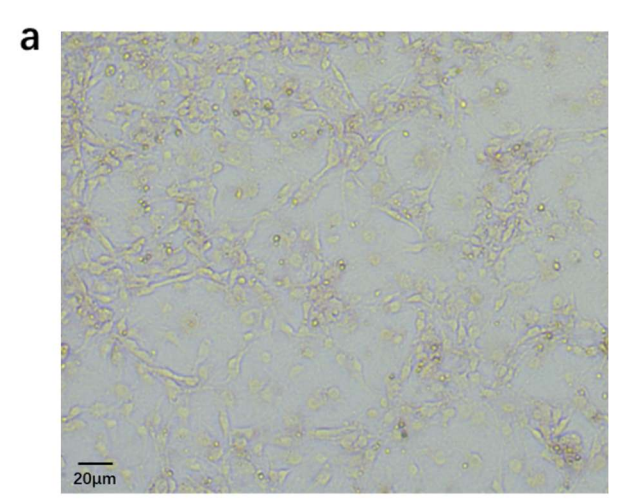
Bone marrow derived NK cells can be classified into four subtypes based on the expression of IL6R and CSF1R. Compared with conventional double-negative NK cells, the obesity-associated NK cells that are either single-positive or double-positive exhibit elevated expression of the fatty acid transporter CD36 as well as NK maturation marker CD11b (Figure 13). The above results indicate that fatty acids can induce the differentiation of HSPCs into NK cells which exhibit phenotypic characteristics similar to those of obesity-associated NK cells isolated from the adipose tissue of obese mice.

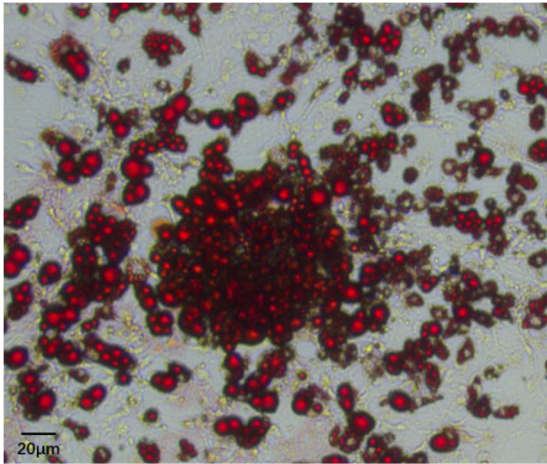
4.3 Simulating obesity conditions through co-culture with adipocytes to investigate the effects on NK cell differentiation and phenotype

To further support the hypothesis that a high-fat microenvironment can induce the development of obesity-associated NK cells, we co-cultured adipocytes derived from fibroblasts with bone marrow stem cells to simulate the in vivo obese microenvironment.

4.3.1 Establishment of an in vitro adipocyte induction and NK cell co-culture differentiation model

Adipocytes were generated from the 3T3-L1 cell line through differentiation induced by specific pharmacological agents (Augustyniak et al. 2024), and the accumulation of lipid droplets within these cells was confirmed by Oil Red O staining (Figure 14a). Mouse bone marrow cells were then added to culture dishes containing either fibroblasts or adipocytes, with mature lymphocytes isolated from the spleen serving as controls (Figure 14b). The cells underwent a 16-day differentiation process, during which flow cytometry analyses were performed at designated time points.





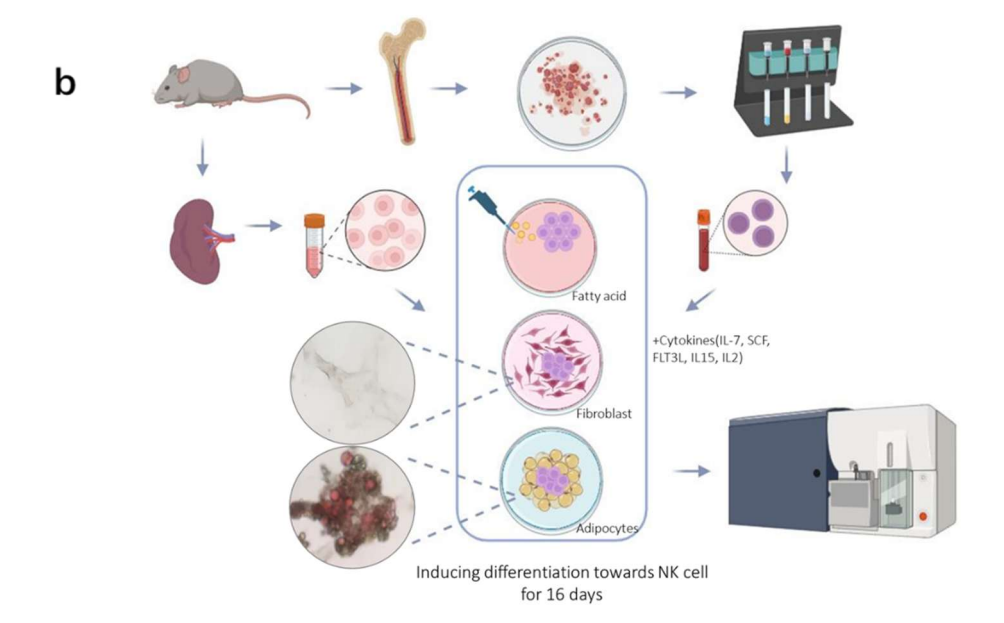


Figure 14 Fibroblast and adipocyte morphology and experimental workflow for NK Cell differentiation in coculture model. a) microscopic images of fibroblasts and 3T3-L1 induced adipocytes, with Oil Red O staining revealing the accumulated lipid droplets in adipocytes; b) experimental setup for murine NK cell differentiation and cultivation from spleen or bone marrow in different coculture condition with adipocytes or Fibroblasts plus palmitate.

Cell viability was monitored throughout the entire culture process. Unlike the high cytotoxicity observed with 200 μ M palmitate, cell viability in the adipocyte co-culture consistently remained above 90% (Figure 15).

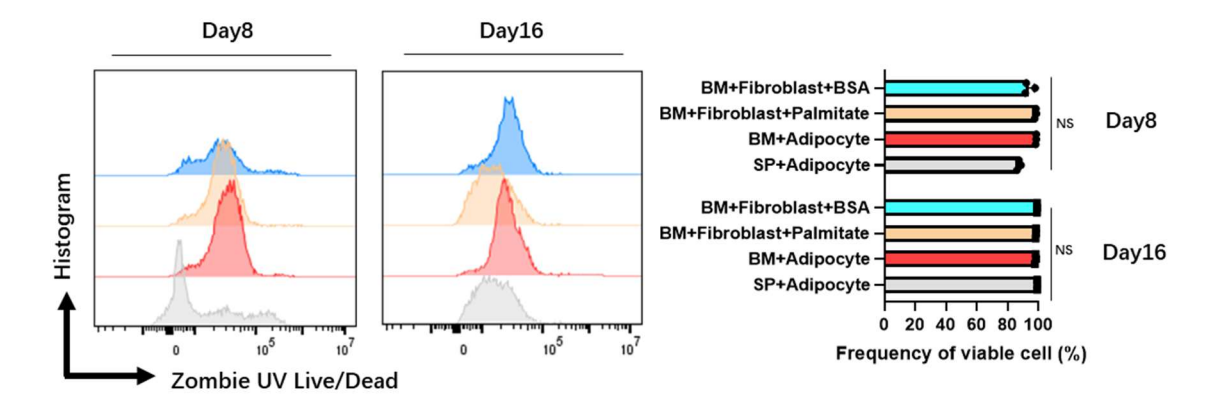


Figure 15 Cell viability during NK cell differentiation in diverse coculture conditions. Flow cytometry analysis demonstrating the viability of cells during NK cell differentiation across different coculture conditions at D8 and D16, cells were gated on single cells. BM: bone marrow; SP: splenocytes; BSA: Bovine serum albumin. Overlaid histogram plots and quantification reveal the percentage of viable cells for each experimental condition: bone marrow and spleen cultures with fibroblasts, adipocytes, or palmitate treatments. Error bars represent standard deviation from n=3 independent experiments.

4.3.2 Dynamic changes in the frequency of different lineage cells in the coculture differentiation model

At the end of differentiation, we assessed the proportions of various cell lineages within the coculture system. As shown in the figure 16, NK cells accounted for approximately 20–30% under all conditions, with T cells exhibiting a similar proportion to NK cells and NKT cells constituting around 10%. Apart from the control group using spleen cells, the bone marrow-derived samples still retained a certain proportion of myeloid cells by the end of the differentiation period. These results indicate that, in the presence of feeder cells, bone marrow hematopoietic stem and progenitor cells can be successfully induced to differentiate into NK cells in vitro.

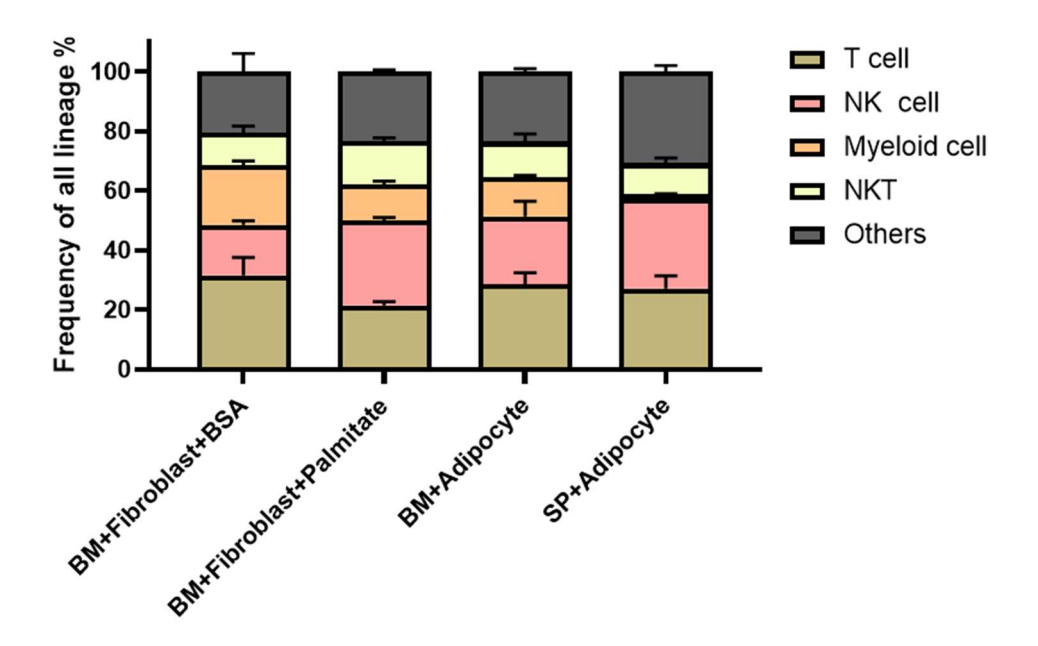


Figure 16 Cell lineage composition on day 16 in diverse coculture conditions. Stacked bar graph depicting the percentage distribution of cell lineages on Day 16 across different experimental culture conditions. BM: bone marrow; SP: splenocytes; BSA: Bovine serum albumin. Error bars indicate standard deviation from n=3 independent experiments.

4.3.3 Increasing frequency of obesity-associated NK cell subsets in the adipocyte co-culture differentiation model

We further investigated whether the adipocyte co-cultured obese microenvironment could induce the upregulation of obesity-associated markers CSF1R and IL6R in NK cells, and compared these changes across various cell lineages. The results indicated that on day 8, NK cells had already started to upregulated both markers, with statistically significant differences observed (Figure 17).

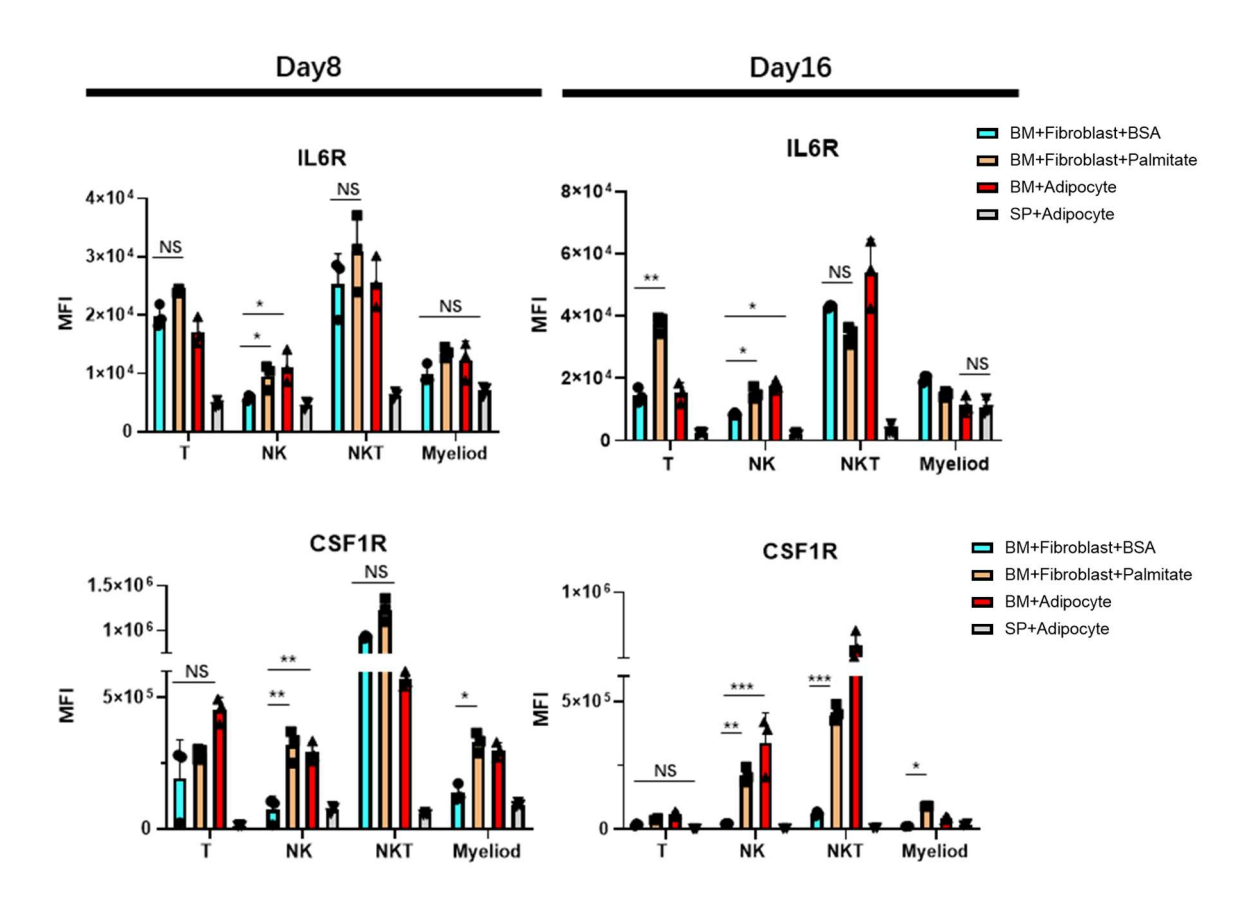
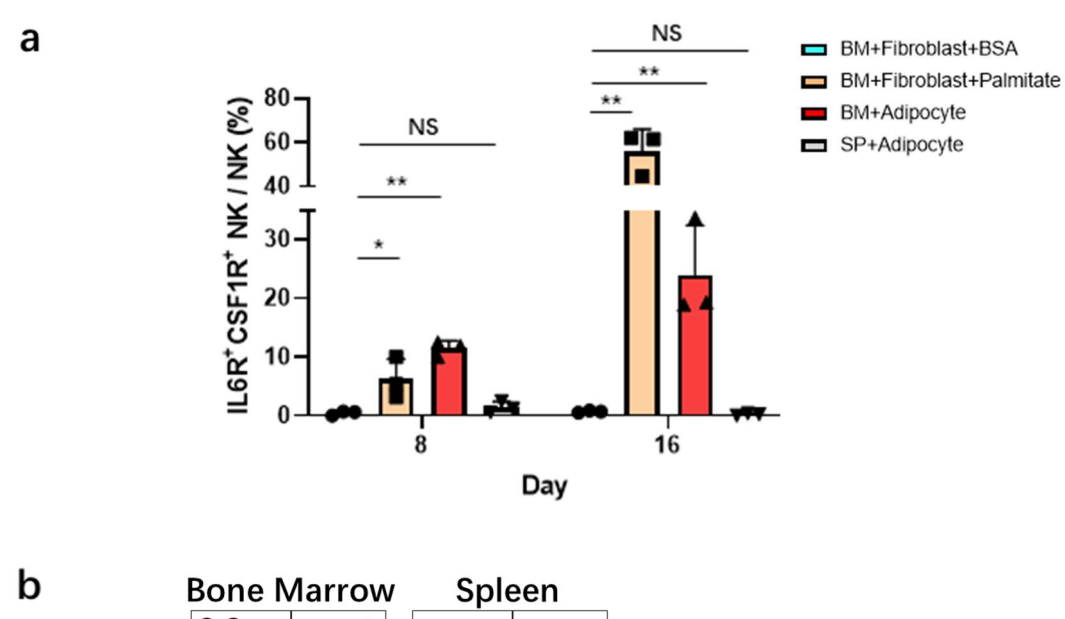


Figure 17 Dynamic changes in IL6R and CSF1R expression across cell lineages in different culture conditions. The mean fluorescence intensity of IL6R and CSF1R expression in T cells, NK cells, NKT cells, and Myeloid cells were measured across different experimental culture conditions at D8 and D16. Error bars indicate standard deviation from n=3 independent experiments. Statistical significance was calculated by one-way ANOVA and indicated with * (p<0.05), *** (p<0.01), ***(p<0.001) or NS (non-significant).

On day 16, NK cells in both the adipocyte co-culture and palmitate treatment groups continued to exhibit elevated expression of CSF1R and IL6R. However, this pattern was not consistently observed in other lineages. We analyzed the proportion of NK cells positive for CSF1R and IL6R (Figure 18), and found significant differences between the adipocyte co-culture and palmitate treatment groups compared to the control. These results suggest that both fatty acids and adipocytes can induce the generation of obesity-associated NK cells from bone marrow hematopoietic progenitor cells, and that this unique NK cell subset cannot be directly derived from mature NK cells in vitro.



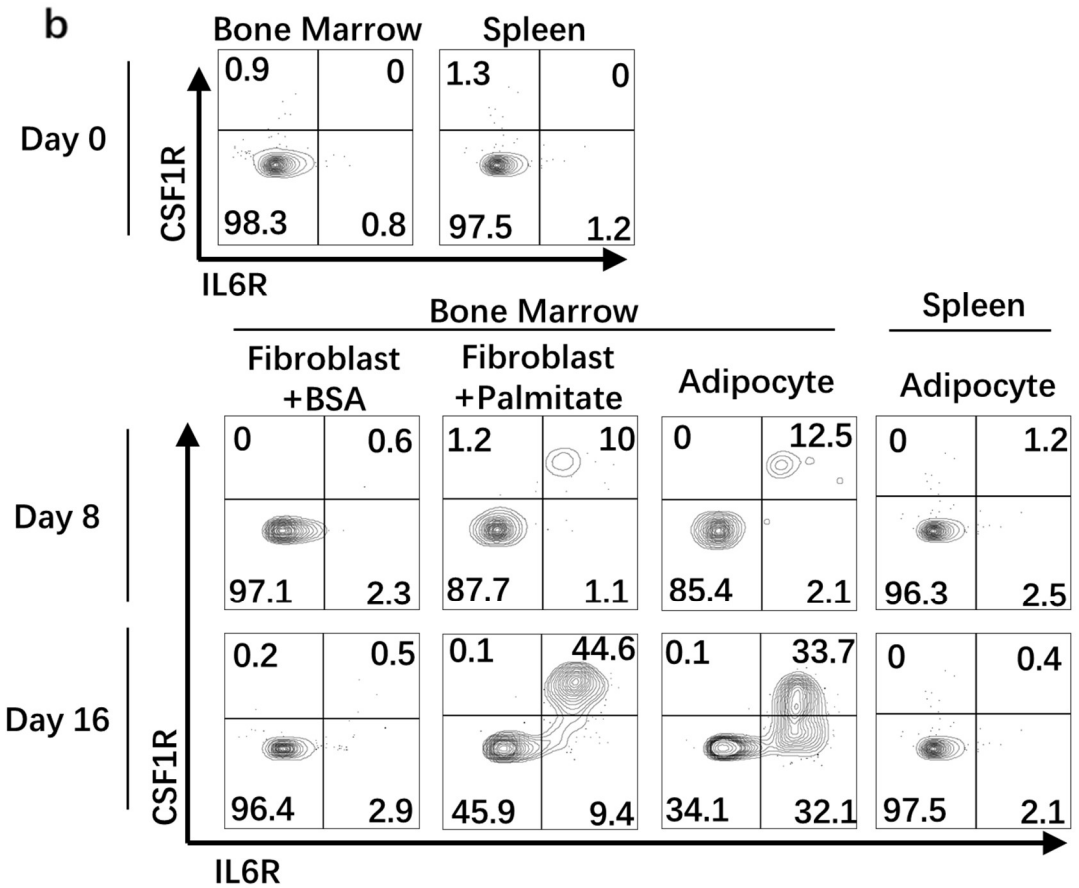


Figure 18 Frequency of bone marrow and spleen derived IL6R and CSF1R positive obesity-associated NK cells in different coculture model. Flow cytometry analysis of the frequency of IL6R and CSF1R double-positive obesity-associated NK cells across different model on D8 and D16, NK cells were gated on CD45⁺ CD3⁻ NK1.1⁺ or NKp46⁺ cells. a) quantifying the percentage of IL6R⁺ CSF1R⁺ obesity associated NK cells, comparing bone marrow and spleen derived across different model on D8 and D16. b) representative flow cytometry dot plots of IL6R and CSF1R expression in bone marrow and spleen derived NK cells at D0 to D16. Error bars represent standard deviation from n=3 independent experiments. Statistical

significance was calculated by one-way ANOVA and indicated with * (p<0.05), ** (p<0.01) or NS (non-significant).

Besides, CD11B and CD27 are classical markers used to assess the maturation status of mouse NK cells (Bi et al. 2020). Based on the expression profiles of IL6R and CSF1R, we found that obesity-associated NK cells (P1) exhibited higher levels of CD11b marker compared to conventional NK cells (P2) (Figure 19).

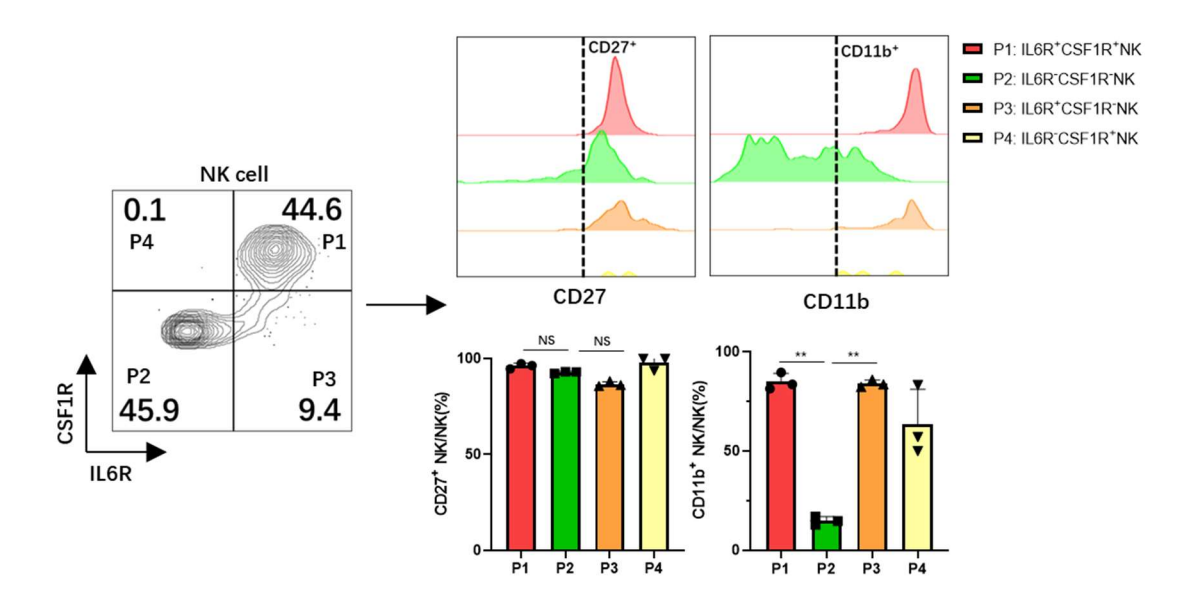


Figure 19 Differential expression of CD27 and CD11b on NK cell subpopulations. Comprehensive flow cytometry analysis revealing the expression patterns of CD27 and CD11b across different NK cell subpopulations based on IL6R and CSF1R expression. NK cells were gated on CD45⁺ CD3⁻ NK1.1⁺ or NKp46⁺ cells. Bar graph shows quantification of the percentage of CD27 and CD11b expression NK, with error bars representing standard deviation from n=3 independent experiments. Statistical significance was calculated by one-way ANOVA and indicated with ** (p<0.01) or NS (non-significant).

4.3.4 Flow cytometry analysis of surface markers of NK cell subsets indicating a distinct expression pattern in obesity-associated NK cell

To further elucidate the differences between NK cells induced under obesity conditions and conventional NK cells, we employed flow cytometry to analyses multiple surface receptors on NK cells. By integrating the data on surface marker expression from both populations, we identified a subpopulation primarily derived from the adipocyte co-culture group (Figure 20a).

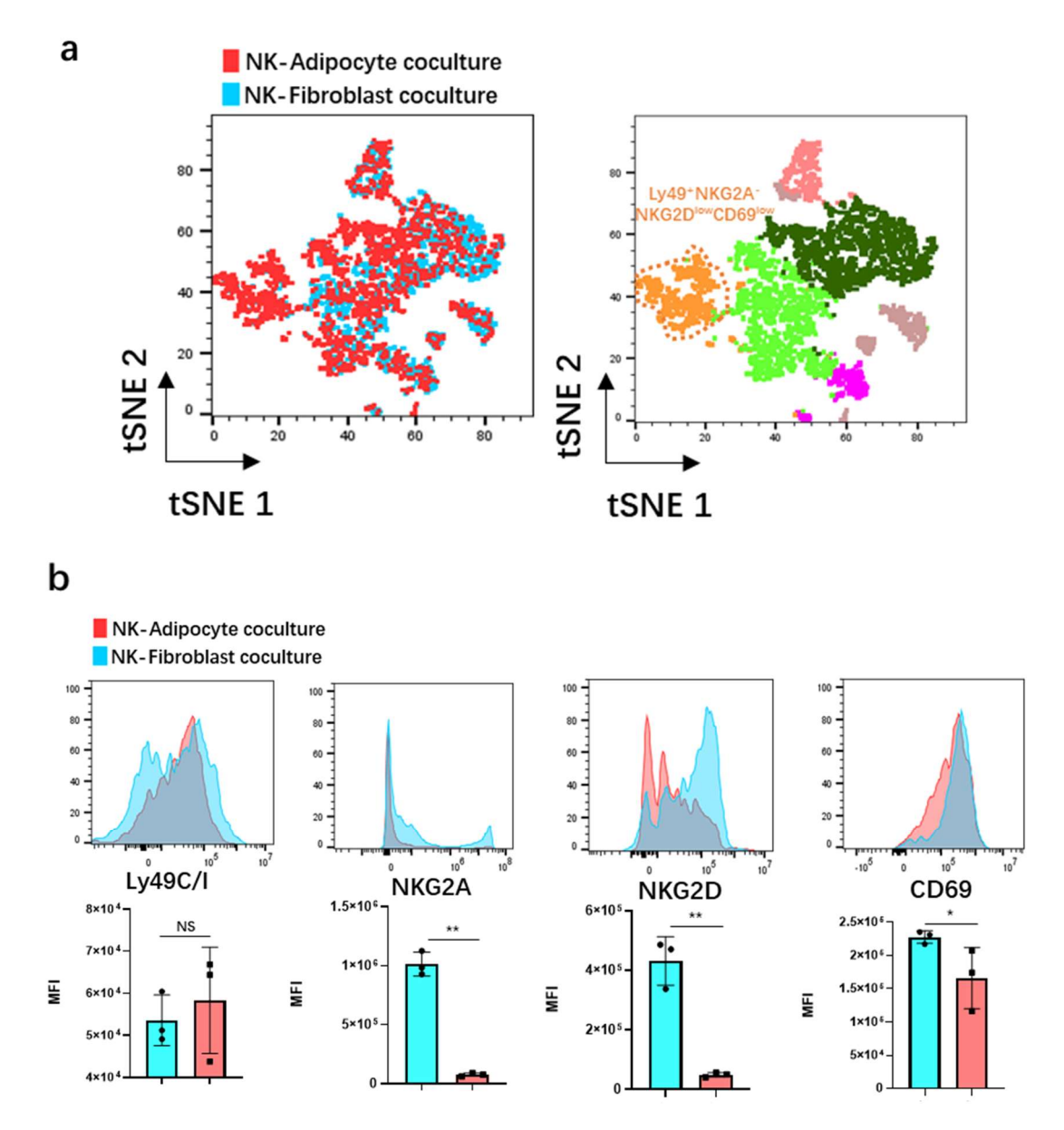


Figure 20 Phenotypic of key receptors between bone marrow derived NK cells co-cultured with adipocytes or fibroblasts. NK cells were first gated on viable CD45⁺ CD3⁻ NK1.1⁺ or NKp46⁺ cells in each coculture condition separately and then concatenated for t-SNE analysis. a) t-SNE plots showing the distribution of pooled NK cells after coculture induction with the left plot color-coded by culture condition and the right plot showing distinct clusters with the Ly49C/I, NKG2A, NKG2D, CD69 and KLRG1 expression pattern. b) histograms and bar graphs comparing the expression of key NK cell receptors between NK cells cocultured with adipocytes versus fibroblasts with error bars representing standard deviation from n=3 independent experiments. Statistical significance was calculated by t-test and indicated with * (p<0.05), *** (p<0.01) or NS (non-significant).

This subset exhibited low expression of the activating receptors NKG2D, NKP46 and CD69, was positive for the inhibitory receptor Ly49C/I, and lacked expression of NKG2A (Figure 20b). Furthermore, NK cells differentiated in the presence of adipocytes not only exhibited elevated expression of the myeloid markers CSF1R, CD11b but also showed increased levels of KLRG1 (Figure 21), a hallmark of terminally differentiated NK cells (Muller-Durovic et al. 2016). These results suggest that obesity-associated NK cells may constitute a subset with reduced cellular

activity and terminal differentiation. We hypothesize that their cellular function such as proliferative capacity and cytotoxic ability probably are diminished compared to conventional NK cells.

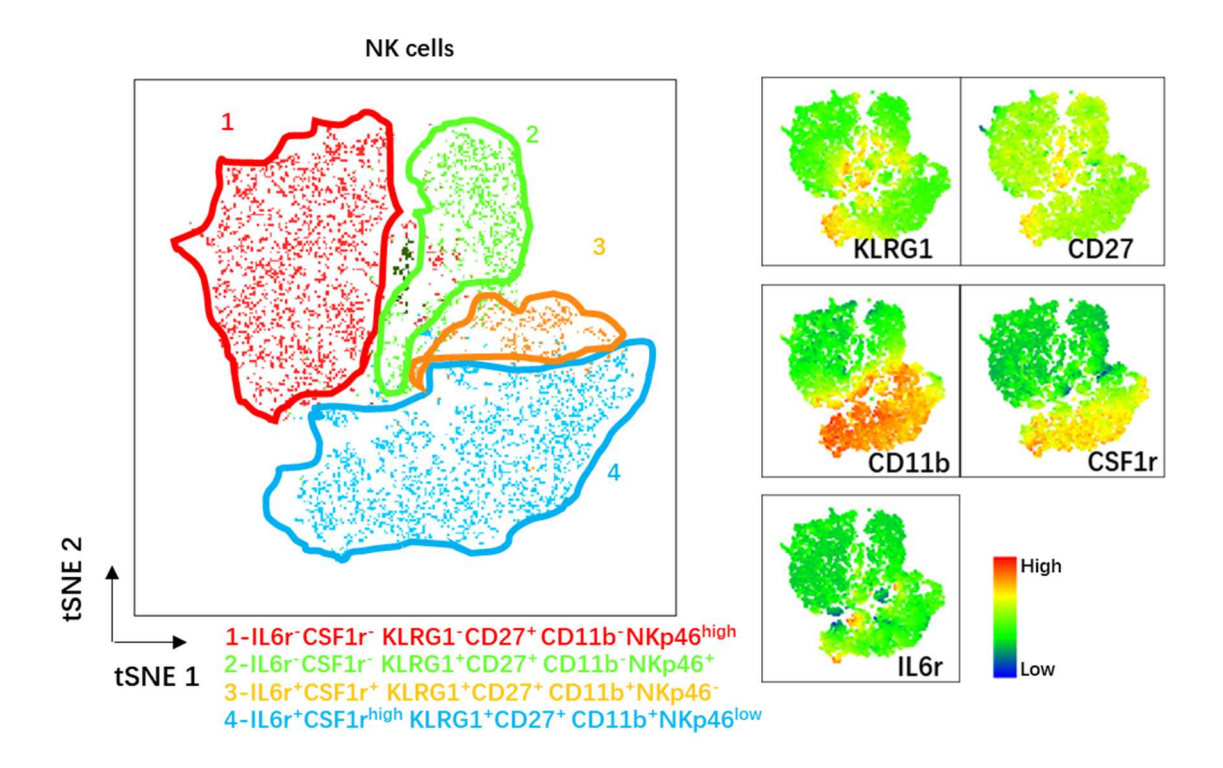


Figure 21 Phenotypic of maturation differences between bone marrow derived NK cells subpopulation. All NK cells cocultured from both adipocytes and fibroblasts coculture are pooled together for analysis. NK cells were gated on viable CD45⁺ CD3⁻ NK1.1⁺ or NKp46⁺ cells. t-SNE plots showing the clusters distribution of bone marrow derived NK cells based on IL6R, CSF1R, CD11b, CD27 and KLRG1 expression pattern and heatmap comparing the expression of different maturation markers between NK cell clusters.

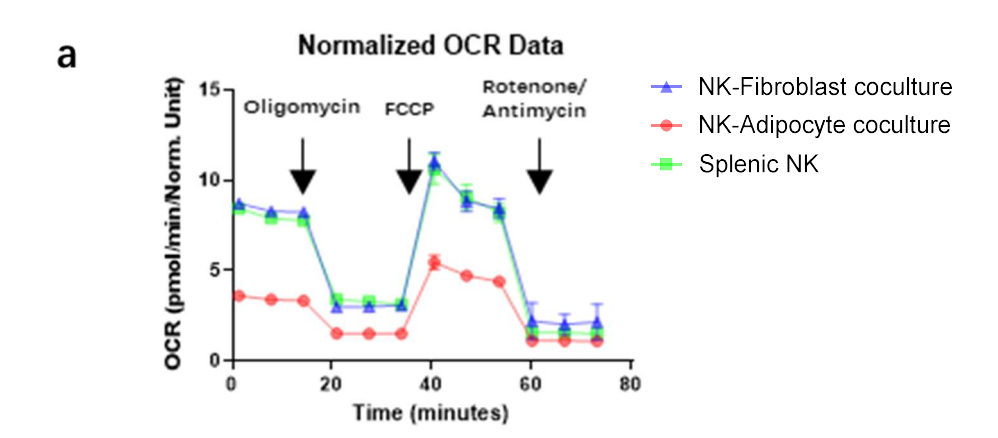
4.4 Analysis of mitochondrial metabolism and cytotoxic function in NK cells induced under obesity conditions

In the preceding section, we detailed the phenotypic characteristics of NK cells, underscoring the differential expression of key markers that distinguish conventional NK cells from their obesity-associated counterparts. To further investigate the functional implications of these phenotypic variations, we next turned our focus to the metabolic properties of NK cells. By employing mitochondrial stress tests and glycolysis assays, we aim to comprehensively assess the bioenergetic profile of these cells, provide critical insights into how the obesity-induced microenvironment impacts NK cell function at a bioenergetic level, thereby bridging our

phenotypic findings with potential mechanistic underpinnings of altered NK cell performance in obesity (Bahr et al. 2020).

4.4.1 NK cells induced in adipocytes co-culture model exhibiting reduced mitochondrial metabolic activity

We collected all the cells after 16 days differentiation in both coculture models and enriched NK cells by CD3* cell depletion first followed by NK1.1* positive selection. Mitochondrial metabolic function was assessed using Seahorse analysis to measure oxygen consumption rate (OCR) across three NK cell populations. The time-course OCR measurements revealed that Fibroblast cocultured NK cells and Splenic NK cells exhibited similar metabolic profiles, with both showing higher oxygen consumption compared to adipocyte cocultured NK cells (Figure 22a). Analysis of specific metabolic parameters showed that adipocyte cocultured NK cells consistently demonstrated reduced mitochondrial activity. Under basal conditions, adipocyte cocultured NK cells showed markedly lower OCR compared to both fibroblast cocultured NK and Splenic NK cells. Similarly, the maximal respiratory capacity was substantially reduced in adipocyte cocultured NK cells compared to fibroblast cocultured NK and Splenic NK cells. The spare respiratory capacity (SRC) followed the same pattern, with adipocyte cocultured NK cells showing the lowest values among the three populations (Figure 22b). These results indicate that NK cells induced in an adipocyte environment exhibit significantly compromised mitochondrial metabolic function compared to NK cells from fibroblast cocultured and splenic counterparts.



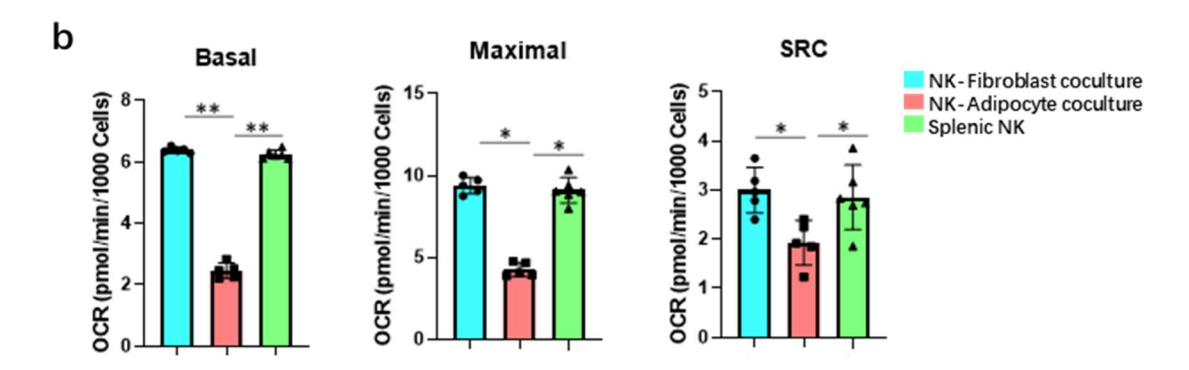


Figure 22 Decreased mitochondrial respiration of NK cells from adipocyte coculture model.

The metabolic profile of different NK cells populations as measured by Seahorse mitochondrial respiratory assay. NK cells are enriched by CD3⁺ depletion and subsequentially NK1.1⁺ positive magnetic cell sorting. **a)** a time-course of OCR normalized to cell number across fibroblast cocultured NK cells, adipocyte cocultured NK cells, and splenic NK cells over 80 minutes. **b)** quantification comparisons of specific metabolic parameters: basal respiration, maximal respiratory capacity and spare respiratory capacity, revealing that adipocyte cocultured NK cells consistently exhibit lower metabolic activity compared to both fibroblast cocultured and splenic NK cells. Error bars represent standard deviation from n=5 or 6 biologic replicates. Statistical significance was calculated by one-way ANOVA and indicated with * (p<0.05), ** (p<0.01).

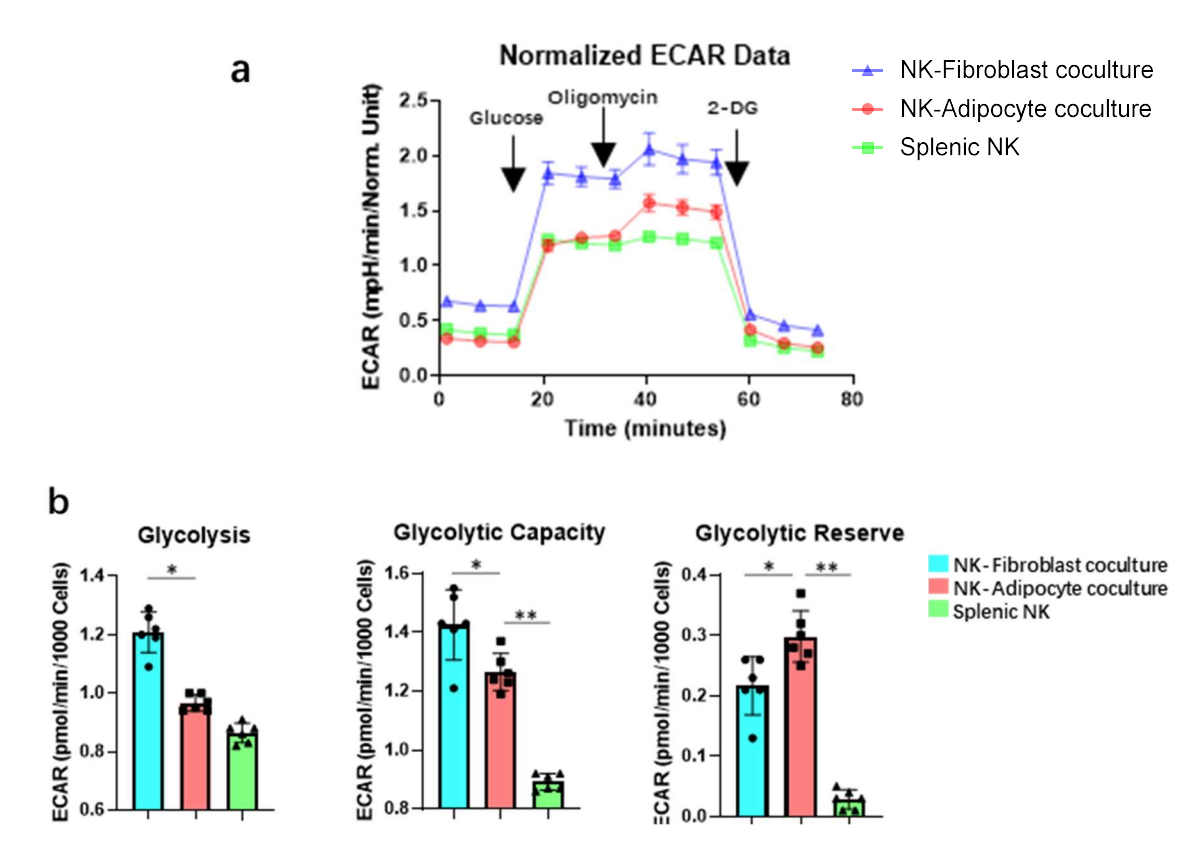


Figure 23 Decreased glycolysis capacity of NK cells from adipocyte coculture model. The metabolic profile of different NK cells populations as measured by Seahorse mitochondrial respiratory assay.

a) a time-course of ECAR normalized to cell number across fibroblast cocultured NK cells, adipocyte cocultured NK cells, and splenic NK cells over 80 minutes. b) quantification comparisons of specific metabolic parameters: glycolysis, glycolytic capacity and reserve, revealing that adipocyte cocultured NK

cells exhibit lower glycolysis in stress compared to fibroblast cocultured NK cells. Error bars represent standard deviation from n=6 biologic replicates. Statistical significance was calculated by one-way ANOVA and indicated with * (p<0.05), ** (p<0.01).

To further characterize the metabolic profile of NK cells, we assessed glycolytic function using Seahorse extracellular acidification rate (ECAR) analysis. The time-course ECAR measurements revealed distinct glycolytic patterns across different NK cell populations (Figure 23a). Glycolysis analysis showed significant differences between cell groups. Fibroblast cocultured NK cells demonstrated the highest basal glycolytic activity, significantly higher than adipocyte cocultured NK cells. Splenic NK cells exhibited the lowest basal glycolytic rate. When examining glycolytic capacity, fibroblast cocultured NK cells again showed the highest ECAR values, with statistically significant differences compared to adipocyte cocultured NK cells. The glycolytic reserve, which represents the cells' potential to increase glycolysis, was markedly higher in adipocyte cocultured NK cells compared to Splenic NK cells, despite their lower basal glycolytic activity (Figure 23b). These results suggest a complex metabolic reprogramming of NK cells in different microenvironmental contexts, with particularly notable alterations in glycolytic metabolism when NK cells are induced in adipose environments.

4.4.2 Analysis of mitochondrial mass, membrane potential, and reactive oxygen species levels elucidated impaired NK cell function in obese environment

To further investigate the mitochondrial characteristics of NK cells, we performed comprehensive flow cytometry analyses measuring four key mitochondrial parameters: Cell ROX (reactive oxygen species), mSOX (mitochondrial superoxide), Mitochondrion Mass, and Mitochondrion Potential (Murphy et al. 2011). Flow cytometry analysis revealed subtle but significant differences between fibroblast cocultured and adipocyte cocultured NK cells. Cell ROX measurements showed comparable levels of reactive oxygen species between the two populations, with similar mean fluorescence intensity values. The mSOX analysis, which specifically detects mitochondrial superoxide, demonstrated no significant difference between fibroblast cocultured and adipocyte cocultured NK cells. Notably, MitoMass analysis revealed a statistically significant difference, with fibroblast cocultured NK cells showing a higher MFI compared to adipocyte cocultured NK cells (Figure 24). This suggests a potential reduction in mitochondrial content or density in NK cells

induced in an adipocyte environment. MitoPotential measurements, which reflect mitochondrial membrane potential, indicated a trend of lower potential in adipocyte cocultured NK cells, although the difference was not as pronounced as in the MitoMass analysis. These findings complement our previous Seahorse metabolic analyses, providing further evidence of metabolic and mitochondrial alterations in NK cells induced in different microenvironmental contexts.

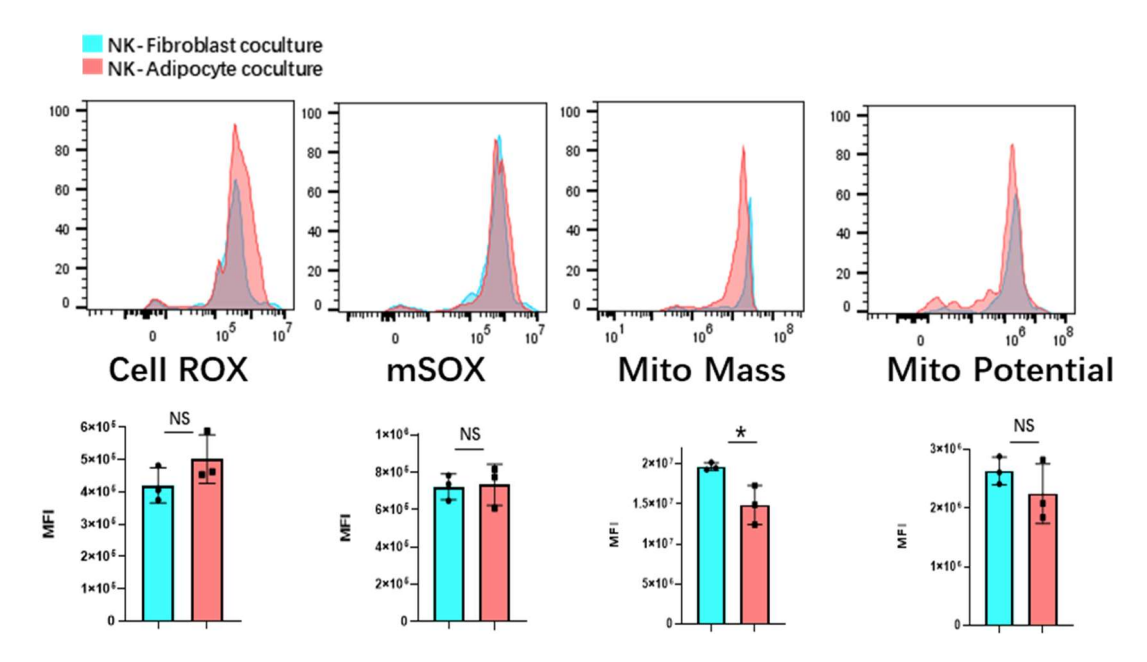


Figure 24 Flow cytometry analysis of oxidative stress and mitochondrial parameters between bone marrow derived fibroblast cocultured and adipocyte cocultured NK Cells. NK cells are enriched by CD3+ depletion and subsequentially NK1.1+ positive magnetic cell sorting. Histogram overlays showing the fluorescence intensity distribution of Cell ROX, mSOX, MitoMass, and MitoPotential between the NK cell populations. The bottom panels quantify these parameters as mean fluorescence intensity suggesting that NK cells induced in adipocytes microenvironments develop lower mitochondrial mass. Error bars represent standard deviation from n=3 biologic replicates. Statistical significance was calculated by t-test and indicated with * (p<0.05) or NS (non-significant).

Fluorescence microscopy was also employed to characterize the mitochondrial dynamics of fibroblast cocultured and adipocyte cocultured NK cells (Figure 25). In the merged images, we observe distinct mitochondrial patterns between fibroblast and adipocyte cocultured NK cells. fibroblast cocultured NK cells display more compact and clustered mitochondrial structures, with pronounced yellow regions indicating co-localization of green and red fluorescence. In contrast, adipocyte cocultured NK cells show a more dispersed mitochondrial distribution, with less intense yellow coloration in the merged image. These microscopic observations complement our

previous Seahorse metabolic and flow cytometry analyses, providing visual evidence of altered mitochondrial characteristics in NK cells induced in different microenvironmental contexts.

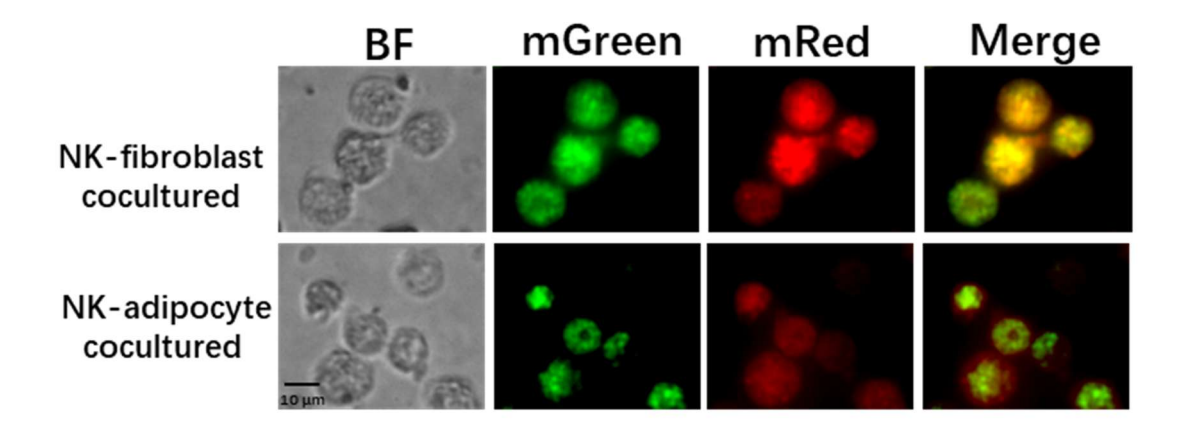


Figure 25 Fluorescence microscopy of mitochondrial mass and potential indicate a fitter mitochondrial of fibroblast cocultured NK cells. NK cells are magnetically enriched and maintained in NK medium with IL-2 20U/mL, stained by MitoTacker Green and Mitotracker Red FM dye. The fluorescent images (X40 fold lens) of mGreen and mRed dyes indicating adipocyte cocultured NK cells have both lower mitochondrial mass and potential compared to NK cells cocultured with fibroblast.

4.4.3 NK cells induced under obesity conditions exhibit reduced tumor cell cytotoxicity

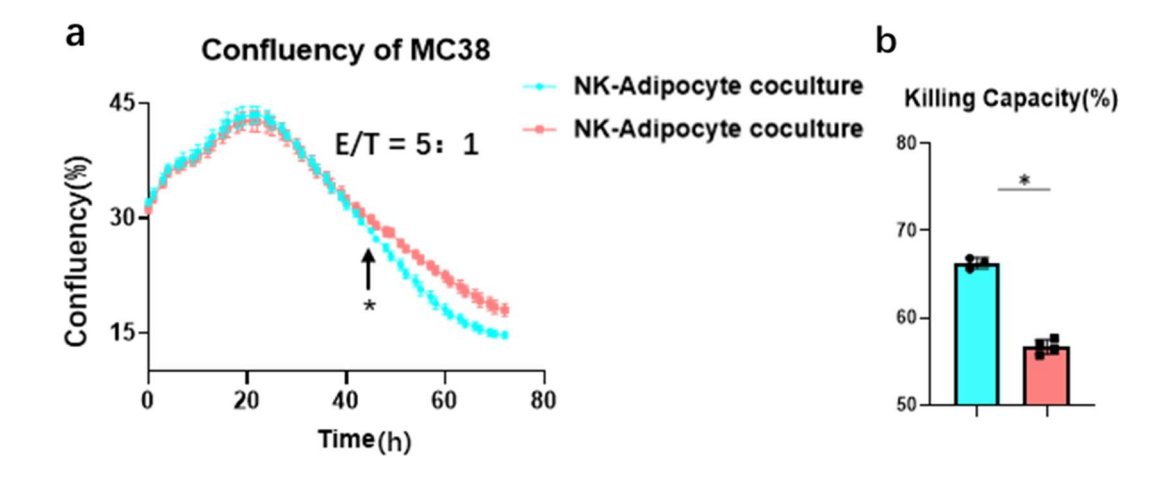


Figure 26 Ex Vivo fibroblast cocultured NK cells exhibit superior killing capacity against MC38 cell line. The killing efficiency of fibroblast cocultured NK cells and adipocyte cocultured NK cells against the MC38 cell line at an effector-to-target ratio of 5:1. a) the confluency of MC38 cells over time, where fibroblast cocultured NK cells exhibit a more pronounced reduction in confluency compared to adipocyte cocultured NK cells, indicating stronger cytotoxic activity. b) quantification of the killing capacity at the end of the experiment. Error bars represented standard deviation from n=4 biologic replicates. Statistical significance was calculated by t-test at each time point and indicated with * (p<0.05).

To assess the functional consequences of metabolic alterations, we performed a killing assay using MC38 target cells at an effector-to-target (E/T) ratio of 5:1 (Ng et al. 2016). The confluency-based killing assay revealed significant differences in the cytotoxic capabilities of fibroblast cocultured and adipocyte cocultured NK cells. The time-course confluency graph demonstrates the progressive reduction in target cell confluence over time (Figure 26). Notably, fibroblast cocultured NK cells exhibited markedly superior killing capacity compared to adipocyte cocultured NK cells. The killing capacity analysis showed a statistically significant difference, with fibroblast cocultured NK cells achieving approximately 67% target cell killing, while adipocyte cocultured NK cells displayed reduced cytotoxicity at around 57% (p<0.05). These results provide compelling evidence that NK cells induced in an adipocyte microenvironment experience not only metabolic reprogramming but also functionally significant impairment in their cytotoxic capabilities. This finding suggests that the obesogenic environment may substantially compromise NK cell anti-tumor functionality.

4.5 Using single-cell RNA sequencing to analyses the impact of obesity conditions on the NK cells from the *in vitro* differentiation model

Obesity has been increasingly recognized as a systemic inflammatory condition that alters immune cell development and function (Andersen et al. 2016). In our *in vitro* model, NK cells differentiation and functional maturation are distinguishably changed by the microenvironment. Aiming to further investigate the potential regulatory mechanisms underlying their differentiation in an obesogenic environment, we utilize single-cell transcriptomic sequencing to analyses gene expression differences in NK cells under distinct environmental conditions.

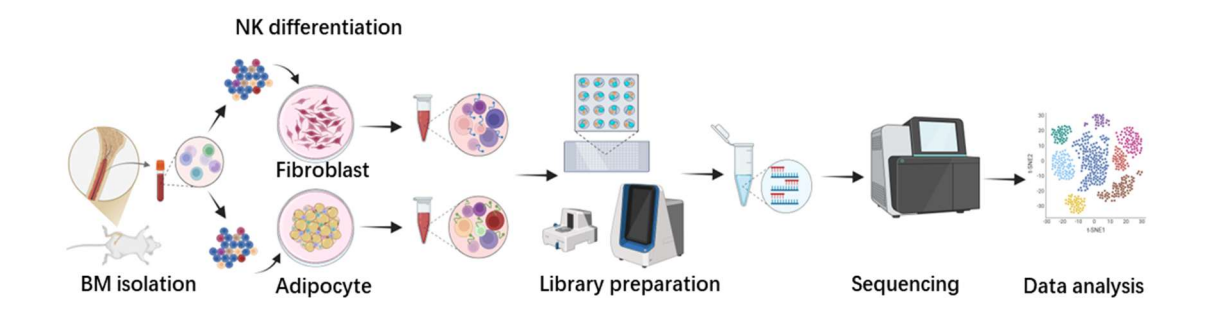


Figure 27 The experimental workflow for analyzing NK cell differentiation under different conditions using single-cell RNA sequencing. Bone marrow cells from six wild-type mouse are isolated and cultured in vitro with either fibroblasts or adipocytes. After 16 days of differentiation, the cells are collected and processed for transcriptomic library preparation with BD Rhapsody platform and sequencing by Illumina Nextseq1000. The transcriptomic data is analyzed using R.

Initially, bone marrow cells were isolated and differentiated into NK cells under obese and nonobese conditions as described before. After collection and labelling, the cells were lysed for transcriptomic library preparation and subsequent sequencing (Figure 27).

4.5.1 Adipocytes induce generally upregulation of pro-inflammatory genes and fatty acid metabolism related genes

Raw data was collected and processed using the Rhapsody Sequence Analysis Pipeline from Seven Bridges Genomics. Further analysis was done in R. Identification of cell populations relies on manual annotation of cell clusters using established marker genes (Sup 2). The Uniform Manifold Approximation and Projection (UMAP) depicts the clustering of different cell types and their distribution across experimental conditions (Figure 28). Different cell types are well-separated, the macrophages form a large, evenly distributed cluster from both conditions, while NK cells form separate clusters, indicating distinct transcriptional profiles.

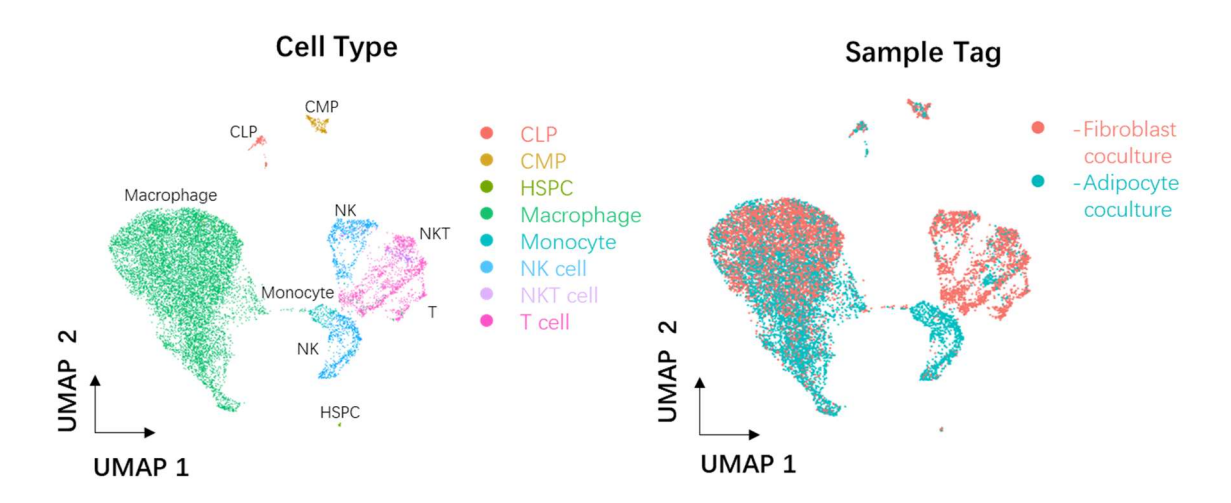
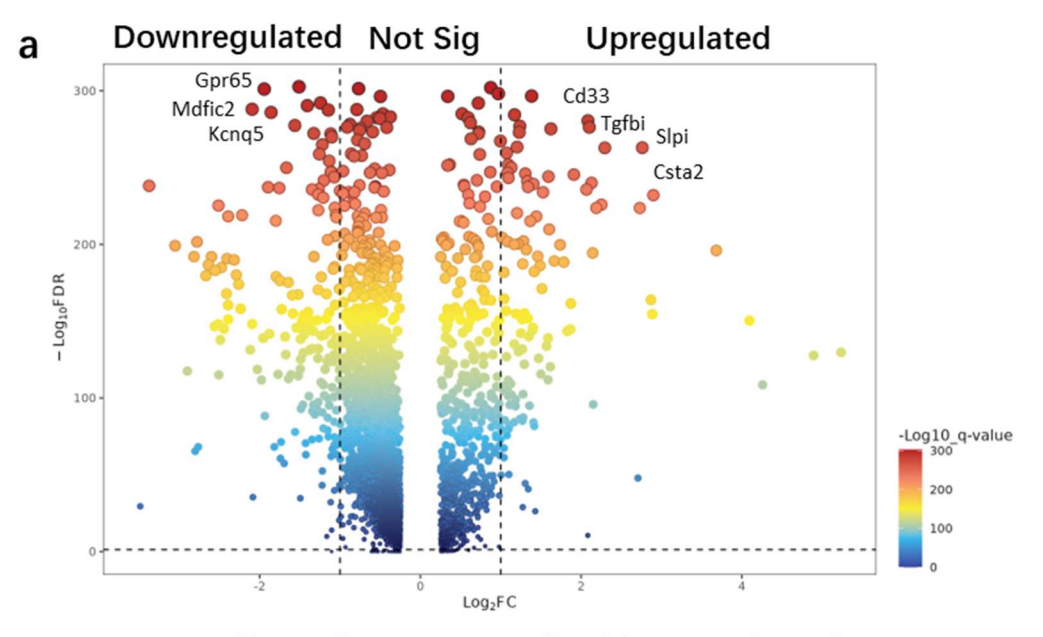


Figure 28 Single-cell RNA sequencing reveals transcriptomic changes of NK cells in different coculture conditions. Single cell RNA sequencing data is represented in UMAP, cell clustering annotated by marker genes and distinguished by different coculture condition.

To further investigate the impact of obesogenic conditions on cell differentiation in general, we compared differentially expressed genes across all cell types. The volcano plot illustrates the differences between the two differentiation conditions, while the left panel displays the

significantly down-regulated genes and upregulated genes on the right. These genes are subsequently enriched in biological regulatory pathways (Figure 29).



Pan-Cells: -Adipocyte VS -Fibroblast cocultured

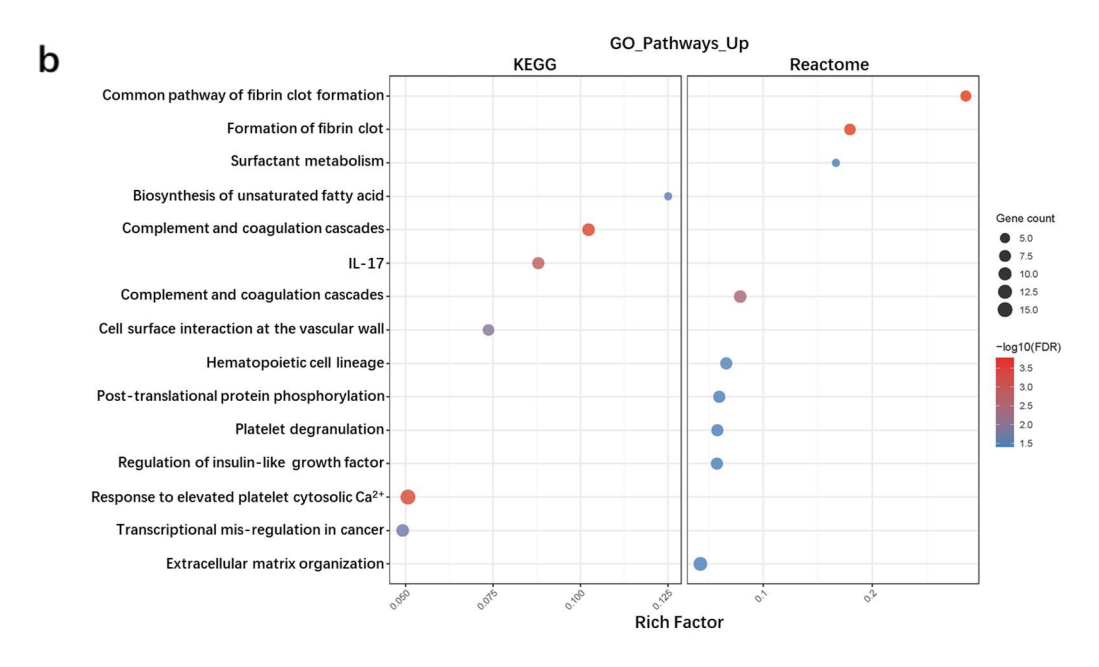


Figure 29 Volcano plots across Pan-cell types show generally transcriptomic variations in different coculture conditions. a) >2 or <0.5-fold changes in gene expression of all cells between adipocyte and fibroblast cocultured differentiation are presented in the volcano plot. b) gene ontology enrichment plot shows significantly altered biological pathways across two databases (KEGG and Reactome). Interestingly, we found that compared to cells induced to differentiate by fibroblasts, cells differentiated by coculturing with adipocytes showed an upregulation of fatty acid biosynthesis pathways. Simultaneously, a comprehensive upregulation of pro-inflammatory responses was

observed, including cell adhesion molecules, cytokine-mediated signaling pathways, leukocyte chemotaxis (Sup 3), complement and coagulation cascades.

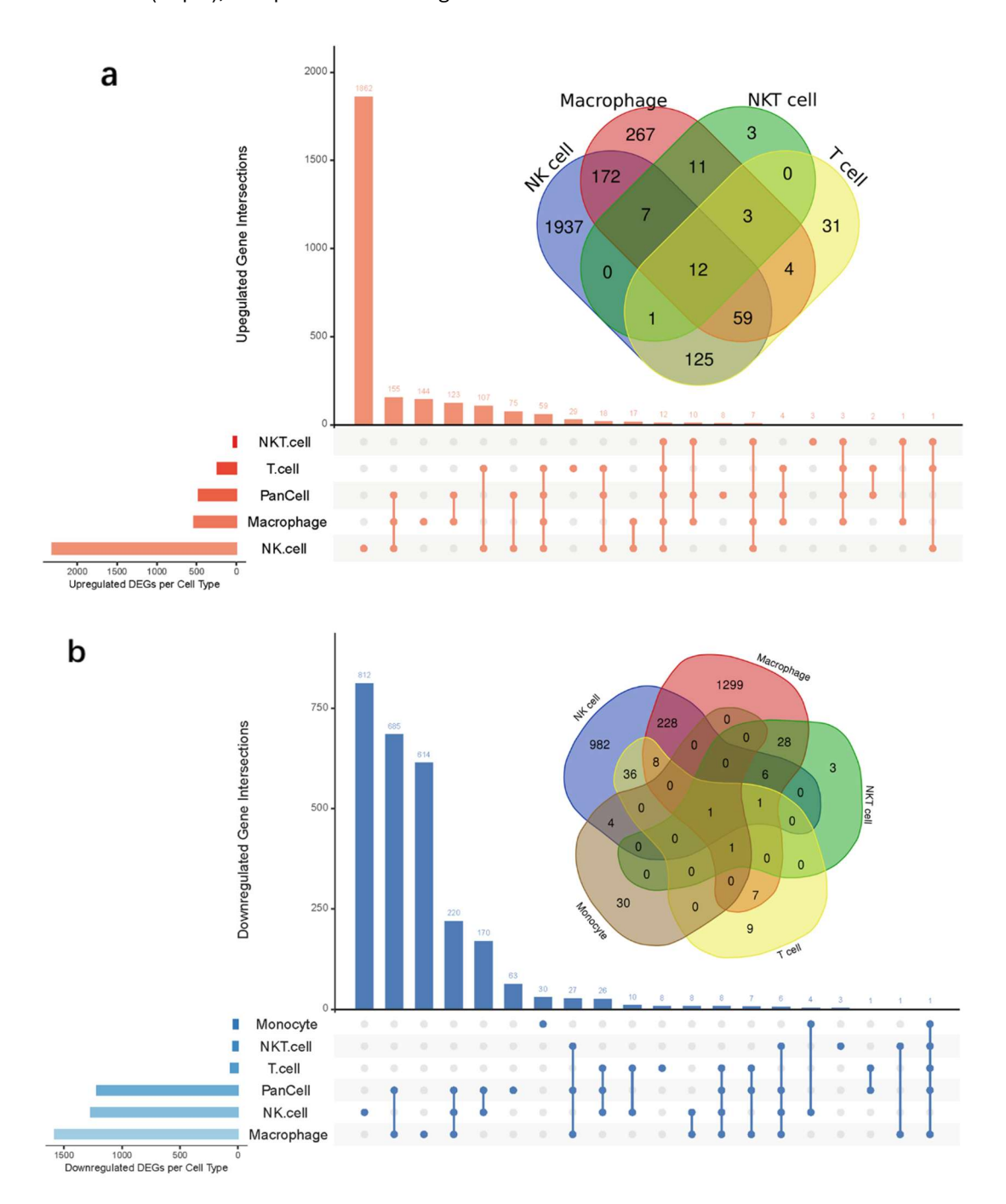


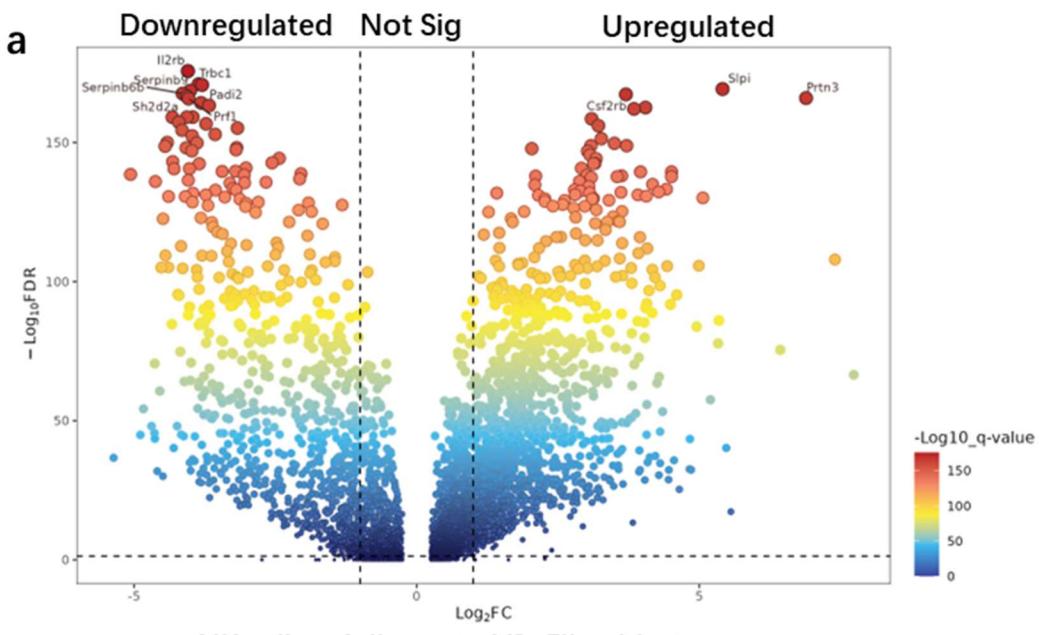
Figure 30 UpSet and Venn plots across all cell types indicate shared up- (a) or down-regulated (b) genes in different cell lineages. The number of upregulated or downregulated differentially expressed genes across different cell types, including NKT cells, T cells, Pan-Cell, Macrophages, and NK cells are showed in UpSet plot. The horizontal bars represent intersections or overlaps between cell types, with each dot indicating which cell types are included in a specific combination.

Next, to investigate the relationship of differentially expressed genes between different lineages, we found that macrophages and NK cells had the highest number of differentially expressed genes

under different differentiation conditions. Among these, 172 genes were co-upregulated (Figure 30a) and 228 genes were co-downregulated (Figure 30b) between these two cell types in the adipose coculture. In all lymphoid cells, only one gene, *Cstb*, was upregulated in NK, NKT, and T cells in the adipose co-culture group, with no genes commonly downregulated among the three populations. This suggests a close tendency and connection between NK cells and myeloid cells under obesogenic conditions.

4.5.2 Identification of obesity-associated NK cell subsets in adipocytes coculture model

We identified NK cells with the following marker genes: CD19⁻ CD3⁻ F4/80⁻ CD14⁻ NKp46⁺ or NK1.1⁺ (Crinier et al. 2018). Interestingly, we observed distinct transcriptomic characteristics between NKp46⁺ and NK1.1⁺ NK cells. Of note, NKp46⁺ NK cells primarily originated from the fibroblast cocultured differentiation model, whereas NK1.1⁺ NK cells were predominantly derived from the adipocyte cocultured model. Transcriptomic analysis revealed that obesity-associated NK1.1⁺ NK cells upregulated genes involved in fatty acid metabolism, as well as inflammatory response related receptors like IL6R and IL1R, and some myeloid lineage differentiation transcription factors (Figure 31). In contrast, NKp46⁺ NK cells showed minimal expression of IL6R. These findings align with our flow cytometry results, which demonstrated that NK cells induced under obesogenic conditions will upregulate the cell surface pro-inflammatory receptors. From Theurich's. *et al* results, gene sets of "myeloid leukocyte differentiation", "inflammatory response", "cell chemotaxis" are upregulated in NK cells isolated from high fat diet fed obese mouse (Theurich et al. 2017). Our *ex vivo* data also suggested the changes consistently happened to NK cell generated in obese condition.



NK cells: -Adipocyte VS -Fibroblast

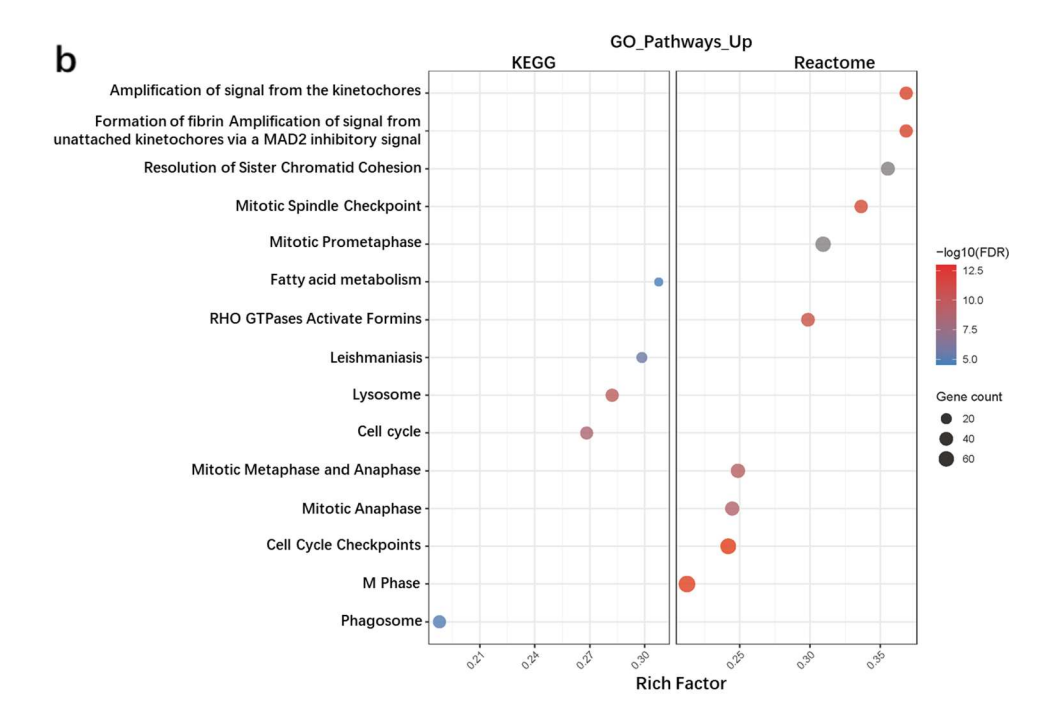


Figure 31 Upregulation of fatty acid metabolism related genes in NK cells induced from adipocyte coculture. a) volcano plots show significantly differentially expressed genes of NK cells induced from adipocyte and fibroblast coculture model; b) gene ontology enrichment of upregulated genes in adipocyte cocultured NK cells across two databases (KEGG and Reactome).

To more thoroughly describe the effects of adipocytes on NK cell differentiation, we manually selected several myeloid cells related genes, transcription factors from different lineages, genes related to fatty acid uptake, inflammation-related receptors, and genes related to NK cell function.

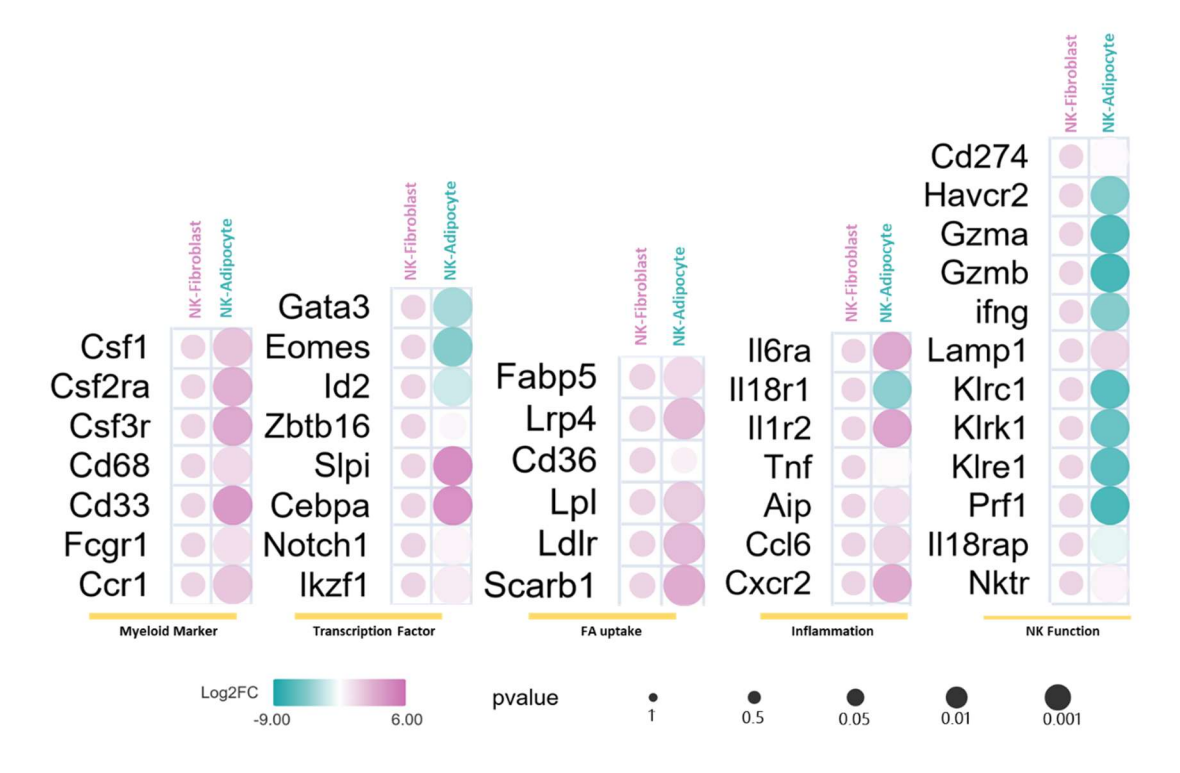
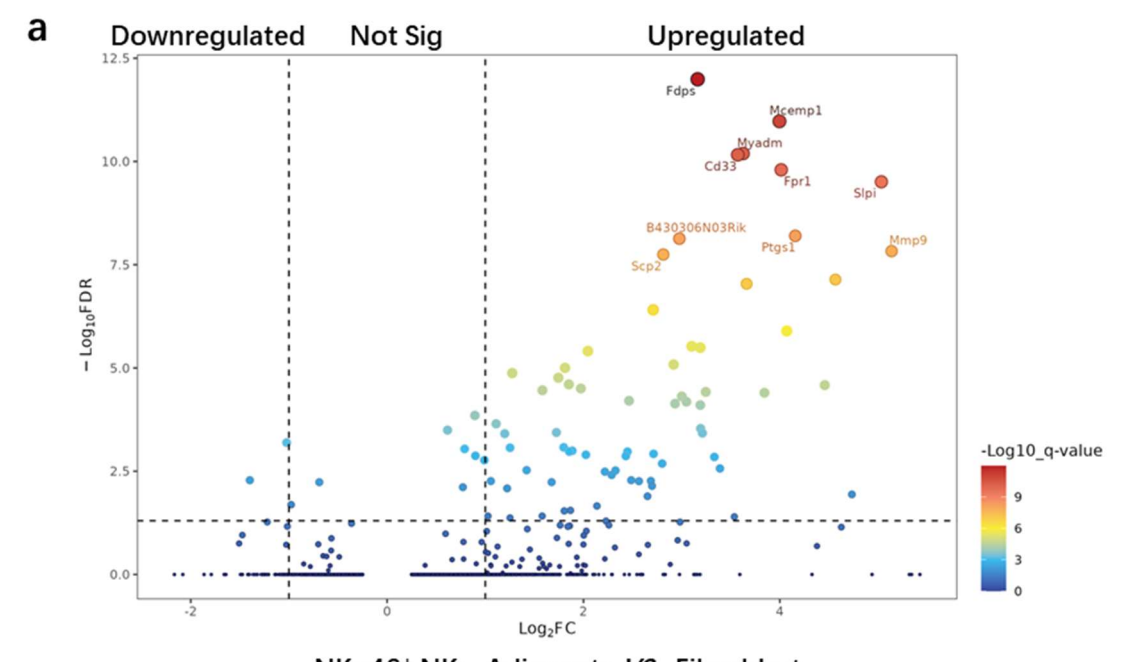


Figure 32 Bubble plot shows differentially expressed genes of NK cells involving myeloid makers, transcription factors, fatty acid uptake, inflammatory response and NK function. The dot plot represents normalized gene expression data organized into different functional categories, the color scale ranges representing Log2 Fold Change, the size of each dot showing the p-value.

We compared their expression with NK cells cocultured with fibroblast. The results revealed that high-fat conditions generally upregulated colony stimulating factor receptors, which are commonly highly expressed in myeloid cells during inflammatory responses (Figure 32). Meanwhile, lymphoid-related transcription factors, except for zbtb16, were suppressed, including gata3, Eomes, and ID2. Fatty acid uptake genes Fabp5, CD36, Lrp4 were increased, while the cytotoxicity function markers of NK cells mostly decreased.

4.5.3 Comparative gene set enrichment analysis of the differential expression genes in NKp46⁺ NK cell subsets

Although the number of NKp46⁺ NK cells differentiated under high-fat conditions was small, in order to minimize the impact of NK1.1⁺ NK cell heterogeneity on the results and to verify the consistency of previous conclusions, we selected only NKp46⁺ NK cells regardless of NK1.1 expression from both induction conditions for differential gene expression analysis.



NKp46+ NK: -Adipocyte VS -Fibroblast

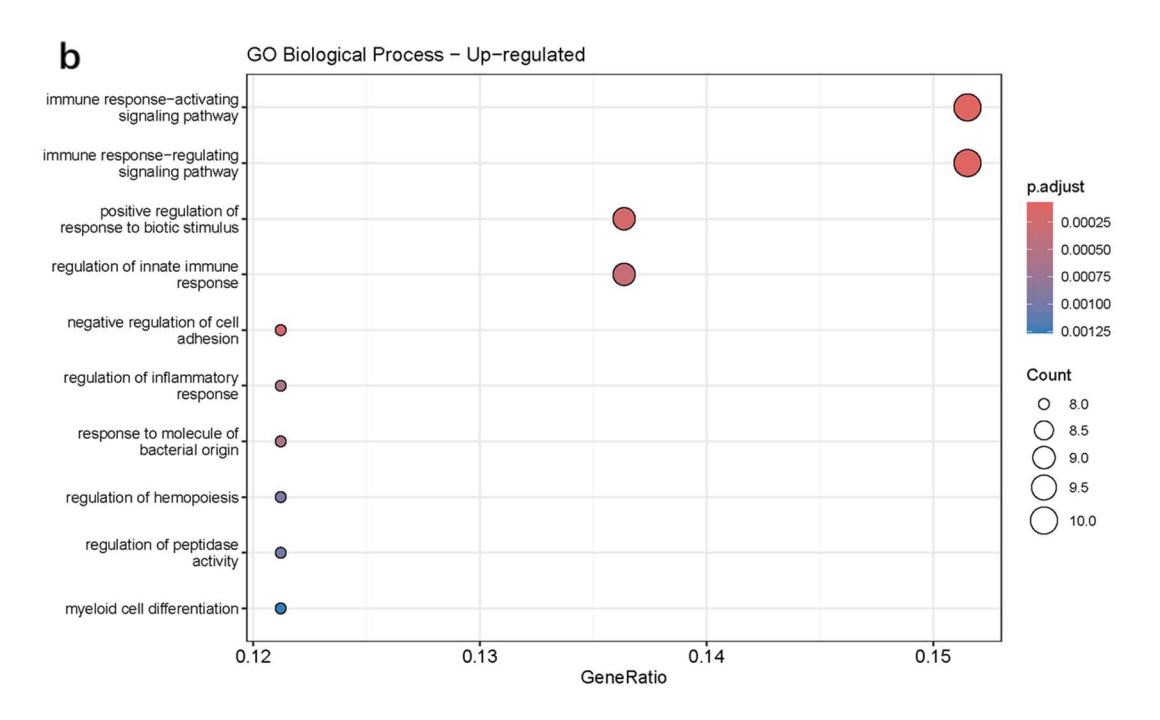


Figure 33 Upregulation of immune response activating signaling pathway and myeloid cell differentiation in NKp46⁺ NK cells from adipocyte coculture. a) volcano plots show significantly differentially expressed genes of NKp46⁺ NK cells induced from adipocyte and fibroblast coculture model; b) biological process gene ontology enrichment of upregulated genes from adipocyte induced NKp46⁺ NK cells. Among all statistically significant differentially expressed genes between the two conditions, 64 genes were upregulated, including CD33, a common myeloid marker, and Slpi, a myeloid-related transcription factor (Figure 33a) (Azevedo et al. 2024). Gene enrichment analysis revealed that these genes were most closely associated with NK cell immune response regulation pathways,

activation signal transduction pathways, and inflammatory responses (Figure 33b). Those results further validate that a high-fat environment leads to activation of NK cells and reveals regulatory differences in their differentiation.

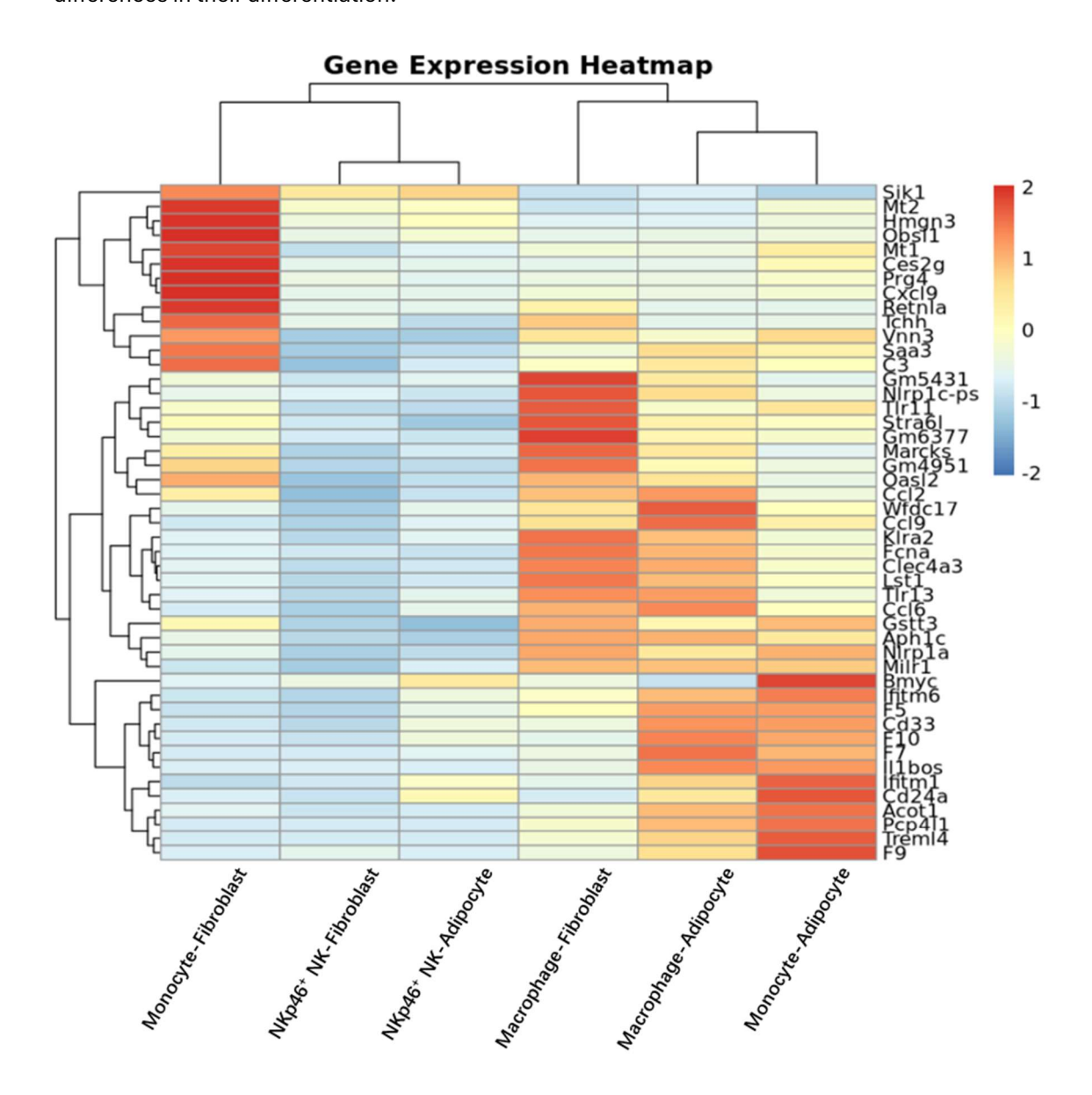


Figure 34 Comprehensive gene expression profiling of myeloid lineage and NKp46⁺ NK subsets from both differentiation conditions. The gene expression heatmap visualizes the differential expression of genes across both NK cell and myeloid lineage, indicating the heterogenicity among myeloid cells while the NKp46⁺ NK cells induced with adipocytes exhibit upregulation of some myeloid relevant markers and transcription factors.

Due to the upregulation of myeloid transcription factors in obesity associated NK cell, we performed unsupervised clustering gene expression analysis on these cell types to further reveal the similarities and distinctions between NK cells and myeloid cells. As shown in the figure 34,

although obesity associated NK cells upregulate certain myeloid markers, their gene expression pattern still exhibits significant heterogeneity compared to macrophages and monocytes while showing closer pattern to non-obese NK cell. This indicates that the high-fat environment can influence NK cell differentiation and regulation, but does not fundamentally alter the inherent characteristics of NK cells as lymphoid cells.

Additionally, we analyzed NKP46⁺ NK1.1⁺ and NKP46⁺ NK1.1⁻ cells, regardless of their group of origin. We performed an unsupervised gene set analysis (Sup 4), which revealed the heterogeneity of these two NK cell populations with higher myeloid transcription factor expression in NKP46⁺ NK1.1⁻ cells.

4.5.4 Pseudo-time analysis showing distinct differentiation regulation pathways of obesity-associated NK cells

Many biological processes manifest as a continuum of dynamic changes in the cellular state (Trapnell et al. 2014), to elucidate the differentiation regulatory patterns of obesity-associated NK cells, we performed pseudo-time trajectory analysis on progenitor cells, two distinct NK cell subtypes and monocytes (Figure 35). CMPs and CLPs occupy the highest positions in the hematopoietic differentiation hierarchy. A subset of CLPs first differentiates into NKp46+ NK cells, while the remaining progenitors give rise to myeloid-lineage monocytes. Under adipocyte cocultured obese condition, a portion of NK cells undergo differential regulation, ultimately giving rise to NK1.1+ obesity-associated NK cell subsets. Notably, cells following the obesity-related trajectory exhibit transcriptional shifts toward a more myeloid-like state, so we assume that obesity can alters NK cell differentiation dynamics leading to the upregulation of some myeloid cell highly expressed and pro-inflammatory genes.

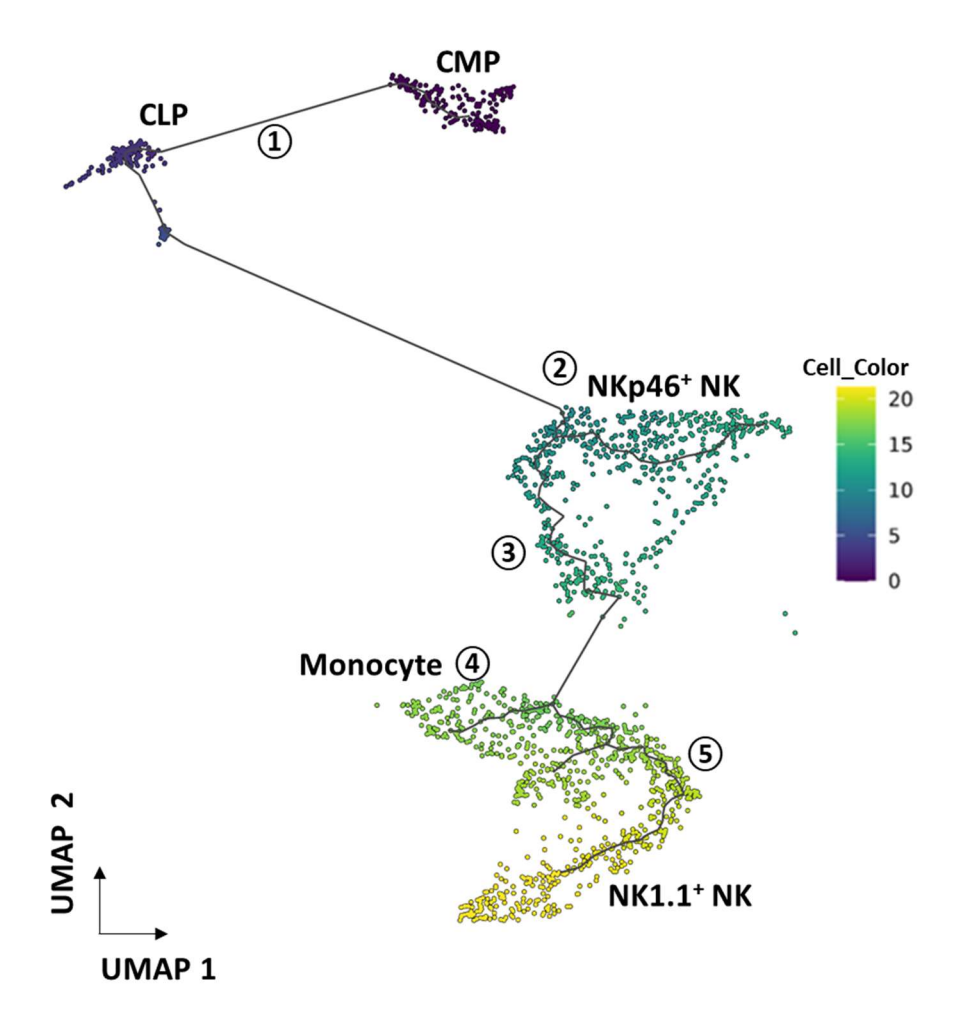


Figure 35 Pseudo-time analysis of single cell transcriptomic data identifies the obesity-associated NK cell differentiation hierarchy. The progenitor cells including CLP (common lymphoid progenitors) and CMP (common myeloid progenitors), distinct NK cell subtypes and monocytes are included in this analysis. The color gradient represents pseudo-time progression, with purple indicating early-stage cells and yellow denoting more differentiated cells. The trajectory reveals distinct lineage branches, suggesting divergence in the differentiation pathways of normal and obesity-associated NK cells.

There are 1740 significantly expressed genes in total were utilized to infer differentiation trajectories, among which we selected the 15 most critical and significantly expressed transcription factors for detailed characterization (Figure 36). We classified the dynamic expression patterns of 1,740 differentially expressed genes into five categories, resulting in five distinct clusters. Among these, 15 transcription factors associated with cell differentiation distributed across four clusters. These included factors highly expressed at the late stage of pseudo-time differentiation (e.g. Hoxa9, Myc, Myb, Cebpa), some upregulated during the intermediate stage (e.g. Irf8, Eomes, Zbtb32), factors predominantly expressed in the early stage (e.g. Irf1, Nfib, Ikzf4), and Cebpd which peaking in both early and late phase.

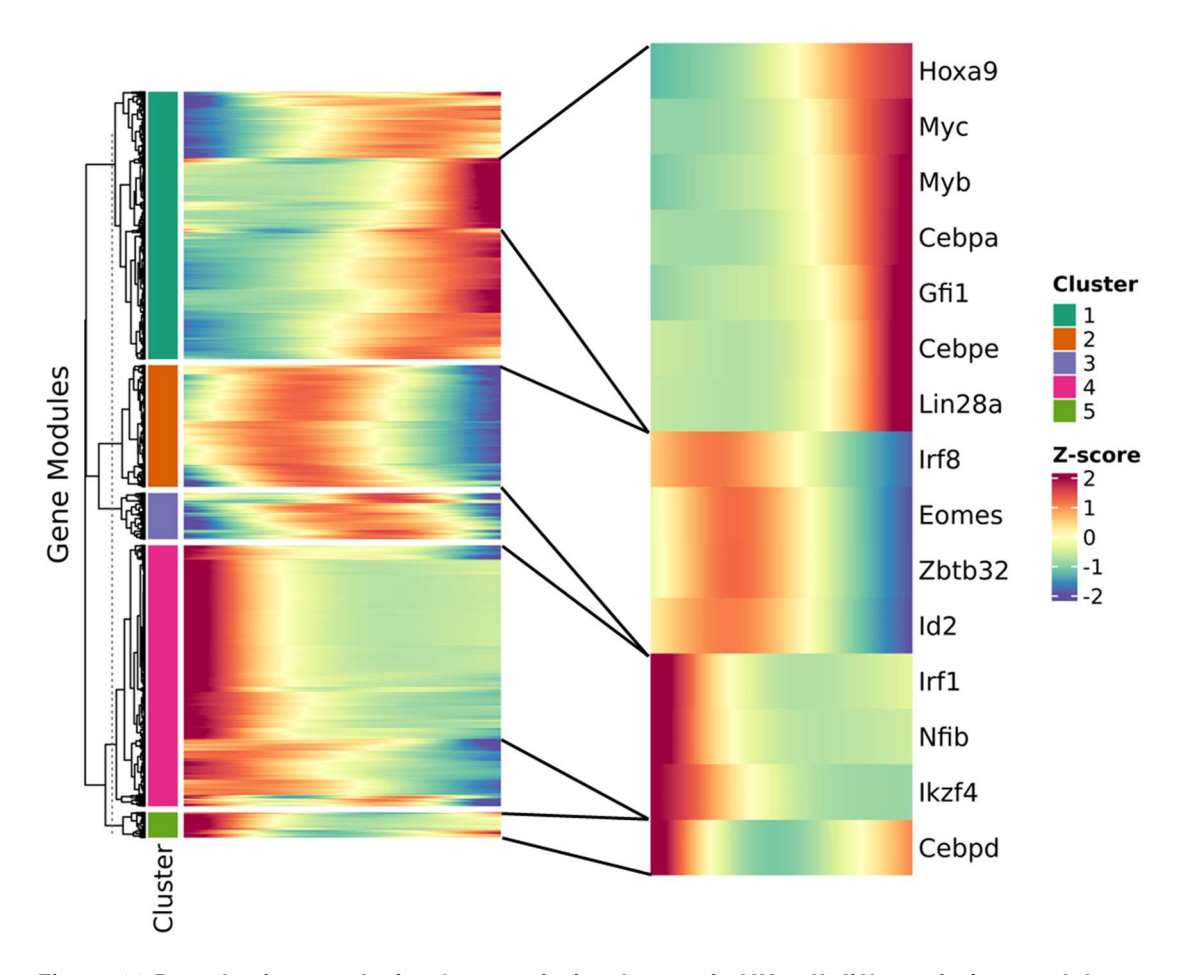


Figure 36 Pseudo-time analysis of transcription factors in NK cell differentiation model. The heatmap displaying gene expression patterns (1,740 genes) across different developmental stages. The right side presents a magnified view of 15 lineage-related and differential expressed transcription factors across these developmental stages from different gene cluster, including Hoxa9, Myc, Myb, Cebpa, Gfi1, Cebpe, Lin28a, Irf8, Eomes, Zbtb32, Id2, Irf1, Nfil3, Ikzf4, and Cebpd.

Next, we analyzed the dynamic changes and differential expression of 15 transcription factors across various lineage cells. We highlighted three transcription factors involved in myeloid and progenitor cell differentiation regulation (Figure 37) and three transcription factors related to lymphoid differentiation regulation (Figure 38). Results demonstrated that compared to NKp46⁺ NK cells, Cebpa, Gfi1, and Hoxa9 exhibited rapid upregulation followed by downregulation in the terminal stage (Figure 37). Cebpa as a key transcription factor drives the commitment of granulocyte and monocyte lineages which promotes myeloid-specific genes activation and repressing cell cycle progression (Porse et al. 2005). While Hoxa9 is important in early myeloid development, aberrant overexpression is associated with leukemogenesis (Sun et al. 2018). Those findings suggested they may be the primary co-regulatory transcription factors potentially participating in the upregulation mechanism of myeloid markers in NK1.1⁺ NK cells.

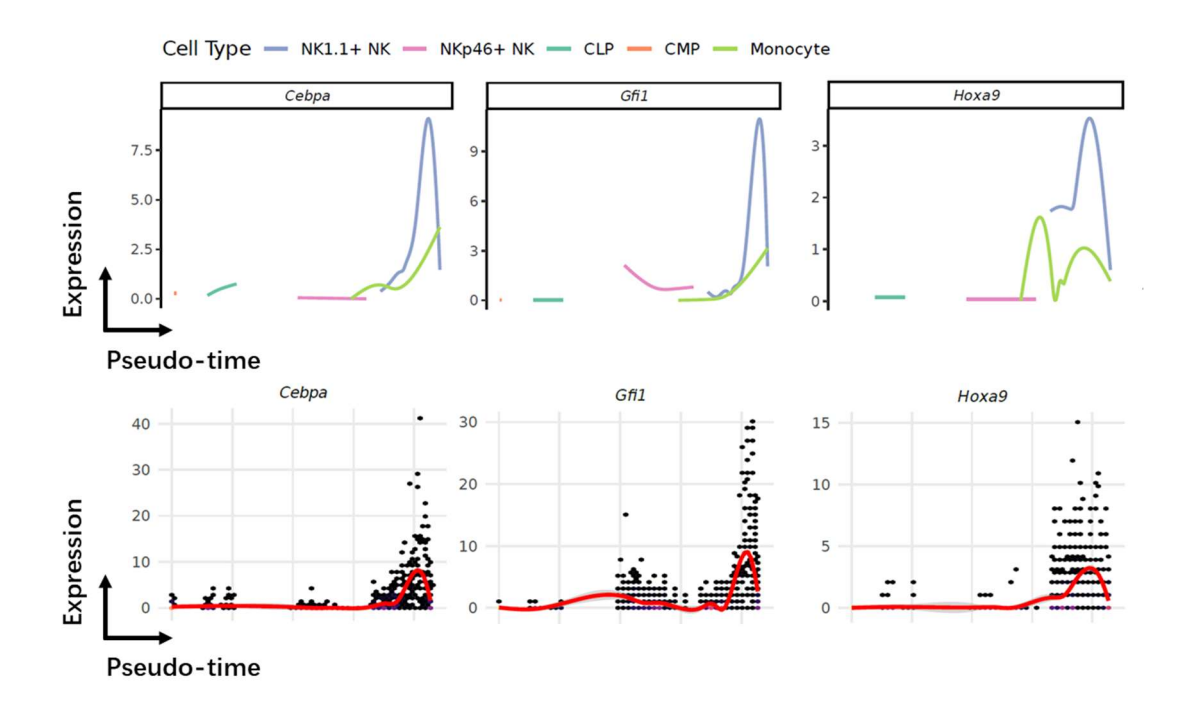


Figure 37 Pseudo-time analysis of Cebpa, Gfi1 and Hoxa9 transcription factors expression during cell lineage differentiation. The plots display the dynamic expression patterns of three myeloid related transcription factors (Cebpa, Gfi1, and Hoxa9) across different hematopoietic cell lineages over pseudo-time. The upper panel shows smoothed expression trajectories for each gene in distinct cell types, including NK1.1⁺ NK, NKp46⁺ NK, CLP (common lymphoid progenitors), CMP (common myeloid progenitors) and monocytes, with colors corresponding to each lineage. The lower panel displays single cell expression data (black dots) overlaid with a fitted red line representing average expression trends.

Additionally, lymphoid-associated transcription factors including Id2, Myb and Myc exhibited upregulation during both the intermediate and terminal stages of pseudo-time analysis in NK cells. We hypothesize that these transcription factors govern the maintenance of lymphoid identity characteristics of NK1.1⁺ cells, with Myc demonstrating the most significant upregulation among them (Figure 38). Myc is a well-known proto-oncogene, a key regulator of cell growth and metabolism (Dang 2012). In lymphoid cells, Myc supports proliferation and expansion during early development and activation, particularly both in T and B cell lineages. Its downregulation is often needed for full terminal differentiation (Dose et al. 2006). So, we hypothesize its increasing may play a vital role in obesity-associated NK cell formation.

Overall, these findings provide insights into how obesity reshapes NK cell fate and development into obesity-associated phenotype, which may contribute to improve functional impairments observed in metabolic disorders and obesity associated cancers.

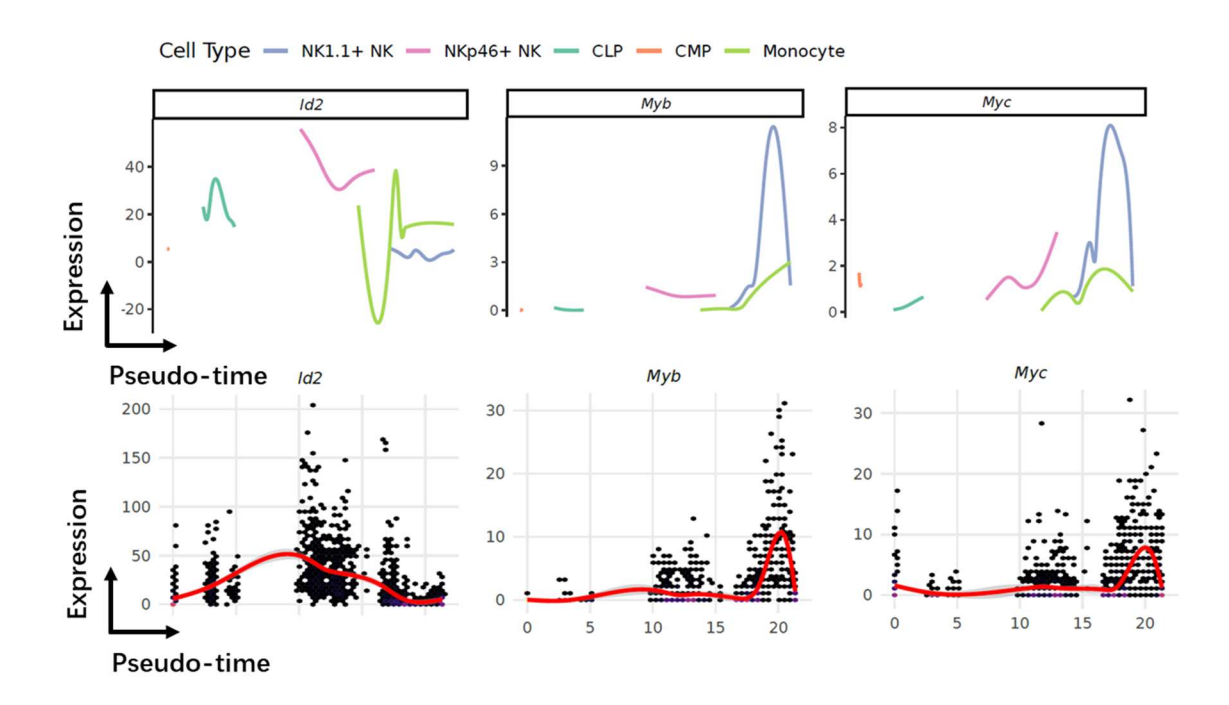


Figure 38 Pseudo-time analysis of Id2, Myb and Myc transcription factors expression during cell lineage differentiation. The plots display the dynamic expression patterns of three lymphoid related transcription factors (Id2, Myb and Myc) across different hematopoietic cell lineages over pseudo-time. The upper panel shows smoothed expression trajectories for each gene in distinct cell types. The lower panel displays single cell expression data (black dots) overlaid with a fitted red line representing average expression trends.

Discussion

5.1 Summary of the results

The herein presented data reveals we have established an in vitro model to differentiate NK cells from hematopoietic stem and progenitor cells. To investigate the impact of obesity on NK cell development and function, we incorporated palmitate in the culture medium or co-cultured the developing NK cells with adipocytes. Our results demonstrate that NK cells can be successfully generated in vitro under these conditions, and importantly, they upregulate pro-inflammatory receptors such as IL6R in response to the obese microenvironment. Additionally, High concentrations of palmitate (exceeding 100 µM) exhibit cytotoxic effects on various bone marrowderived cell lineages, with NK cells being the most affected. During the in vitro differentiation process, bone marrow-derived B cells gradually diminish due to the absence of stimulation, whereas T cells, NK cells, and NKT cells undergo expansion in response to IL-2 and IL-15 stimulation while myeloid cells remain viable throughout the differentiation process. Flow cytometry analysis revealed that under obesogenic conditions, in vitro-induced NK cells exhibit increased surface expression of the fatty acid transporter CD36, reduced activation levels, and decreased expression of both activating and inhibitory receptors. In contrast, the expression of myeloid-associated markers and inflammation-related receptors was upregulated. In functional assays, NK cells induced under obesogenic conditions displayed lower mitochondrial activity, reduced maximal oxygen consumption rate, and impaired glycolytic capacity compared to NK cells induced under normal conditions. Additionally, these NK cells exhibited a weakened ability to directly kill tumor cells. Single-cell transcriptomic RNA sequencing further confirmed transcriptional differences between the two NK cell populations. In obesity-associated NK cells, functional pathways were suppressed, while myeloid- and inflammation-related pathways were upregulated. Differences in differentiation trajectories were also observed, with obesityassociated NK cells exhibiting increased expression of myeloid-related transcription factors at the end of the pseudo-time trajectory. These findings closely resemble the NK cell phenotype and genetical regulation that we observed in obese mice from our previous research (Theurich et al. 2017).

5.2 The NK cell generation facilitated by cytokines in vitro

NK cell differentiation from HSCs in vitro typically requires a specific combination of cytokines that guide the development through various stages. Here we use the key cytokines include SCF, Flt-3L, IL-7, IL-2 and IL-15 to successfully induce NK differentiation from HSPCs. SCF could activate the c-kit receptor expressed on HSCs, triggering signaling pathways that prevent apoptosis and promote cell cycle entry (Zhang et al. 2008). It often works synergistically with other cytokines such as Flt-3L and interleukins to enhance HSC expansion and differentiation. Flt-3L that acts through the Flt3 receptor, a tyrosine kinase receptor expressed on primitive hematopoietic progenitors, to expand early multipotent progenitors and common lymphoid progenitors, providing a significant proliferative stimulus (Zriwil et al. 2018). IL-7 promotes survival of lymphoid progenitors by upregulating anti-apoptotic proteins like Bcl-2 and Mcl-1 while suppressing pro-apoptotic factors (D. Chen et al. 2021). Many publications (Grzywacz et al. 2006; Luevano et al. 2012; McCullar et al. 2008; Euchner et al. 2021; Dezell et al. 2012) show the high yield efficiency of those cytokines to promote NK cell differentiation from human or mouse stem cells. In our assays, with the combination of three cytokines in the first 8 days, the frequency of NK cells could be expanded to 10% from no more than 3% on the first day. On later stage, IL-2 and IL-15 signal through receptors containing the common gamma chain and IL-2/IL-15R beta chain, but differ in alpha chains to drive the development and differentiation of NK cells. IL-15 or IL-15Ra knockout mice show profound deficiencies in NK cell numbers (Koka et al. 2003). IL-15 is the primary cytokine supporting NK cell survival by upregulating anti-apoptotic molecules as well as promoting mitochondrial function, while IL-2 potently stimulates NK cell proliferation and activation, particularly at high doses. IL-2 typically provides strong but more transient activation signals compared to IL-15's more sustained effects (Waldmann 2015). Our experimental results indicate that by the final day, the proportion of NK cells ranges from 15% to 25% across different conditions. However, due to the presence of a mixed cell population in the culture system, T cell proliferation partially reduces the final proportion of NK cells. In summary, our differentiation protocol could eventually drive NK cell production from HSPCs.

5.3 Phenotypic differences in obesity-associated NK cells

In *in vivo* experiments, obesity associated NK cell is typically induced in mice with a high-fat diet. However, in our in vitro NK cell differentiation experiments, we simulated the obesogenic microenvironment using two approaches: (1) supplementing the culture medium with varying concentrations of palmitate, the most common saturated fatty acid, and (2) co-culturing cells with adipocytes.

Flow cytometry analysis showed that both approaches produced similar effects, leading to the differentiation of NK cells from HSPCs that exhibited upregulated IL6R and CSF1R expression. These NK cells shared key characteristics with those observed in the peripheral blood and adipose tissue of high-fat diet fed mice. Of note, this obesity-associated NK cell phenotype could not be directly induced from mature splenic NK cells, suggesting that their differentiation originates from earlier progenitor stages. Grzywacz. B (Grzywacz et al. 2011) use hydrocortisone and stromal cells to successfully drive the human myeloid progenitor cells including common myeloid progenitors and granulocytic-monocytic precursors differentiated into the NK-cell lineage. Interestingly, those NK cells have transient myeloid antigen expression along with developing. Our single-cell RNA sequencing results further also revealed that the obesogenic microenvironment induces increased expression of other myeloid markers in NK cells, such as CD11b and CD33. Additionally, several studies have previously examined the impact of obesity on murine NK cells, reporting variations in NK cell numbers and phenotypes across peripheral blood and organs (Bahr et al. 2020). However, the findings remain inconsistent. These discrepancies may stem from speciesor strain-specific metabolic differences, as well as variations in NK cell development, degradation, or migration dynamics. In our experiment, we observed that the obesogenic microenvironment led to a reduction in the activating receptor NKG2D, an increase in the inhibitory receptor KLRG1, and lower expression of the activation marker CD69 in NK cells. While other markers, such as Ly49C/I and NKG2A, exhibited differential expression compared to the control. These NK cell phenotypic findings are consistent with subsequent functional validation results.

5.4 Impaired NK cell function in obese environment

Obesity could be viewed as a low-grade chronic inflammation, the accumulation of lipids leads to

adipocyte hypertrophy, which induces the activation of pro-inflammatory pathways, especially by the NF_KB pathway (Cavaliere et al. 2023). The inflammatory cascades may result in an increase of reactive oxygen species generation and oxidative stress response. In mitochondrial stress and glycolysis assays, we observed a trend toward increased intracellular ROS and mitochondrial ROS levels in NK cells induced under obesogenic conditions, though the differences were not statistically significant. However, mitochondrial mass showed a significant reduction, and mitochondrial membrane potential exhibited a decreasing trend. These findings are consistent with results reported by other researchers (Gu et al. 2024; Poznanski et al. 2021; Zong et al. 2024). The obesity-associated alterations not only causing NK cell mitochondrial dysfunction, but impacting their functional parameters. Numerous studies have demonstrated obesity significantly impairs NK cell degranulation capacity and cytotoxicity against malignant cells (O'Shea et al. 2019; Bahr et al. 2020; Laue et al. 2015; Mylod et al. 2022). It has been proposed that the hyperactivated NK cells in obese individuals undergo more rapid exhaustion upon target cell exposure compared to those from individuals with normal weight, ultimately leading to a diminished ability to combat tumors and virus-infected cells (Canter et al. 2024). In ex vivo NK cell cytotoxicity assays, we also observed a significant reduction in the killing capacity against MC38 cell line of NK cells induced under obesogenic conditions after long-term coculture. In general, the obesogenic environment leads to mitochondrial dysfunction in NK cells, accompanied by a reduction in their cytotoxic function.

5.5 Transcriptomic profile differences of NK cells induced in different micro-environment

The obesity associated impact on immune cells are evaluated phenotypically and functionally. Furthermore, we utilize single-cell transcriptomic sequencing to analyses gene expression differences and developments in NK cells under distinct environmental conditions. Our data suggested a comprehensive upregulation of pro-inflammatory responses across different cell lineages, including cell adhesion molecules, cytokine-mediated signaling pathways, leukocyte chemotaxis related genes. Interestingly, fibroblast cocultured NK cells have higher expression of NKp46⁺, while the majority of adipocyte cocultured NK cells are NK1.1⁺. They form separate

clusters, indicating distinct transcriptional profiles. Myeloid relevant transcription factors and genes, fatty acid transporters, inflammation-related receptors are upregulated in obesity associated NK cell while genes related to NK cell function are downregulated. Those features also indicate how obesity increased meta-inflammation and impaired NK cell function. Ultimately, we performed pseudo-time analysis of single cell transcriptomic data identifying the obesity-associated NK cell differentiation hierarchy. The trajectory reveals distinct lineage branches, suggesting divergence in the differentiation pathways of normal and obesity-associated NK cells. Many transcription factors are involved in these regulatory interactions including Eomes, Zbtb32, Cebpe, Id2, Irf8 and so on. Among them, Cebpa, Gfi1, and Hoxa9 may be the primary co-regulatory transcription factors participating in the upregulation mechanism of myeloid markers in NK1.1+ NK cells. Nevertheless, Id2, Myb and Myc may govern the maintenance of lymphoid identity characteristics of NK1.1+ cells. All above, our data suggested a differential regulation of obesity associated NK cell development.

5.6 Clinical perspective in obesity associated cancer

In clinical research, the relationship between obesity, NK cell dysfunction, and increased cancer incidence represents a significant area of investigation. Studies have demonstrated that obesity impairs NK cell function through multiple mechanisms, contributing to obesity-associated cancer development such as liver cancer, colorectal cancer (Kolb et al. 2016). In obese individuals, NK cells exhibit reduced cytotoxicity and surveillance capacity, allowing pre-cancerous cells to evade immune detection. This dysfunction is partly due to obesity-associated alterations in activating receptors such as NKG2D and NKp46, which impair NK cells' ability to recognize stress ligands expressed on malignant cells (Naujoks et al. 2020). Additionally, expanded adipose tissue creates an immunosuppressive microenvironment with elevated inhibitory factors (IL-10, TGF-β) that further suppress NK cell function in tissues where obesity-associated cancers frequently develop (Q. Wu et al. 2021). The chronic inflammatory state characteristic of obesity simultaneously contributes to NK cell exhaustion while promoting genetic instability and tumor-promoting inflammation. Furthermore, metabolic competition between tumor cells and NK cells in the tumor microenvironment particularly disadvantages the already metabolically compromised NK cells in obese individuals. So, restoring NK cell function in obesity-associated cancers is a compelling

area of research with significant clinical implications. For example, NK cell could be applied to enhance the efficacy of conventional cancer treatments: chemotherapy-induced stress ligands could be better recognized by functionally competent NK cells (Okita et al. 2019); Antibody-based therapies would benefit from improved antibody-dependent cellular cytotoxicity of NK cell (Beelen et al. 2023); checkpoint inhibitor therapies might show enhanced efficacy with complementary NK cell activity (Andre et al. 2018).

The hypothesis that NK cell restoration improves outcomes is supported by several observations from clinical and preclinical studies. For instance, weight loss interventions in obese individuals have been associated with both improved NK cell function and reduced cancer risk (Bohm et al. 2022). Additionally, animal models of obesity show that adoptive transfer of functional NK cells can reduce tumor growth (Mylod et al. 2022). Also, Early-phase clinical trials of NK-based immunotherapies show signals of efficacy in cancers common in obesity (Morcillo-Martín-Romo et al. 2025). Last but not least, some data suggests that enhanced conditions favoring robust NK cell function correlate with better cancer outcomes (Freund-Brown et al. 2018).

Our research identifying upregulated biomarkers and uncovering regulatory mechanisms by transcription factors in NK cells from obese coculture environment represents a potentially valuable discovery that might lead to novel therapeutic approaches. Target pathway modulation from identified transcription factors such as Cebpa, Gfi1 which has enhanced activity in obesity, with small molecule inhibitors to restore normal NK cell differentiation. This approach allows for more precise intervention than general immune stimulation but of course need validation in further experiments. Besides, the upregulated biomarkers of IL6R or CSF1R that we discovered could serve as predictive biomarkers to identify which obese patients might benefit most from NK-restoring therapies or prognosis evaluation, enabling personalized treatment approaches. In summary, our research represents a perspective to understand the immune-microenvironment of obesity associated alterations in NK cells and reveals potential immunotherapeutic approaches to restore anti-tumor immunity in obesity-associated cancers.

Conclusion and Outlook

Conclusion

In this study, we investigated the impact of an obesogenic environment on NK cell differentiation and function using flow cytometry, functional assays and in vitro single-cell RNA sequencing. Our findings demonstrate that obesity alters the differentiation trajectory of NK cells, leading to a distinct transcriptional and phenotypic profile compared to NK cells generated under normal conditions. Specifically, NK cells induced in an obesogenic environment exhibit a shift toward a more myeloid-like phenotype, characterized by upregulation of myeloid-associated transcription factors and pro-inflammatory receptors. These changes are consistent with those observed in high fat diet fed obese mice, suggesting that obesity reshapes NK cell development at an early progenitor stage rather than solely modifying mature NK cells.

Functionally, obesity-associated NK cells exhibit impaired metabolic and cytotoxic capacity, as evidenced by reduced mitochondrial respiration and glycolysis, increased exhaustion receptor expression. Mitochondrial dysfunction, including decreased mitochondrial mass and membrane potential, as well as increased oxidative stress, likely contributes to the functional exhaustion of these NK cells. Importantly, long-term coculture experiments confirmed that obesity-induced NK cells have a diminished ability to eliminate target cells, reinforcing the link between metabolic stress and NK cell dysfunction.

Outlook

These findings provide important insights into the mechanisms by which obesity shapes NK cell differentiation and function, with potential implications for immune surveillance and metabolic disorders. However, several questions remain open for future exploration. First, the precise molecular pathways driving NK cell reprogramming in an obesogenic environment warrant further investigation, particularly the role of metabolic regulators and epigenetic modifications. Second, whether these obesity-associated NK cells contribute to systemic inflammation or immune dysfunction in human remains to be clarified, necessitating further validation in human studies. Additionally, targeting metabolic pathways to restore NK cell function presents a promising therapeutic avenue. Strategies such as modulating fatty acid metabolism, enhancing mitochondrial fitness, or reversing myeloid-like reprogramming could be tried to rescue NK cell

Conclusion

cytotoxicity in obesity-related diseases. Future research should explore whether metabolic interventions, can restore NK cell function and improve immune surveillance in obesity-related conditions. Overall, this study highlights the profound effects of obesity on NK cell differentiation and function, underscoring the need for further research into metabolic-immune interactions and potential therapeutic strategies to counteract obesity-induced immune dysfunction.

Supplementary

Supplementary Figures

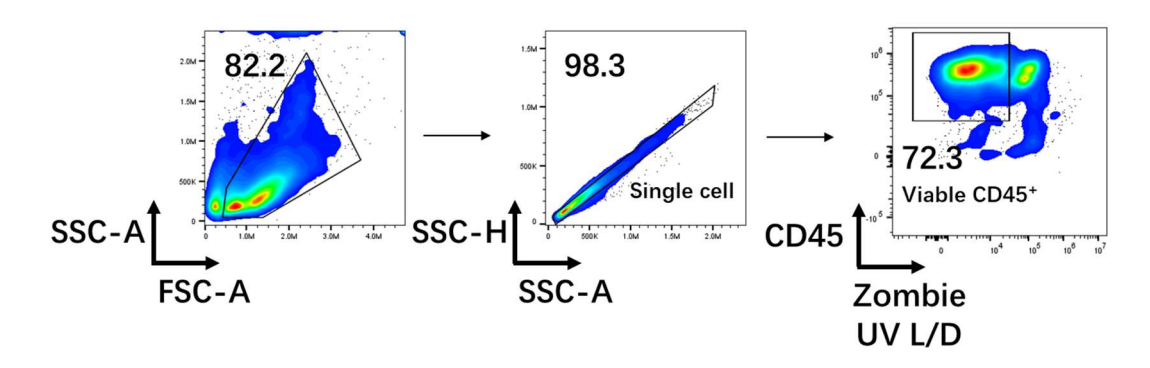


Figure S1 Gating strategy of viable hematopoietic cells. The viable cells for further lineage analysis were gated on mononuclear cell, single cell and Zombie UV Live/Dead negative but CD45 positive cell.

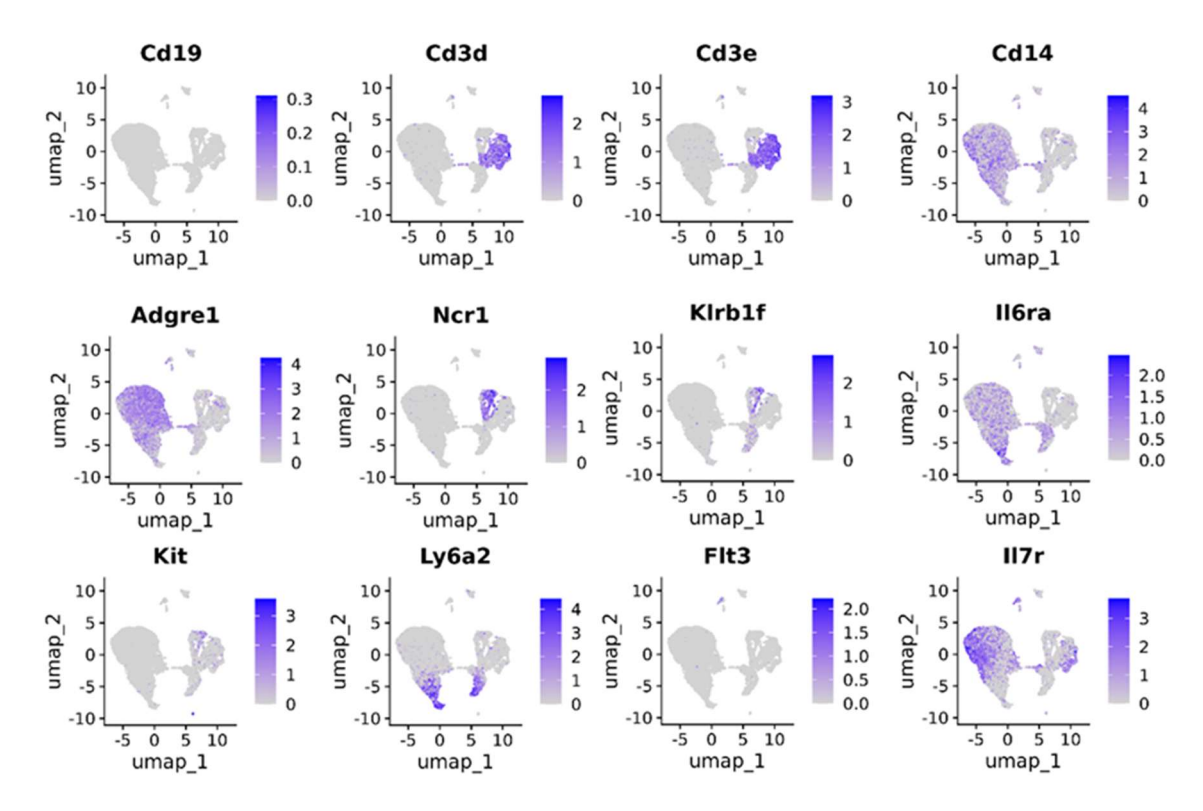


Figure S2 Single cell RNA-seq analysis of key marker genes for cell type annotation. Genes used for cell type annotation including: B cell CD19⁺ CD3⁻ F4/80⁻ CD14⁻ Ncr Klrb1f⁻ Kit⁻ Sca1⁻ Flt3⁻ IL7r; T cell CD19⁻ CD3⁺ F4/80⁻ CD14⁻ Ncr⁻ Klrb1f⁻ IL7r^{-/+}; NKT cell CD19⁻ CD3⁺ F4/80⁻ CD14⁻ Ncr⁺ Klrb1f⁺ IL7r^{-/+}; Macrophage or Monocyte CD19⁻ CD3⁻ F4/80⁺ CD14⁺ Ncr Klrb1f⁻ IL7r^{-/+}; NK cell CD19⁻ CD3⁻ F4/80⁻ CD14⁻ Ncr⁺ or Klrb1f⁺ IL7r^{-/+}; HSPC Lin⁻ Sca1⁻ c-kit⁺; CMP Lin⁻ Sca1⁻ c-kit⁺ Il7r⁺.

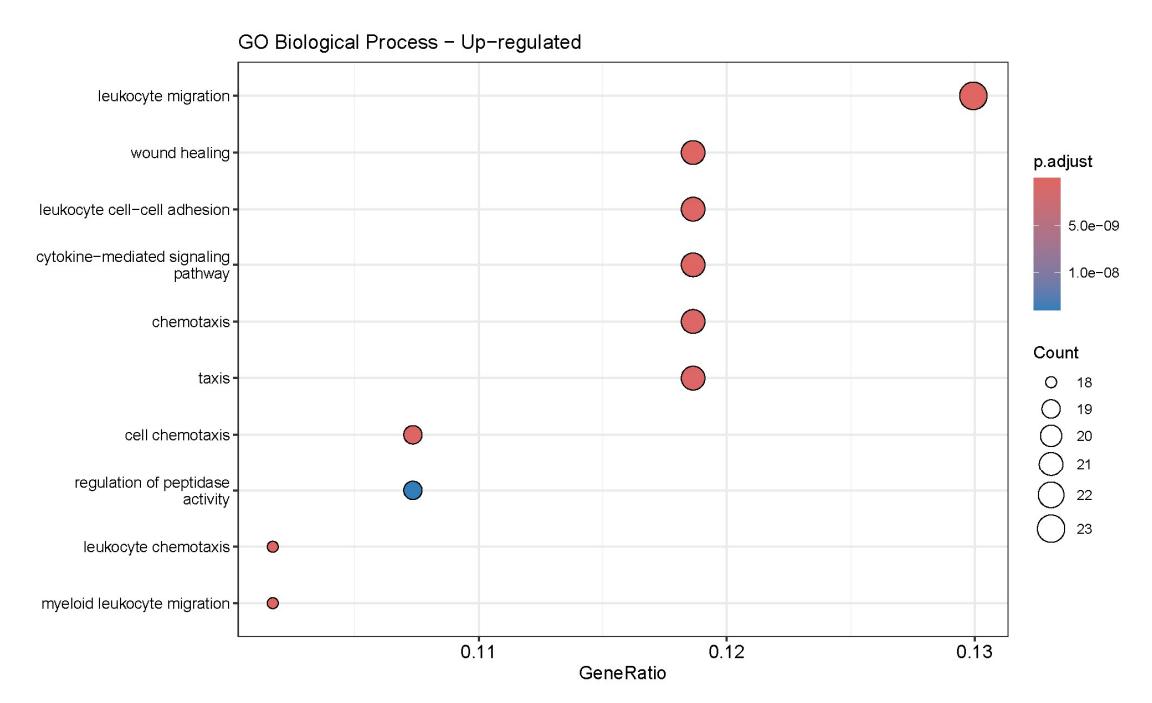


Figure S3 Upregulation of adhesion molecules, cytokine-mediated signaling pathways, leukocyte chemotaxis in cells induced from adipocyte coculture. Biological process gene ontology is enriched by upregulated genes of adipocyte cocultured cells.

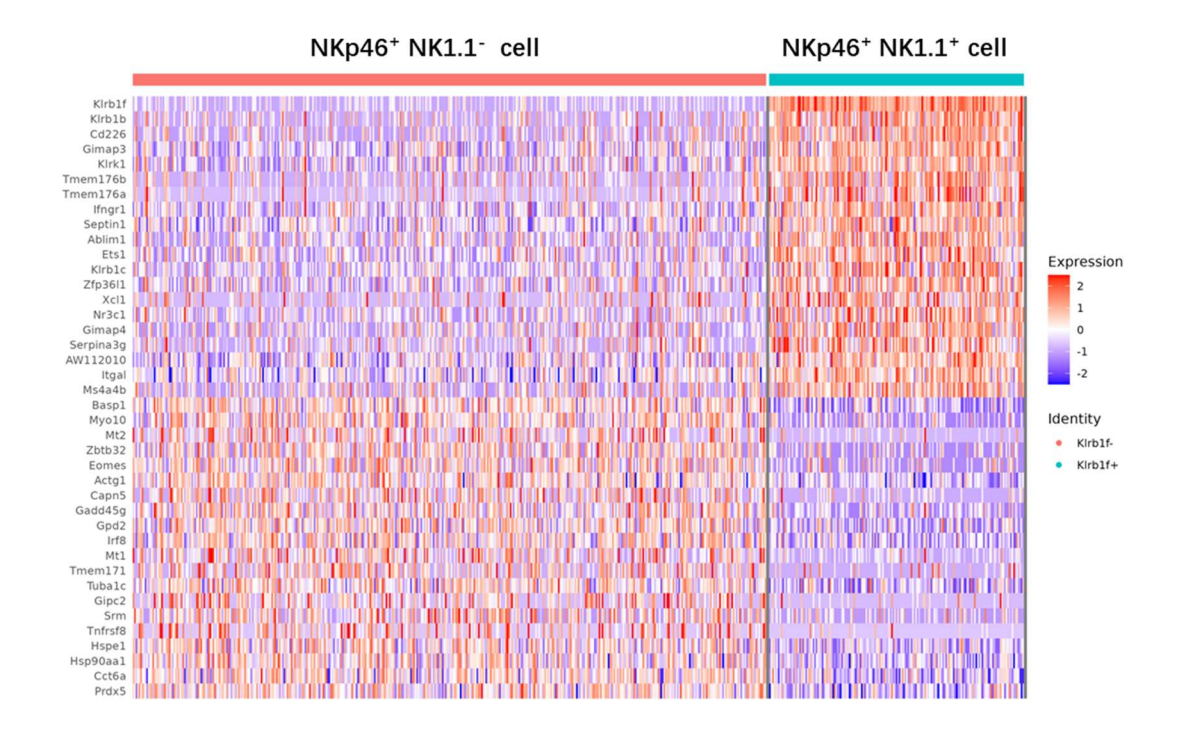


Figure S4 Unsupervised gene set analysis revealed higher myeloid transcription factor expression in NKP46⁺ NK1.1⁻ cells. NKP46⁺ NK1.1⁺ and NKP46⁺ NK1.1⁻ cells regardless of their origin were analyzed by unsupervised gene set analysis revealing the heterogeneity within NKp46⁺ cells.

List of Figures

Figure 1 Key makers of murine NK cell at distinct developmental stages from HSC.	5
Figure 2 Mechanism of NK cell recognition and killing against target cell.	8
Figure 3 Phenotypically and functionally adaptation of NK cell in obesity.	12
Figure 4 Schematic presentation of project objectives.	14
Figure 5 Identification of hematopoietic stem cells, NK cell progenitors, and NK cells in murin	ne
bone marrow.	26
Figure 6 In Vitro NK cell differentiation protocol.	27
Figure 7 Dynamic changes in lymphoid and myeloid lineage populations during in vitro NK ce	ll
differentiation.	29
Figure 8 Dose-dependent cytotoxicity of palmitate on different cell lineages during NK cell	
differentiation.	30
Figure 9 Dose-dependent effects of palmitate on cell lineage composition on D16.	31
Figure 10 Palmitate-induced CD36 expression variations in different cell lineages.	32
Figure 11 Palmitate-induced IL6R and CSF1R expression variations in different cell lineages.	33
Figure 12 Frequency of bone marrow and spleen derived IL6R and CSF1R positive obesity-	
associated NK cells.	34
Figure 13 Differential expression of CD36 and CD11b on NK cell subpopulations.	35
Figure 14 Fibroblast and adipocyte morphology and experimental workflow for NK Cell	
differentiation in coculture model.	37
Figure 15 Cell viability during NK cell differentiation in diverse coculture conditions.	37
Figure 16 Cell lineage composition on day 16 in diverse coculture conditions.	38
Figure 17 Dynamic changes in IL6R and CSF1R expression across cell lineages in different	
culture conditions.	39
Figure 18 Frequency of bone marrow and spleen derived IL6R and CSF1R positive obesity-	
associated NK cells in different coculture model.	40
Figure 19 Differential expression of CD27 and CD11b on NK cell subpopulations.	41
Figure 20 Phenotypic of key receptors between bone marrow derived NK cells co-cultured wi	th
adipocytes or fibroblasts.	42
Figure 21 Phenotypic of maturation differences between bone marrow derived NK cells	
subpopulation.	43
Figure 22 Decreased mitochondrial respiration of NK cells from adipocyte coculture model.	45
Figure 23 Decreased glycolysis capacity of NK cells from adipocyte coculture model.	45
Figure 24 Flow cytometry analysis of oxidative stress and mitochondrial parameters between	1
bone marrow derived fibroblast cocultured and adipocyte cocultured NK Cells.	47
Figure 25 Fluorescence microscopy of mitochondrial mass and potential indicate a fitter	
mitochondrial of fibroblast cocultured NK cells.	48
Figure 26 Ex Vivo fibroblast cocultured NK cells exhibit superior killing capacity against MC38	
cell line.	48
Figure 27 The experimental workflow for analyzing NK cell differentiation under different	
conditions using single-cell RNA sequencing.	50
Figure 28 Single-cell RNA sequencing reveals transcriptomic changes of NK cells in different	
coculture conditions.	50

Figure 29 Volcano plots across Pan-cell types show generally transcriptomic variations in				
different coculture conditions.	51			
Figure 30 UpSet and Venn plots across all cell types indicate shared up- or down-regulated				
genes in different cell lineages.	52			
Figure 31 Upregulation of fatty acid metabolism related genes in NK cells induced from				
adipocyte coculture.	54			
Figure 32 Bubble plot shows differentially expressed genes of NK cells involving myeloid makers,				
transcription factors, fatty acid uptake, inflammatory response and NK function.	55			
Figure 33 Upregulation of immune response activating signaling pathway and myeloid cell				
differentiation in NKp46 ⁺ NK cells from adipocyte coculture.	56			
Figure 34 Comprehensive gene expression profiling of myeloid lineage and NKp46 ⁺ NK subsets				
from both differentiation conditions.	57			
Figure 35 Pseudo-time analysis of single cell transcriptomic data identifies the obesity-				
associated NK cell differentiation hierarchy.	59			
Figure 36 Pseudo-time analysis of transcription factors in NK cell differentiation model.	60			
Figure 37 Pseudo-time analysis of Cebpa, Gfi1 and Hoxa9 transcription factors expression during				
cell lineage differentiation.	61			
Figure 38 Pseudo-time analysis of Id2, Myb and Myc transcription factors expression during cell				
lineage differentiation.	62			
Figure S1 Gating strategy of viable hematopoietic cells.	71			
Figure S2 Single cell RNA-seq analysis of key marker genes for cell type annotation.	71			
Figure S3 Upregulation of adhesion molecules, cytokine-mediated signaling pathways, leukocyte				
chemotaxis in cells induced from adipocyte coculture.	72			
Figure S4 Unsupervised gene set analysis revealed higher myeloid transcription factor				
expression in NKP46 ⁺ NK1.1 ⁻ cells.	72			

List of Abbreviations

μM	Micromolar
2-DG	2-Deoxyglucose
ADCC	Antibody-Dependent Cellular Cytotoxicity
BM	Bone Marrow
BSA	Bovine Serum Albumin
CCL	C-C Motif Chemokine Ligand
CD	Cluster of Differentiation
CLP	Common Lymphoid Progenitor
СМР	Common Myeloid Progenitor
CMV	Cytomegalovirus
CSF1R	Colony Stimulating Factor 1 Receptor
CXCL	C-X-C Motif Chemokine Ligand
DAMPs	Damage-Associated Molecular Patterns
ECAR	Extracellular Acidification Rate
GM-CSF	Granulocyte-Macrophage Colony-Stimulating Factor
HSC	Hematopoietic Stem Cell
IFN-γ	Interferon-gamma
IL6R	Interleukin 6 Receptor
iNK	immature NK cell
KIR	Killer Cell Immunoglobulin-Like Receptor
LSK	Lin ⁻ Sca-1 ⁺ c-Kit ⁺
MFI	Mean Fluorescent Intensity
MHC-I	Major Histocompatibility Complexes I
MLP	Multi-Lymphoid Progenitor
mM	Millimolar
mNK	Mature NK
mSOX	Mitochondrial Superoxide
NAFLD	Non-Alcoholic Fatty Liver Disease
NCR	Natural Cytotoxicity Receptor
NK	Natural Killer
NKP	NK Cell Progenitor
NS	Non-Significant
OCR	Oxygen Consumption Rate
OXPHOS	Oxidative Phosphorylation
PAMPs	Pathogen-associated molecular patterns
ROS	Reactive Oxygen Species
SCF	Stem Cell Factor
scRNA-seq	Single-Cell RNA Sequencing
SP	Splenocyte
SRC	Spare Respiratory Capacity
TLR	Toll-like Receptors

TNF-α	Tumor Necrosis Factor-alpha
TRAIL	Tumor necrosis factor-related apoptosis-inducing ligand
UMAP	Uniform Manifold Approximation and Projection
XCL	X-C Motif Chemokine Ligand

References

- Ali, A. K., Nandagopal, N., & Lee, S. H. (2015). IL-15-PI3K-AKT-mTOR: A Critical Pathway in the Life Journey of Natural Killer Cells. *Front Immunol*, 6, 355. doi:10.3389/fimmu.2015.00355
- Andersen, C. J., Murphy, K. E., & Fernandez, M. L. (2016). Impact of Obesity and Metabolic Syndrome on Immunity. *Adv Nutr, 7*(1), 66-75. doi:10.3945/an.115.010207
- Andre, P., Denis, C., Soulas, C., Bourbon-Caillet, C., Lopez, J., Arnoux, T., Blery, M., Bonnafous, C., Gauthier, L., Morel, A., Rossi, B., Remark, R., Breso, V., Bonnet, E., Habif, G., Guia, S., Lalanne, A. I., Hoffmann, C., Lantz, O., Fayette, J., Boyer-Chammard, A., Zerbib, R., Dodion, P., Ghadially, H., Jure-Kunkel, M., Morel, Y., Herbst, R., Narni-Mancinelli, E., Cohen, R. B., & Vivier, E. (2018). Anti-NKG2A mAb Is a Checkpoint Inhibitor that Promotes Anti-tumor Immunity by Unleashing Both T and NK Cells. *Cell*, *175*(7), 1731-1743 e1713.
- Augustyniak, K., Lesniak, M., Golan, M. P., Latka, H., Wojtan, K., Zdanowski, R., Kubiak, J. Z., & Malek, K. (2024). Chemical Landscape of Adipocytes Derived from 3T3-L1 Cells Investigated by Fourier Transform Infrared and Raman Spectroscopies. *Int J Mol Sci*, 25(22). doi:10.3390/ijms252212274
- Azevedo, P. L., Maradei, S., de Sa Bigni, R., Santos Ramires Aragao, J., Abdelhay, E., & Binato, R. (2024). SLPI overexpression in hMSCs could be implicated in the HSC gene expression profile in AML. *Sci Rep, 14*(1), 15550. doi:10.1038/s41598-024-66400-7
- Bahr, I., Spielmann, J., Quandt, D., & Kielstein, H. (2020). Obesity-Associated Alterations of Natural Killer Cells and Immunosurveillance of Cancer. *Front Immunol, 11*, 245. doi:10.3389/fimmu.2020.00245
- Bald, T., Krummel, M. F., Smyth, M. J., & Barry, K. C. (2020). The NK cell-cancer cycle: advances and new challenges in NK cell-based immunotherapies. *Nat Immunol*, *21*(8), 835-847. doi:10.1038/s41590-020-0728-z
- Baranek, T., Morello, E., Valayer, A., Aimar, R. F., Brea, D., Henry, C., Besnard, A. G.,
 Dalloneau, E., Guillon, A., Dequin, P. F., Narni-Mancinelli, E., Vivier, E., Laurent,
 F., Wei, Y., Paget, C., & Si-Tahar, M. (2017). FHL2 Regulates Natural Killer Cell
 Development and Activation during Streptococcus pneumoniae Infection. Front
 Immunol, 8, 123. doi:10.3389/fimmu.2017.00123
- Barnes, S., Schilizzi, O., Audsley, K. M., Newnes, H. V., & Foley, B. (2020). Deciphering the Immunological Phenomenon of Adaptive Natural Killer (NK) Cells and Cytomegalovirus (CMV). *Int J Mol Sci, 21*(22). doi:10.3390/ijms21228864
- Batlle, E., & Massague, J. (2019). Transforming Growth Factor-beta Signaling in Immunity and Cancer. *Immunity*, *50*(4), 924-940. doi:10.1016/j.immuni.2019.03.024
- Beaulieu, A. M. (2021). Transcriptional and epigenetic regulation of memory NK cell responses. *Immunol Rev, 300*(1), 125-133. doi:10.1111/imr.12947
- Beelen, N. A., Aberle, M. R., Bruno, V., Olde Damink, S. W. M., Bos, G. M. J., Rensen, S. S., & Wieten, L. (2023). Antibody-dependent cellular cytotoxicity-inducing

- antibodies enhance the natural killer cell anti-cancer response against patient-derived pancreatic cancer organoids. *Front Immunol, 14*, 1133796. doi:10.3389/fimmu.2023.1133796
- Benayoun, B. A., Pollina, E. A., Ucar, D., Mahmoudi, S., Karra, K., Wong, E. D., Devarajan, K., Daugherty, A. C., Kundaje, A. B., Mancini, E., Hitz, B. C., Gupta, R., Rando, T. A., Baker, J. C., Snyder, M. P., Cherry, J. M., & Brunet, A. (2014). H3K4me3 breadth is linked to cell identity and transcriptional consistency. *Cell*, *158*(3), 673-688. doi:10.1016/j.cell.2014.06.027
- Berbudi, A., Khairani, S., & Tjahjadi, A. I. (2025). Interplay Between Insulin Resistance and Immune Dysregulation in Type 2 Diabetes Mellitus: Implications for Therapeutic Interventions. *Immunotargets Ther, 14*, 359-382. doi:10.2147/ITT.S499605
- Bi, J., & Wang, X. (2020). Molecular Regulation of NK Cell Maturation. *Front Immunol, 11*, 1945. doi:10.3389/fimmu.2020.01945
- Bjorkstrom, N. K., Strunz, B., & Ljunggren, H. G. (2022). Natural killer cells in antiviral immunity. *Nat Rev Immunol*, 22(2), 112-123. doi:10.1038/s41577-021-00558-3
- Bohm, M. S., Sipe, L. M., Pye, M. E., Davis, M. J., Pierre, J. F., & Makowski, L. (2022). The role of obesity and bariatric surgery-induced weight loss in breast cancer.

 Cancer Metastasis Rev, 41(3), 673-695. doi:10.1007/s10555-022-10050-6
- Brookheart, R. T., Michel, C. I., & Schaffer, J. E. (2009). As a matter of fat. *Cell Metab,* 10(1), 9-12. doi:10.1016/j.cmet.2009.03.011
- Canter, R. J., Judge, S. J., Collins, C. P., Yoon, D. J., & Murphy, W. J. (2024). Suppressive effects of obesity on NK cells: is it time to incorporate obesity as a clinical variable for NK cell-based cancer immunotherapy regimens? *J Immunother Cancer*, 12(3). doi:10.1136/jitc-2023-008443
- Cavaliere, G., Cimmino, F., Trinchese, G., Catapano, A., Petrella, L., D'Angelo, M., Lucchin, L., & Mollica, M. P. (2023). From Obesity-Induced Low-Grade Inflammation to Lipotoxicity and Mitochondrial Dysfunction: Altered Multi-Crosstalk between Adipose Tissue and Metabolically Active Organs.

 Antioxidants (Basel), 12(6). doi:10.3390/antiox12061172
- Chan, C. J., Smyth, M. J., & Martinet, L. (2014). Molecular mechanisms of natural killer cell activation in response to cellular stress. *Cell Death Differ, 21*(1), 5-14. doi:10.1038/cdd.2013.26
- Chen, D., Tang, T.-X., Deng, H., Yang, X.-P., & Tang, Z.-H. (2021). Interleukin-7 Biology and Its Effects on Immune Cells: Mediator of Generation, Differentiation, Survival, and Homeostasis. *Frontiers in Immunology, 12*. doi:10.3389/fimmu.2021.747324
- Chen, X., Shi, C., He, M., Xiong, S., & Xia, X. (2023). Endoplasmic reticulum stress: molecular mechanism and therapeutic targets. *Signal Transduct Target Ther,* 8(1), 352. doi:10.1038/s41392-023-01570-w
- Chen, Y., Zhang, J., Cui, W., & Silverstein, R. L. (2022). CD36, a signaling receptor and fatty acid transporter that regulates immune cell metabolism and fate. *J Exp Med*, 219(6). doi:10.1084/jem.20211314
- Crinier, A., Milpied, P., Escaliere, B., Piperoglou, C., Galluso, J., Balsamo, A., Spinelli, L.,

- Cervera-Marzal, I., Ebbo, M., Girard-Madoux, M., Jaeger, S., Bollon, E., Hamed, S., Hardwigsen, J., Ugolini, S., Vely, F., Narni-Mancinelli, E., & Vivier, E. (2018). High-Dimensional Single-Cell Analysis Identifies Organ-Specific Signatures and Conserved NK Cell Subsets in Humans and Mice. *Immunity, 49*(5), 971-986 e975. doi:10.1016/j.immuni.2018.09.009
- Damele, L., Montaldo, E., Moretta, L., Vitale, C., & Mingari, M. C. (2018). Effect of Tyrosin Kinase Inhibitors on NK Cell and ILC3 Development and Function. *Front Immunol*, 9, 2433. doi:10.3389/fimmu.2018.02433
- Dang, C. V. (2012). MYC on the path to cancer. *Cell, 149*(1), 22-35. doi:10.1016/j.cell.2012.03.003
- de Andrade, A. G., Vanderley, S. E. R., de Farias Marques, L., Almeida, F. S., Cavalcante-Silva, L. H. A., & Keesen, T. S. L. (2025). Leptin, NK cells, and the weight of immunity: Insights into obesity. *Int Immunopharmacol, 147*, 113992. doi:10.1016/j.intimp.2024.113992
- De Barra, C., O'Shea, D., & Hogan, A. E. (2023). NK cells vs. obesity: A tale of dysfunction & redemption. *Clin Immunol*, 255, 109744. doi:10.1016/j.clim.2023.109744
- Dezell, S. A., Ahn, Y. O., Spanholtz, J., Wang, H., Weeres, M., Jackson, S., Cooley, S., Dolstra, H., Miller, J. S., & Verneris, M. R. (2012). Natural killer cell differentiation from hematopoietic stem cells: a comparative analysis of heparin- and stromal cell-supported methods. *Biol Blood Marrow Transplant*, 18(4), 536-545. doi:10.1016/j.bbmt.2011.11.023
- Di Vito, C., Mikulak, J., & Mavilio, D. (2019). On the Way to Become a Natural Killer Cell. Front Immunol, 10, 1812. doi:10.3389/fimmu.2019.01812
- Dose, M., Khan, I., Guo, Z., Kovalovsky, D., Krueger, A., von Boehmer, H., Khazaie, K., & Gounari, F. (2006). c-Myc mediates pre-TCR-induced proliferation but not developmental progression. *Blood*, *108*(8), 2669-2677. doi:10.1182/blood-2006-02-005900
- Euchner, J., Sprissler, J., Cathomen, T., Fürst, D., Schrezenmeier, H., Debatin, K.-M., Schwarz, K., & Felgentreff, K. (2021). Natural Killer Cells Generated From Human Induced Pluripotent Stem Cells Mature to CD56brightCD16+NKp80+/-In-Vitro and Express KIR2DL2/DL3 and KIR3DL1. *Frontiers in Immunology, 12*. doi:10.3389/fimmu.2021.640672
- Freund-Brown, J., Chirino, L., & Kambayashi, T. (2018). Strategies to enhance NK cell function for the treatment of tumors and infections. *Crit Rev Immunol*, 38(2), 105-130. doi:10.1615/CritRevImmunol.2018025248
- Grzywacz, B., Kataria, N., Kataria, N., Blazar, B. R., Miller, J. S., & Verneris, M. R. (2011).

 Natural killer-cell differentiation by myeloid progenitors. *Blood, 117*(13), 3548-3558. doi:10.1182/blood-2010-04-281394
- Grzywacz, B., Kataria, N., Sikora, M., Oostendorp, R. A., Dzierzak, E. A., Blazar, B. R., Miller, J. S., & Verneris, M. R. (2006). Coordinated acquisition of inhibitory and activating receptors and functional properties by developing human natural killer cells. *Blood*, *108*(12), 3824-3833. doi:10.1182/blood-2006-04-020198
- Gu, M., Zhang, Y., Lin, Z., Hu, X., Zhu, Y., Xiao, W., Jia, X., Chen, W., Lu, G., & Gong, W. (2024). Decrease in UCP1 by sustained high lipid promotes NK cell necroptosis

- to exacerbate nonalcoholic liver fibrosis. *Cell Death Dis, 15*(7), 518. doi:10.1038/s41419-024-06910-4
- Haugstoyl, M. E., Cornillet, M., Strand, K., Stiglund, N., Sun, D., Lawrence-Archer, L.,
 Hjellestad, I. D., Busch, C., Mellgren, G., Bjorkstrom, N. K., & Ferno, J. (2023).
 Phenotypic diversity of human adipose tissue-resident NK cells in obesity. Front
 Immunol, 14, 1130370. doi:10.3389/fimmu.2023.1130370
- Horowitz, A., Strauss-Albee, D. M., Leipold, M., Kubo, J., Nemat-Gorgani, N., Dogan, O.
 C., Dekker, C. L., Mackey, S., Maecker, H., Swan, G. E., Davis, M. M., Norman, P.
 J., Guethlein, L. A., Desai, M., Parham, P., & Blish, C. A. (2013). Genetic and environmental determinants of human NK cell diversity revealed by mass cytometry. Sci Transl Med, 5(208), 208ra145. doi:10.1126/scitranslmed.3006702
- Iikuni, N., Lam, Q. L., Lu, L., Matarese, G., & La Cava, A. (2008). Leptin and Inflammation. Curr Immunol Rev, 4(2), 70-79. doi:10.2174/157339508784325046
- Jiao, Y., Yan, Z., & Yang, A. (2023). The Roles of Innate Lymphoid Cells in the Gastric Mucosal Immunology and Oncogenesis of Gastric Cancer. *Int J Mol Sci, 24*(7). doi:10.3390/ijms24076652
- Jin, X., Qiu, T., Li, L., Yu, R., Chen, X., Li, C., Proud, C. G., & Jiang, T. (2023).

 Pathophysiology of obesity and its associated diseases. *Acta Pharm Sin B, 13*(6), 2403-2424. doi:10.1016/j.apsb.2023.01.012
- Johnson, A. R., Milner, J. J., & Makowski, L. (2012). The inflammation highway: metabolism accelerates inflammatory traffic in obesity. *Immunol Rev, 249*(1), 218-238. doi:10.1111/j.1600-065X.2012.01151.x
- Karamitros, D., Stoilova, B., Aboukhalil, Z., Hamey, F., Reinisch, A., Samitsch, M., Quek, L., Otto, G., Repapi, E., Doondeea, J., Usukhbayar, B., Calvo, J., Taylor, S., Goardon, N., Six, E., Pflumio, F., Porcher, C., Majeti, R., Gottgens, B., & Vyas, P. (2018). Single-cell analysis reveals the continuum of human lympho-myeloid progenitor cells. *Nat Immunol, 19*(1), 85-97. doi:10.1038/s41590-017-0001-2
- Kawai, T., Autieri, M. V., & Scalia, R. (2021). Adipose tissue inflammation and metabolic dysfunction in obesity. *Am J Physiol Cell Physiol*, *320*(3), C375-C391. doi:10.1152/ajpcell.00379.2020
- Koka, R., Burkett, P. R., Chien, M., Chai, S., Chan, F., Lodolce, J. P., Boone, D. L., & Ma, A. (2003). Interleukin (IL)-15R[alpha]-deficient natural killer cells survive in normal but not IL-15R[alpha]-deficient mice. *J Exp Med, 197*(8), 977-984. doi:10.1084/jem.20021836
- Kolb, R., Sutterwala, F. S., & Zhang, W. (2016). Obesity and cancer: inflammation bridges the two. *Curr Opin Pharmacol*, *29*, 77-89. doi:10.1016/j.coph.2016.07.005
- Kumar, S., & Geiger, H. (2017). HSC Niche Biology and HSC Expansion Ex Vivo. *Trends Mol Med*, *23*(9), 799-819. doi:10.1016/j.molmed.2017.07.003
- Lau, C. M., Wiedemann, G. M., & Sun, J. C. (2022). Epigenetic regulation of natural killer cell memory. *Immunol Rev, 305*(1), 90-110. doi:10.1111/imr.13031
- Laue, T., Wrann, C. D., Hoffmann-Castendiek, B., Pietsch, D., Hubner, L., & Kielstein, H. (2015). Altered NK cell function in obese healthy humans. *BMC Obes, 2*, 1. doi:10.1186/s40608-014-0033-1

- Leischner, C., Burkard, M., Pfeiffer, M. M., Lauer, U. M., Busch, C., & Venturelli, S. (2016). Nutritional immunology: function of natural killer cells and their modulation by resveratrol for cancer prevention and treatment. *Nutr J, 15*(1), 47. doi:10.1186/s12937-016-0167-8
- Leone, R. D., & Powell, J. D. (2020). Metabolism of immune cells in cancer. *Nat Rev Cancer*, 20(9), 516-531. doi:10.1038/s41568-020-0273-y
- Leong, J. W., Sullivan, R. P., & Fehniger, T. A. (2014). microRNA management of NK-cell developmental and functional programs. *Eur J Immunol, 44*(10), 2862-2868. doi:10.1002/eji.201444798
- Li, J. H., Hepworth, M. R., & O'Sullivan, T. E. (2023). Regulation of systemic metabolism by tissue-resident immune cell circuits. *Immunity*, *56*(6), 1168-1186. doi:10.1016/j.immuni.2023.05.001
- Littwitz-Salomon, E., Moreira, D., Frost, J. N., Choi, C., Liou, K. T., Ahern, D. K., O'Shaughnessy, S., Wagner, B., Biron, C. A., Drakesmith, H., Dittmer, U., & Finlay, D. K. (2021). Metabolic requirements of NK cells during the acute response against retroviral infection. *Nat Commun*, *12*(1), 5376. doi:10.1038/s41467-021-25715-z
- Liu, T., Zhang, L., Joo, D., & Sun, S. C. (2017). NF-kappaB signaling in inflammation. Signal Transduct Target Ther, 2, 17023-. doi:10.1038/sigtrans.2017.23
- Long, Y., Mao, C., Liu, S., Tao, Y., & Xiao, D. (2024). Epigenetic modifications in obesity-associated diseases. *MedComm (2020)*, 5(2), e496. doi:10.1002/mco2.496
- Luevano, M., Madrigal, A., & Saudemont, A. (2012). Generation of natural killer cells from hematopoietic stem cells in vitro for immunotherapy. *Cell Mol Immunol*, 9(4), 310-320. doi:10.1038/cmi.2012.17
- Luo, L., Feng, P., Yang, Q., Lv, W., Meng, W., Yin, Z., Li, Z., Sun, G., Dong, Z., & Yang, M. (2023). Transcription factor TOX maintains the expression of Mst1 in controlling the early mouse NK cell development. *Theranostics*, 13(7), 2072-2087. doi:10.7150/thno.81198
- Ma, M., Jiang, W., & Zhou, R. (2024). DAMPs and DAMP-sensing receptors in inflammation and diseases. *Immunity*, *57*(4), 752-771. doi:10.1016/j.immuni.2024.03.002
- McCullar, V., Oostendorp, R., Panoskaltsis-Mortari, A., Yun, G., Lutz, C. T., Wagner, J. E., & Miller, J. S. (2008). Mouse fetal and embryonic liver cells differentiate human umbilical cord blood progenitors into CD56-negative natural killer cell precursors in the absence of interleukin-15. *Exp Hematol*, *36*(5), 598-608. doi:10.1016/j.exphem.2008.01.001
- Michelet, X., Dyck, L., Hogan, A., Loftus, R. M., Duquette, D., Wei, K., Beyaz, S., Tavakkoli, A., Foley, C., Donnelly, R., O'Farrelly, C., Raverdeau, M., Vernon, A., Pettee, W., O'Shea, D., Nikolajczyk, B. S., Mills, K. H. G., Brenner, M. B., Finlay, D., & Lynch, L. (2018). Metabolic reprogramming of natural killer cells in obesity limits antitumor responses. *Nat Immunol*, *19*(12), 1330-1340. doi:10.1038/s41590-018-0251-7
- Morcillo-Martín-Romo, P., Valverde-Pozo, J., Ortiz-Bueno, M., Arnone, M., Espinar-Barranco, L., Espinar-Barranco, C., & García-Rubiño, M. E. (2025). The Role of NK

- Cells in Cancer Immunotherapy: Mechanisms, Evasion Strategies, and Therapeutic Advances. *Biomedicines*, *13*(4). doi:10.3390/biomedicines13040857
- Muller-Durovic, B., Lanna, A., Covre, L. P., Mills, R. S., Henson, S. M., & Akbar, A. N. (2016). Killer Cell Lectin-like Receptor G1 Inhibits NK Cell Function through Activation of Adenosine 5'-Monophosphate-Activated Protein Kinase. *J Immunol*, 197(7), 2891-2899. doi:10.4049/jimmunol.1600590
- Murphy, M. P., Holmgren, A., Larsson, N. G., Halliwell, B., Chang, C. J., Kalyanaraman, B., Rhee, S. G., Thornalley, P. J., Partridge, L., Gems, D., Nystrom, T., Belousov, V., Schumacker, P. T., & Winterbourn, C. C. (2011). Unraveling the biological roles of reactive oxygen species. *Cell Metab*, *13*(4), 361-366. doi:10.1016/j.cmet.2011.03.010
- Murru, E., Manca, C., Carta, G., & Banni, S. (2022). Impact of Dietary Palmitic Acid on Lipid Metabolism. *Front Nutr*, 9, 861664. doi:10.3389/fnut.2022.861664
- Mylod, E., Lysaght, J., & Conroy, M. J. (2022). Natural killer cell therapy: A new frontier for obesity-associated cancer. *Cancer Lett*, 535, 215620. doi:10.1016/j.canlet.2022.215620
- Naujoks, W., Quandt, D., Hauffe, A., Kielstein, H., Bahr, I., & Spielmann, J. (2020).

 Characterization of Surface Receptor Expression and Cytotoxicity of Human NK

 Cells and NK Cell Subsets in Overweight and Obese Humans. *Front Immunol*,

 11, 573200. doi:10.3389/fimmu.2020.573200
- Ng, S., Deng, J., Chinnadurai, R., Yuan, S., Pennati, A., & Galipeau, J. (2016). Stimulation of Natural Killer Cell-Mediated Tumor Immunity by an IL15/TGFbeta-Neutralizing Fusion Protein. *Cancer Res*, *76*(19), 5683-5695. doi:10.1158/0008-5472.CAN-16-0386
- Nguyen, S., Dhedin N Fau Vernant, J.-P., Vernant Jp Fau Kuentz, M., Kuentz M Fau Al Jijakli, A., Al Jijakli A Fau Rouas-Freiss, N., Rouas-Freiss N Fau Carosella, E. D., Carosella Ed Fau Boudifa, A., Boudifa A Fau Debré, P., Debré P Fau Vieillard, V., & Vieillard, V. (2005). NK-cell reconstitution after haploidentical hematopoietic stem-cell transplantations: immaturity of NK cells and inhibitory effect of NKG2A override GvL effect. *Blood*, *105(10)*, *4135–4142*. doi:10.1182/blood-2004-10-4113
- O'Shea, D., & Hogan, A. E. (2019). Dysregulation of Natural Killer Cells in Obesity. *Cancers (Basel), 11*(4). doi:10.3390/cancers11040573
- O'Sullivan, T. E., Sun, J. C., & Lanier, L. L. (2015). Natural Killer Cell Memory. *Immunity,* 43(4), 634-645. doi:10.1016/j.immuni.2015.09.013
- Oh, H., & Ghosh, S. (2013). NF-kappaB: roles and regulation in different CD4(+) T-cell subsets. *Immunol Rev, 252*(1), 41-51. doi:10.1111/imr.12033
- Okita, R., Maeda, A., Shimizu, K., Nojima, Y., Saisho, S., & Nakata, M. (2019). Effect of platinum-based chemotherapy on the expression of natural killer group 2 member D ligands, programmed cell death-1 ligand 1 and HLA class I in non-small cell lung cancer. *Oncol Rep, 42*(2), 839-848. doi:10.3892/or.2019.7185
- Omer, N., Nicholls, W., Ruegg, B., Souza-Fonseca-Guimaraes, F., & Rossi, G. R. (2021).

- Enhancing Natural Killer Cell Targeting of Pediatric Sarcoma. *Front Immunol, 12,* 791206. doi:10.3389/fimmu.2021.791206
- Ouchi, N., Parker, J. L., Lugus, J. J., & Walsh, K. (2011). Adipokines in inflammation and metabolic disease. *Nat Rev Immunol*, 11(2), 85-97. doi:10.1038/nri2921
- Paul, S., & Lal, G. (2017). The Molecular Mechanism of Natural Killer Cells Function and Its Importance in Cancer Immunotherapy. *Front Immunol, 8*, 1124. doi:10.3389/fimmu.2017.01124
- Persyn, E., Wahlen, S., Kiekens, L., Taveirne, S., Van Loocke, W., Van Ammel, E., Van Nieuwerburgh, F., Taghon, T., Vandekerckhove, B., Van Vlierberghe, P., & Leclercq, G. (2022). TXNIP Promotes Human NK Cell Development but Is Dispensable for NK Cell Functionality. *Int J Mol Sci*, *23*(19). doi:10.3390/ijms231911345
- Porse, B. T., Bryder, D., Theilgaard-Monch, K., Hasemann, M. S., Anderson, K., Damgaard, I., Jacobsen, S. E., & Nerlov, C. (2005). Loss of C/EBP alpha cell cycle control increases myeloid progenitor proliferation and transforms the neutrophil granulocyte lineage. *J Exp Med*, 202(1), 85-96. doi:10.1084/jem.20050067
- Poznanski, S. M., Singh, K., Ritchie, T. M., Aguiar, J. A., Fan, I. Y., Portillo, A. L., Rojas, E. A., Vahedi, F., El-Sayes, A., Xing, S., Butcher, M., Lu, Y., Doxey, A. C., Schertzer, J. D., Hirte, H. W., & Ashkar, A. A. (2021). Metabolic flexibility determines human NK cell functional fate in the tumor microenvironment. *Cell Metab*, 33(6), 1205-1220 e1205. doi:10.1016/j.cmet.2021.03.023
- Qiu, X., Hill, A., Packer, J., Lin, D., Ma, Y. A., & Trapnell, C. (2017). Single-cell mRNA quantification and differential analysis with Census. *Nat Methods, 14*(3), 309-315. doi:10.1038/nmeth.4150
- Quail, D. F., & Dannenberg, A. J. (2019). The obese adipose tissue microenvironment in cancer development and progression. *Nat Rev Endocrinol, 15*(3), 139-154. doi:10.1038/s41574-018-0126-x
- Rados, M., Landegger, A., Schmutzler, L., Rabidou, K., Taschner-Mandl, S., & Fetahu, I. S. (2024). Natural killer cells in neuroblastoma: immunological insights and therapeutic perspectives. *Cancer Metastasis Rev, 43*(4), 1401-1417. doi:10.1007/s10555-024-10212-8
- Richard, A. J., & Stephens, J. M. (2014). The role of JAK-STAT signaling in adipose tissue function. *Biochim Biophys Acta, 1842*(3), 431-439. doi:10.1016/j.bbadis.2013.05.030
- Riggan, L., Shah, S., & O'Sullivan, T. E. (2021). Arrested development: suppression of NK cell function in the tumor microenvironment. *Clin Transl Immunology, 10*(1), e1238. doi:10.1002/cti2.1238
- Rizzatti, V., Boschi, F., Pedrotti, M., Zoico, E., Sbarbati, A., & Zamboni, M. (2013). Lipid droplets characterization in adipocyte differentiated 3T3-L1 cells: size and optical density distribution. *Eur J Histochem*, *57*(3), e24. doi:10.4081/ejh.2013.e24
- Rosenstock, P., Bork, K., Massa, C., Selke, P., Seliger, B., & Horstkorte, R. (2020). Sialylation of Human Natural Killer (NK) Cells is Regulated by IL-2. *J Clin Med*, 9(6). doi:10.3390/jcm9061816

- Schrors, B., Hos, B. J., Yildiz, I. G., Lower, M., Lang, F., Holtstrater, C., Becker, J., Vormehr, M., Sahin, U., Ossendorp, F., & Diken, M. (2023). MC38 colorectal tumor cell lines from two different sources display substantial differences in transcriptome, mutanome and neoantigen expression. *Front Immunol, 14*, 1102282. doi:10.3389/fimmu.2023.1102282
- Segovis, C. M., Schoon, R. A., Dick, C. J., Nacusi, L. P., Leibson, P. J., & Billadeau, D. D. (2009). PI3K links NKG2D signaling to a CrkL pathway involved in natural killer cell adhesion, polarity, and granule secretion. *J Immunol*, *182*(11), 6933-6942. doi:10.4049/jimmunol.0803840
- Shaver, K. A., Croom-Perez, T. J., & Copik, A. J. (2021). Natural Killer Cells: The Linchpin for Successful Cancer Immunotherapy. *Front Immunol, 12*, 679117. doi:10.3389/fimmu.2021.679117
- Sheppard, S., Srpan, K., Lin, W., Lee, M., Delconte, R. B., Owyong, M., Carmeliet, P., Davis, D. M., Xavier, J. B., Hsu, K. C., & Sun, J. C. (2024). Fatty acid oxidation fuels natural killer cell responses against infection and cancer. *Proc Natl Acad Sci U S A, 121*(11), e2319254121. doi:10.1073/pnas.2319254121
- Sordo-Bahamonde, C., Vitale, M., Lorenzo-Herrero, S., Lopez-Soto, A., & Gonzalez, S. (2020). Mechanisms of Resistance to NK Cell Immunotherapy. *Cancers (Basel),* 12(4). doi:10.3390/cancers12040893
- Spielmann, J., Hanke, J., Knauf, D., Ben-Eliyahu, S., Jacobs, R., Stangl, G. I., Bahr, I., & Kielstein, H. (2017). Significantly enhanced lung metastasis and reduced organ NK cell functions in diet-induced obese rats. *BMC Obes, 4*, 24. doi:10.1186/s40608-017-0161-5
- Stiglund, N., Strand, K., Cornillet, M., Stal, P., Thorell, A., Zimmer, C. L., Naslund, E., Karlgren, S., Nilsson, H., Mellgren, G., Ferno, J., Hagstrom, H., & Bjorkstrom, N. K. (2019). Retained NK Cell Phenotype and Functionality in Non-alcoholic Fatty Liver Disease. *Front Immunol, 10*, 1255. doi:10.3389/fimmu.2019.01255
- Stokic-Trtica, V., Diefenbach, A., & Klose, C. S. N. (2020). NK Cell Development in Times of Innate Lymphoid Cell Diversity. *Front Immunol*, *11*, 813. doi:10.3389/fimmu.2020.00813
- Sun, Y., Zhou, B., Mao, F., Xu, J., Miao, H., Zou, Z., Phuc Khoa, L. T., Jang, Y., Cai, S., Witkin, M., Koche, R., Ge, K., Dressler, G. R., Levine, R. L., Armstrong, S. A., Dou, Y., & Hess, J. L. (2018). HOXA9 Reprograms the Enhancer Landscape to Promote Leukemogenesis. *Cancer Cell*, 34(4), 643-658 e645. doi:10.1016/j.ccell.2018.08.018
- Syed, M., Parmar, C., & Pouwels, S. (2024). The effects of exercise therapy on immune cells and function in patients with overweight or obesity: A systematic review. Brain Behavior and Immunity Integrative, 8. doi:10.1016/j.bbii.2024.100093
- Terren, I., Orrantia, A., Vitalle, J., Astarloa-Pando, G., Zenarruzabeitia, O., & Borrego, F. (2020). Modulating NK cell metabolism for cancer immunotherapy. *Semin Hematol*, *57*(4), 213-224. doi:10.1053/j.seminhematol.2020.10.003
- Theurich, S., Tsaousidou, E., Hanssen, R., Lempradl, A. M., Mauer, J., Timper, K., Schilbach, K., Folz-Donahue, K., Heilinger, C., Sexl, V., Pospisilik, J. A., Wunderlich, F. T., & Bruning, J. C. (2017). IL-6/Stat3-Dependent Induction of a

- Distinct, Obesity-Associated NK Cell Subpopulation Deteriorates Energy and Glucose Homeostasis. *Cell Metab*, *26*(1), 171-184 e176. doi:10.1016/j.cmet.2017.05.018
- Trapnell, C., Cacchiarelli, D., Grimsby, J., Pokharel, P., Li, S., Morse, M., Lennon, N. J., Livak, K. J., Mikkelsen, T. S., & Rinn, J. L. (2014). The dynamics and regulators of cell fate decisions are revealed by pseudotemporal ordering of single cells. *Nat Biotechnol*, 32(4), 381-386. doi:10.1038/nbt.2859
- Waldmann, T. A. (2015). The shared and contrasting roles of IL2 and IL15 in the life and death of normal and neoplastic lymphocytes: implications for cancer therapy. Cancer Immunol Res, 3(3), 219-227. doi:10.1158/2326-6066.CIR-15-0009
- Wu, Q., Li, B., Li, J., Sun, S., Yuan, J., & Sun, S. (2021). Cancer-associated adipocytes as immunomodulators in cancer. *Biomark Res*, 9(1), 2. doi:10.1186/s40364-020-00257-6
- Wu, S. Y., Fu, T., Jiang, Y. Z., & Shao, Z. M. (2020). Natural killer cells in cancer biology and therapy. *Mol Cancer*, *19*(1), 120. doi:10.1186/s12943-020-01238-x
- Yang, L., Bryder, D., Adolfsson, J., Nygren, J., Mansson, R., Sigvardsson, M., & Jacobsen, S. E. (2005). Identification of Lin(-)Sca1(+)kit(+)CD34(+)Flt3- short-term hematopoietic stem cells capable of rapidly reconstituting and rescuing myeloablated transplant recipients. *Blood*, *105*(7), 2717-2723. doi:10.1182/blood-2004-06-2159
- Yu, L., Zhang, X., Ye, S., Lian, H., Wang, H., & Ye, J. (2022). Obesity and COVID-19: Mechanistic Insights From Adipose Tissue. *J Clin Endocrinol Metab*, 107(7), 1799-1811. doi:10.1210/clinem/dgac137
- Zatterale, F., Longo, M., Naderi, J., Raciti, G. A., Desiderio, A., Miele, C., & Beguinot, F. (2019). Chronic Adipose Tissue Inflammation Linking Obesity to Insulin Resistance and Type 2 Diabetes. *Front Physiol*, *10*, 1607. doi:10.3389/fphys.2019.01607
- Zhang, C. C., & Lodish, H. F. (2008). Cytokines regulating hematopoietic stem cell function. *Curr Opin Hematol*, *15*(4), 307-311. doi:10.1097/MOH.0b013e3283007db5
- Zong, Y., Li, H., Liao, P., Chen, L., Pan, Y., Zheng, Y., Zhang, C., Liu, D., Zheng, M., & Gao, J. (2024). Mitochondrial dysfunction: mechanisms and advances in therapy. Signal Transduct Target Ther, 9(1), 124. doi:10.1038/s41392-024-01839-8
- Zriwil, A., Boiers, C., Kristiansen, T. A., Wittmann, L., Yuan, J., Nerlov, C., Sitnicka, E., & Jacobsen, S. E. W. (2018). Direct role of FLT3 in regulation of early lymphoid progenitors. *Br J Haematol*, *183*(4), 588-600. doi:10.1111/bjh.15578

Acknowledgments

As I bring my PhD journey to a close, I would like to take this opportunity to express my deepest gratitude to the many people and institutions who have supported, encouraged, and inspired me along the way. This thesis would not have been possible without your presence in both my academic and personal life.

First and foremost, I extend my heartfelt appreciation to my supervisor, Professor Sebastian Theurich, for his invaluable guidance, trust, and mentorship throughout the entirety of my doctoral studies. I am truly grateful for the opportunity to work under his supervision and for the freedom he gave me to develop and pursue the research.

I would also like to express my sincere thanks to my TAC members, Professor Nößner and Professor Kobold, for their insightful suggestions, critical feedback, and continued support during my Thesis Advisory Committee meetings. Their perspectives helped me refine my research and stay focused on scientific questions. I deeply appreciate their time and dedication.

I am incredibly grateful to my colleagues Amar, Martin, Sabine, Adriano, Ludo, Lena and Anneli for their encouragement, and constant support throughout my PhD years. Working with such intelligent, kind, and generous people has made every challenge more manageable and every success more rewarding. Whether we were solving problems at the bench or simply enjoying good conversation over lunch, your friendship made a lasting impact on both my work and my life. Special thanks go to Ziming, who performed the RNA-seq data analysis for my project. His technical expertise and willingness to collaborate were essential and significantly strengthened the quality of my research.

I would like to acknowledge the generous financial support from the China Scholarship Council (CSC), which made it possible for me to pursue my PhD studies at Ludwig-Maximilians-Universität München (LMU). I am honored to have received this scholarship, and I recognize the responsibility and opportunity it represents.

Completing my PhD in LMU has been a truly transformative experience. The academic atmosphere, world-class facilities, and opportunity to engage with brilliant researchers

have helped me grow both professionally and personally. I am proud to have been a part of this vibrant and internationally renowned institution.

To my family in China, words cannot fully express my gratitude for your unwavering love, sacrifices, and encouragement. Despite the distance, you have always been by my side in spirit. Your belief in me has been the foundation of all my achievements.

To my friends, near and far—thank you for keeping me grounded, for making me laugh when I needed it, and for reminding me of life beyond the lab. Your kindness and support helped me navigate the ups and downs of this journey with balance and perspective.

As I look back on these years, I am filled with gratitude. This thesis represents the result of collective effort, shared ideas, and the support of a truly remarkable community. Thank you all for being an essential part of this chapter in my life.

Affidavit



LUDWIG-MAXIMILIANS-UNIVERSITÄT MÜNCHEN

Promotionsbüro Medizinische Fakultät





Affidavit Tu, Jingke

Surname, first name

I hereby declare, that the submitted thesis entitled:

The Impact of Obesity-Associated Environment on Differentiation, Metabolism and Function of Natural Killer Cells

is my own work. I have only used the sources indicated and have not made unauthorized use of services of a third party. Where the work of others has been quoted or reproduced, the source is always given.

I further declare that the dissertation presented here has not been submitted in the same or similar form to any other institution for the purpose of obtaining an academic degree.

Munich 09.10.2025

Jingke Tu

Place and date

Signature doctoral candidate

Confirmation of congruency



LUDWIG-MAXIMILIANS-UNIVERSITÄT MÜNCHEN

Promotionsbüro Medizinische Fakultät





Confirmation of congruency between printed and electronic version of the doctoral thesis

the doctoral thesis				
Tu, Jingke				
Surname, first name				
I hereby declare, that the submitted thesis entitled:				
The Impact of Obesity-Associated Environment on Differentiation, Metabolism and				
Function of Natural Killer Cells				
is congruent with the printed version both in content and format.				
Munich 09.10.2025	Jingke Tu			
Place and date	Signature doctoral candidate			